Asymptotic analysis of nonlinear tides in Wadden systems - the role of momentum sinks

by

Tjebbe Hepkema

a thesis submitted to the Department of Mathematics
at Utrecht University for the degree of

Master of Mathematical Sciences

supervisors: Huib de Swart (IMAU) & Antonios Zagaris (CVI-WUR)

second reader: Rob Bisseling (UU)

30th June 2016

Universiteit Utrecht

Abstract

This study aims to contribute to a better understanding of physical mechanisms in tidal channels as present in, for example, the Dutch Wadden Sea. Understanding these mechanisms will contribute to effective management of the Wadden Sea and help preventing flooding in coastal areas. In this study we consider a tidal channel with tidal flats on both sides, that is connected on two sides to an open sea. The model is an idealized version of the channel connecting the Marsdiep and the Vlie in the Netherlands.

The specific mechanism studied is that of momentum dissipation on tidal flats. Rising water level leads to water masses flowing onto the flats, carrying momentum. The water flows back into the channel during the falling tide after being temporarily stored on the flats. However, due to large friction on the shallow flats, the momentum dissipates rapidly. This is a momentum sink. The terms arising from the mass storage and the momentum dissipation are nonlinear and give rise to overtides of the primary (semi-diurnal lunar) tide, which in turn affect net sediment transport.

Here, we build on and extend a recent numerical study so as to better understand the effect of momentum sink on characteristics of the primary tide and of its overtides. This is done by constructing an asymptotic approximation to the solution of the cross sectionally averaged shallow water equations that model the hydrodynamics in a tidal channel. The analytic approach enables assessment of the effect of the momentum sink and quantification of the differences between solutions that do or do not account for it. Multiple effects of the momentum sink on the hydrodynamics are found. In particular, when the tidal flats are approximately of the same width as the main channel no significant effects of momentum sink are found. However, when the tidal channel has wide tidal flats compared to the main channel, the momentum sink causes significant tidal distortion.

Acknowledgements

I would like to thank everyone that helped me write this thesis. First of all, Huib de Swart with whom I had weekly meetings. Thank you for your patience with a non-physicist. I enjoyed working together and sharing the interest in the Wadden Sea. Second, thank you Antonios Zagaris. Thank you for introducing me to the subject of asymptotics. I learned lots from the way you approach mathematical problems and I appreciated our informal working relationship a lot. Third, thank you Wim Ridderinkhof and Niels Alebregtse for showing me the existence of the research area of tidal channels. Then of course, a thanks to all the students in the IMAU students room: Brenda, Aleid, René, Robby, Stef, Stan, Anna, Henry and Klaas. Having people to share an office, coffee and lunch breaks with greatly helped with the motivation. Lastly, thank you Oscar van der Heide giving tips on how to write and thank you Maxim van Oldenbeek for the bike rides and the occasional mathematical consult.

Contents

Abstract i

Acknowledgements iii

Chapter 1. Introduction 1
1.1. Context and problem description 2
1.2. Prerequisites 4
1.2.1. Tides and its overtides 4
1.2.2. Perturbation methods 8

Chapter 2. The model 11
2.1. Domain 11
2.2. The depth averaged shallow water equations 14
2.3. Cross sectionally averaged continuity equation 16
2.4. Cross sectionally averaged momentum balance 17

Chapter 3. Model Analysis 21
3.1. Scaling 21
3.2. Asymptotic approximation 26
3.2.1. The $O(1)$ problem 26
3.2.2. The $O(\varepsilon)$ problem 29

Chapter 4. Results 37
4.1. Default configuration 37
4.2. Analytical difference 44
4.3. Effects of the momentum sink on hydrodynamics 47
4.4. Additional remarks on results of the model 65

Chapter 5. Discussion 67
5.1. On the model 67
5.2. On the model analysis 67
5.3. On context with literature 68

Chapter 6. Conclusions 71

Appendix A. Details on the cross sectionally averaging 73

Appendix B. Calculations from Chapter 3 81

Appendix C. The depth averaged shallow water equations 89

Bibliography 97

CHAPTER 1

Introduction

The Dutch Wadden Sea is a coastal body of water in the north of the Netherlands, situated between the northern islands (the 'Wadden eilanden') and the coast of the mainland. The Wadden Sea continues on the north coast of Germany and on the west coast of Denmark. Large parts of the Wadden Sea are very shallow. A consequence of this shallowness is that during low tide, large parts of the sea fall dry and the bottom of the Wadden Sea becomes visible and accessible. For a great number of birds the Wadden Sea, with its dry falling parts, is essential for their survival. The Wadden Sea is also highly appreciated by mankind. The opinion that it is a special and beautiful place for both animals and humans which should be conserved is confirmed by the fact that since 2009 the Wadden Sea is part of the UNESCO World Heritage List.

This study is meant to contribute to a better understanding of physical mechanisms in the Wadden Sea. In particular, we are interested in gaining a better understanding of the hydrodynamics in the Wadden Sea. The hydrodynamics give rise to net sediment transport and is therefore important for the morphodynamical stability of the Wadden Sea. Understanding the physics in order to make sensible decisions in the conservation of the Wadden Sea may seem like a second order necessity of life. However, it becomes a first order necessity, if understanding the physics helps to prevent flooding of inhabited coastal areas of the Netherlands.

Figure 1.1. photo by: B. G. Hepkema.

1.1. Context and problem description

The focus of this study is on modeling and understanding the hydrodynamics in a tidal channel with tidal flats on both sides that is connected on two sides to an open sea. In particular, of both the free surface elevation and the current velocity, the overtides of the lunar semi-diurnal constituent and the residuals are investigated. The model represents a highly idealized version of the channel connecting the Marsdiep and the Vlie in the Dutch Wadden Sea. In the next few paragraphs (and last two sentences) certain terminology is used that is common in the field of coastal systems. An explanation of these terms will be given in Section 1.2.1.

When the water level rises, water masses flow from the channel onto the flats, carrying with them momentum. The mass is temporarily stored on the flats, until it flows back into the channel during the falling tide. The momentum, however, dissipates rapidly due to large friction on the tidal flats. That is, the tidal flats act like momentum sinks (Dronkers, 1964). The terms arising from the mass storage and the momentum dissipation are nonlinear and give rise to overtides of the dominant primary (semi-diurnal lunar) tide, which in turn affect net sediment transport. Overtides contribute to asymmetries in the curves representing the free surface and the current velocity, which, in turn, causes a net transport of sediment. This is shown in, among others, Boon and Byrne (1981). Net sediment transport is interesting for many reasons. For example, without a net import of sediment the Wadden Sea will disappear rapidly when the sea level rises due to climate change. Dredging companies can also benefit from knowledge of sediment transport mechanisms. Furthermore, understanding mechanisms that influence the amplitude of the free surface elevation helps to prevent flooding of coastal areas.

The mass storage is investigated in, for example, Speer and Aubrey (1985), Friedrichs and Aubrey (1988) and Ridderinkhof et al. (2014). Less attention has been paid to the momentum sink and only recently Alebregtse et al. (2015), investigated its role numerically. This is done in a semi-enclosed basin. His research focused on channels with various tidal flat geometries contained in a semi-enclosed basin. In Speer and Aubrey (1985), it is found that in a short channel (i.e. the channel length is much smaller than the tidal wavelength), without tidal flats the asymmetry in the free surface is characterized by a tide where the falling time is longer than the rising time. The asymmetry increases as friction is increased. The asymmetries in the velocity are such that the velocity is larger during the flood than during the ebb. However, in channels with tidal flats, a longer period of rising tide than falling tide and stronger currents during the ebb was found. In Ridderinkhof et al. (2014), it is found that the currents during the flood become stronger as the length of the channel is increased. All of this is done in a channel that is open at one side and closed on the other. In Alebregtse et al. (2015), the role of the momentum sink is investigated in a channel with various geometries of the tidal flats. In each case the channel is closed at one end. The investigation is done with a numerical model, but also a brief analytical analysis by a harmonic decomposition of the momentum sink term is given. The effect of the momentum sink is found to be sensitive to the area of the tidal flats, the lateral tidal flat profile and the along channel distribution of the flats. It is shown that the effect of the momentum sink on the sediment transport is limited for both coarse and fine sediment.

Here, we build on and extend Alebregtse's work so as to better understand the effect of momentum sink on characteristics of the main tide and of its overtides. There are three major differences. First, our approach is analytic in nature and we explicitly construct the solution of the cross sectionally averaged shallow water equations with asymptotic methods, using the Froude number as a small parameter. Second, to mimic a system as the Marsdiep-Vlie system in

the Dutch Wadden Sea, we exchange Alebregtse's semi enclosed geometry for an open channel with an M_2 wave entering at both ends. Third, in Alebregtse et al. (2015) the effects of the momentum sink on the current velocity is investigated. Here, also the effects of the momentum sink on the free surface elevation are quantified and analyzed. The asymptotic methods allow us to derive analytical expressions for the solutions of the first and second order problems as the Froude number approaches zero. This makes it possible to calculate the free surface elevation and current velocity at any point in space and time without calculating adjacent points in space or time. Furthermore, the analytic approach enables assessment of the effect of the momentum sink and quantify the difference between solutions that do or do not account for it. The advantages of considering a channel open on both ends is that we can model what happens when the two waves that enter the channel differ in amplitude or phase, as typically occurs in nature. For example, the moment of high water at the Marsdiep differs approximately 1,5 hours from the time of high water at the Vlie.

In Chapter 2, the cross sectionally averaged shallow water equations are derived, which is a system of nonlinear first order partial differential equations. In Chapter 3 asymptotic (perturbation) methods are used to find an approximate solution to the equations. With the approximate solutions to the cross sectionally averaged shallow water equations we investigate the effects of the momentum sink on the hydrodynamics in Chapter 4. The results in Chapter 4 are followed by a discusion and a conclusion in Chapters 5 and 6.

Certain calculations in Chapter 2 are far from rigorous. In Appendix A these calculations are investigated in further detail. Appendix B contains some elaborated calculations from Chapter 3. Appendix C contains a derivation of the depth averaged shallow water equations that form the starting point of Chapter 2.

To finish this subsection, a small note on the writing style. Many people prefer to investigate a subject of interest together with someone rather than alone. To create the idea of having company while reading this thesis, the author chose to use the word 'we'. With 'we' is meant: the author together with the reader. The author did not get delusional by thinking he became plural.

1.2. Prerequisites

1.2.1. Tides and its overtides.

This section contains a short introduction into some basic concepts and terminology used in this thesis, mainly coming from the field of coastal physics. It is by no means a general introduction to the theory of tides but should provide the reader with the background necessary to understand the rest of this thesis. A general introduction to the theory of tides is obtained by reading, for example, Open University Course Team (2001), Parker (1991) or, if the basics are enough, the popular scientific book by McCully (2006). Besides reading books about the tides, it is highly recommended to find someone who has been sailing on the Wadden Sea for some time and make a trip with him or her. For inspiration consult Vandersmissen (1993). The internet also provides a lot of information about the tides. For example, `getij.rws.nl`, `waterberichtgeving.rws.nl`, `www.wadvaarders.nl` and `tidesandcurrents.noaa.gov`.

Describing the hydrodynamics in a tidal channel consists of describing the free surface elevation, ξ, and the velocity of the water, u. The free surface elevation can for now be thought of as the height of the water. In Chapter 2 a precise definition is given. Both ξ and u depend on both a time coordinate, t, and a spacial coordinate, x.

1.2.1.1. *Overtides and tidal distortion.*

The hydrodynamics in shallow water are often modeled by the shallow water equations. These equations are a system evolution equations that are of first order in time and contain nonlinear terms. The nonlinear terms are linked to, for example, friction or advection of momentum. That is, including friction or advection of momentum in the model causes nonlinear terms to appear in the equations governing the model. These nonlinear terms (or processes, that are represented by these terms) give rise to so called 'overtides'[1]. The term overtides is explained by the following example. Consider a one dimensional model where the current velocity, u, is given by a single cosine induced by the gravitational field due to the Moon,

$$u(x,t) = U(x)\cos(\sigma t - \phi_u(x)), \tag{1.1}$$

with $U(x)$ the amplitude, σ the angular frequency and $\phi_u(x)$ the phase. The cosine in Equation 1.1 represents the so called M_2 constituent. The 'M' stands for Moon and the '2' represents the fact that it produces a tidal wave with a period of approximately half a day (2 periods fit in one day). The period of the M_2 constituent is in fact very close to 12 hours and 25 minutes[2]. That is, σ equals 2π divided by 12 hours and 25 minutes. Often the word 'constituent' is left out, so the M_2 constituent is abbreviated as the M_2.

A nonlinear term[3] in the shallow water equations reads

$$u\frac{\partial u}{\partial x}. \tag{1.2}$$

Substituting (1.1) in (1.2) yields

$$\begin{aligned} u\frac{\partial u}{\partial x} &= U\cos(\sigma t - \phi_u)\left[\frac{\partial U}{\partial x}\cos(\sigma t - \phi_u) + U\sin(\sigma t - \phi_u)\frac{\partial \phi_u}{\partial x}\right] \\ &= \frac{U}{2}\frac{\partial U}{\partial x} + \frac{U}{2}\frac{\partial U}{\partial x}\cos(2(\sigma t - \phi_u)) + \frac{U^2}{2}\frac{\partial \phi_u}{\partial x}\sin(2(\sigma t - \phi_u)). \end{aligned} \tag{1.3}$$

[1] Similar to a 'overtone' in music.

[2] Half a lunar day.

[3] This term discribes the advection of momentum (per mass), u, by the velocity u.

In Equation (1.3) there is a cosine and sine with frequency 2σ and a term independent of time. This means that, because of the nonlinear term (1.2), a signal of half the period and a time independent signal enters the story. The signal with half the period is called the M_4 constituent and is the first overtide of the M_2 constituent. The time independent signal is a residual signal and is called the M_0; when taking the average over one tidal period this term is the only one that does not vanish. The next overtide is the M_6, with a period three times as short as that of M_2. In general, for $m \in \mathbb{N}_{\geq 2}$, the $(m-1)$-th overtide of the M_2 constituent is M_{2m}, with a period m times as short as that of M_2, such that $2m$ periods fit in one day.

Loosely speaking, the tide coming from a very deep sea looks like a cosine and when this cosine enters shallow water, nonlinear terms start to play a role. In these nonlinear terms the cosine is multiplied by another (co)sine. Then, because

$$\sin(t)\cos(t) = \frac{1}{2}\sin(2t),$$

overtides are created.

If the M_4 is added to the M_2 the tidal curve is no longer a perfect cosine but the sum of two cosines. A typical curve for the free surface elevation, ξ, at a certain point in space is depicted in Figure 1.2. Free surface elevation curves like this occur at multiple places along the Dutch

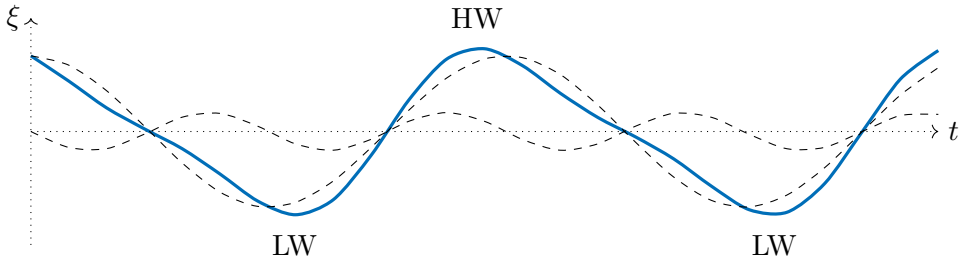

Figure 1.2. A typical curve for the free surface elevation, ξ, at a certain point in space. The time of falling tide is longer than the time of rising tide.

coast, for example, in Harlingen. Because of the nonlinear effects in the shallow Wadden Sea, the period between high water (HW) and low water (LW) is longer than the period between low water and high water[4]. The distortion of sinusoidal curve (called tidal distortion) is visible in plots with the time on one of the axis as in Figure 1.2. However, often we are interested in the tidal distortion at every point in space. It would therefore be preferable to define certain parameters only dependent on x that tell us the main information about the tidal distortion. One way to do this is introduced in Friedrichs and Aubrey (1988). Their idea is based on the fact that the main tidal distortion is due to the first overtide of the M_2, the M_4. A measure of the tidal distortion is given by the ratio between the amplitude of the M_4 and M_2. The characteristics of the tidal distortion is given by the so called 'relative phase' between the M_2 and M_4. From Figure 1.2, it is clear that when the M_4 is shifted with respect to the M_2 the curve of ξ will change. To investigate these shifts of phases, assume ξ consists of a M_2 and a M_4 signal,

$$\xi(t,x) = Z_{M_2}\cos(\sigma t - \phi_{\xi,M_2}) + Z_{M_4}\cos(2\sigma t - \phi_{\xi,M_4}).$$

[4]Sailors that are used to rely on the $1/12, 2/12, 3/12$-rule might want to be careful at these locations.

In Friedrichs and Aubrey (1988) the relative phase between the M_2 and M_4 of the free surface elevation and the velocity is defined as

$$2\phi_{\xi,M_2} - \phi_{\xi,M_4} \quad \text{and} \quad 2\phi_{u,M_2} - \phi_{u,M_4},$$

respectively. The relative phases are understood to be modulo 2π. For different relative phases the resulting curves are shown in Figure 1.3, some of them occur more often in nature than others.

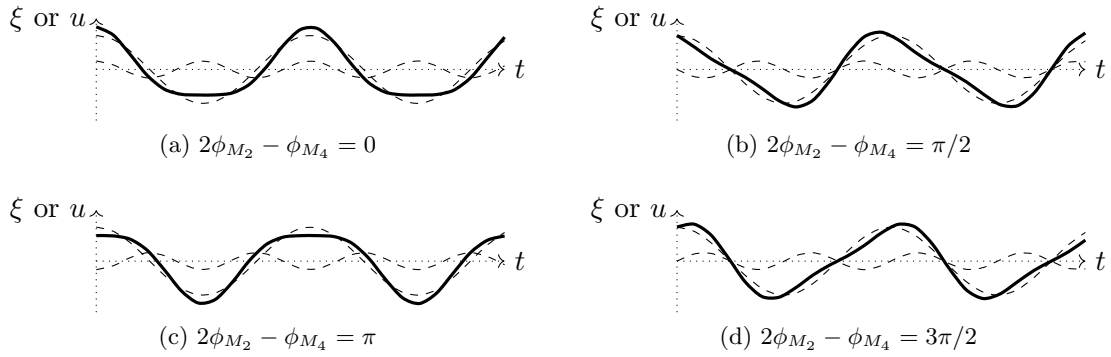

(a) $2\phi_{M_2} - \phi_{M_4} = 0$ (b) $2\phi_{M_2} - \phi_{M_4} = \pi/2$

(c) $2\phi_{M_2} - \phi_{M_4} = \pi$ (d) $2\phi_{M_2} - \phi_{M_4} = 3\pi/2$

Figure 1.3. Curves for the free surface elevation, ξ, or the current velocity, u for different relative phases between M_2 and M_4.

Based on Friedrichs and Aubrey (1988), we will now introduce some terminology in the distortion of the perfect cosine due to the M_4 signal for both the free surface elevation and the current velocity. First, we consider the tidal distortion in the free surface elevation, ξ. Figure 1.3 shows multiple variations of tidal distortion in ξ. The period between high water and the successive low water is called the falling of the tide. Likewise is the period between low water and the successive high water called the rising of the tide. The first tidal distortion is that the rising and the falling of the tide are equal (as in Figures 1.3a and 1.3c). The second is that the falling of the tide is longer than the rising of the tide (as in Figure 1.3b) and the third is that the falling of the tide is shorter than the rising of the tide (as in Figure 1.3d). Figures 1.3a and 1.3c show two other types of tidal distortion. In Figure 1.3a the absolute value of the high water (HW) is larger than the absolute value of the low water (LW). In Figure 1.3c it is the other way around. The relation between the relative phase and the different tidal distortions in ξ is given in Figure 1.4. Note that if the average of the free surface elevation over one tidal period is not equal to zero, the relation between the relative phase and the comparison between the absolute value of the high and low waters might be invalid.

Next, we consider the tidal distortions in the current velocity, u. When studying tidal channels that are closed on one side it is custom to call a moment in time at a location in space ebb if $u < 0$ and flood if $u > 0$. However, when the channel is open on both sides ebb and flood are not well defined anymore. We therefore simply speak of the sign of u being $+$ or $-$. If at a point, x_0, in the channel,

$$|\max_t u(t, x_0)| > |\min_t u(t, x_0)|,$$

the system at that point is called $+$ *dominant* (as in Figure 1.3a). If on the other hand,

$$|\max_t u(t, x_0)| < |\min_t u(t, x_0)|,$$

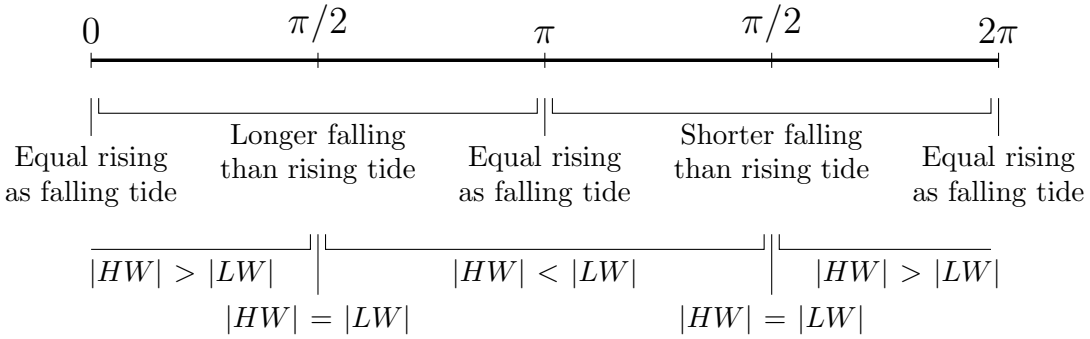

Figure 1.4. Relation between the relative phase, $2\phi_{\xi,M_2} - \phi_{\xi,M_4} \in [0, 2\pi)$, and the type of tidal distortion in the free surface elevation, ξ

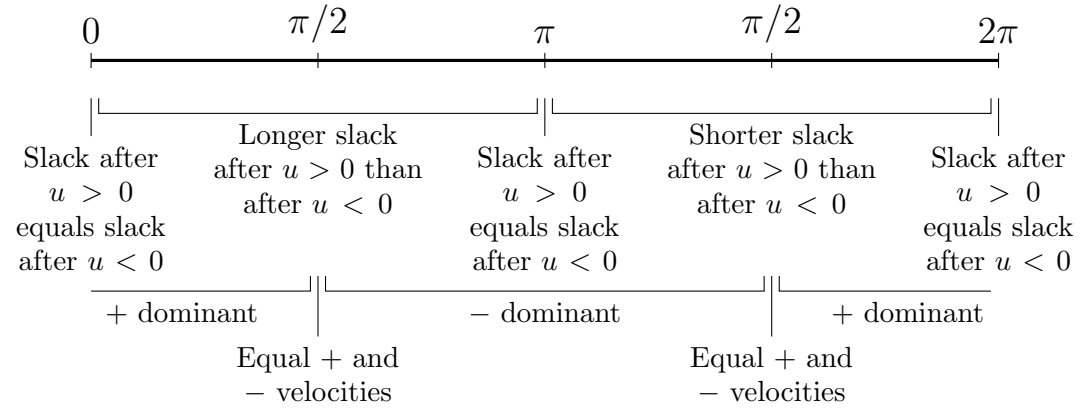

Figure 1.5. Relation between the relative phase, $2\phi_{u,M_2} - \phi_{u,M_4} \in [0, 2\pi)$, and the type of tidal distortion in the current velocity, u.

the system at that point is called − *dominant* (as in Figure 1.3c). The characterization of the system being + or − dominant is an important indicator for the transport of coarse sediment. The period where the velocity is small is called the *slack*. During the slack, suspended sediment can sink to the seabed. In a curve as in Figure 1.3b the slack after the period that the velocity is positive is longer than the slack after the period the velocity is negative. In Figure 1.3d it is the other way around. The difference in slack after positive u and the slack after negative u is an important indicator for the transport of fine sediment. The relation between the different tidal distortions in u and the relative phase is given in Figure 1.5. Note, also for u, that if the average of the current velocity over one tidal period is not equal to zero, the relation between the relative phase and the +/− dominant character of the system might be wrong.

To finish this subsection on overtides and tidal distortion, one last typical curve of ξ in the Wadden Sea is depicted in Figure 1.6. We see that the water level rises, then drops, but then rises again before dropping to LW. There are two 'high' and two 'low' waters. This is called 'shoulder' behaviour. The periods of the dashed lines differ a factor of three. So this shoulder behaviour can occur if, for example, a strong M_6 is created in the tidal channel.

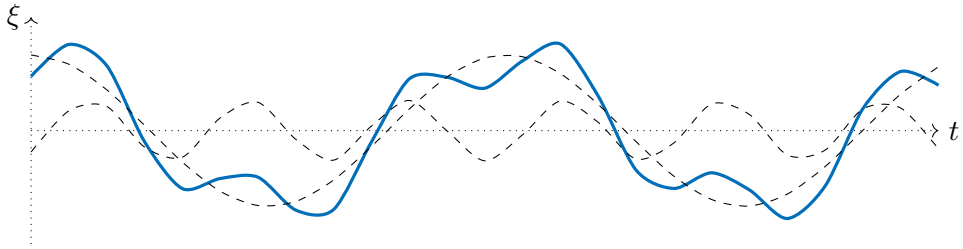

Figure 1.6. Shoulder behaviour of a tidal curve representing the free surface elevation, ξ, versus time, t. The tidal curve includes a M_2 and M_6 signal.

1.2.1.2. *Complex exponentials.*
A labor saving decision is working with complex exponentials instead of with sines and cosines. Allowing every possible overtide, ξ and u are represented as

$$\xi(t,x) = \sum_{m=0}^{\infty} \mathrm{Re}\left\{Z_m(x)e^{-im\sigma t}\right\} = \sum_{m=0}^{\infty} \mathrm{Re}\left\{|Z_m|e^{i\phi_{\xi,m}-im\sigma t}\right\} = \sum_{m=0}^{\infty} |Z_m|\cos(m\sigma t - \phi_{\xi,m}),$$

$$u(t,x) = \sum_{m=0}^{\infty} \mathrm{Re}\left\{U_m(x)e^{-im\sigma t}\right\} = \sum_{m=0}^{\infty} \mathrm{Re}\left\{|U_m|e^{i\phi_{u,m}-im\sigma t}\right\} = \sum_{m=0}^{\infty} |U_m|\cos(m\sigma t - \phi_{u,m}),$$

where σ is the frequency of the M_2 constituent, $\phi_{\xi,m}$ and $\phi_{u,m}$ are the phases of the M_{2m} of ξ and u, respectively. Furthermore,

$$Z_m(x) = |Z_m(x)|e^{i\phi_{\xi,m}(x)} \quad \text{and} \quad U_m(x) = |U_m(x)|e^{i\phi_{u,m}(x)}$$

are complex numbers depending on x but constant in t. We call Z_m and U_m the complex amplitudes of the M_{2m} free surface elevation and M_{2m} velocity respectively. The (real) amplitude of the M_{2m} free surface elevation is the norm of the complex amplitude, $|Z_m(x)|$. Likewise, the (real) amplitude of the velocity is $|U_m(x)|$. As we will see later, the terms in the sums for $m = 0$ are special in the sense that they are real and represent the residual free surface elevation or residual current velocity. In the rest of the thesis we will work with the complex exponential representation of ξ and u.

1.2.2. Perturbation methods.

In this section some basic notions of asymptotic methods are introduced. Asymptotic methods, also called perturbation methods, provide, among other things, a way of approximating functions. In this study the functions to be approximated are the solutions to partial differential equations (pde). The following introduction is borrowed from Holmes (2013). The theorems and definitions are in fact literally copied from Holmes (2013). First, the so called order symbols are introduced. These symbols allow us to describe the behavior of functions as their arguments approach a certain limit. For example, x^2 goes faster to zero than x does, when $x \to 0$.

Definition 1.1.
1. $f = O(\varphi)$ as $\varepsilon \downarrow \varepsilon_0$ means that there are constants k_0 and ε_1 (independent of ε) so that

$$|f(\varepsilon)| \leq k_0|\varphi(\varepsilon)| \quad \text{for} \quad \varepsilon_0 < \varepsilon < \varepsilon_1.$$

We say that 'f is big Oh of φ' as $\varepsilon \downarrow \varepsilon_0$.

2. $f = o(\varphi)$ as $\varepsilon \downarrow \varepsilon_0$ means that for every positive δ there exists an ε_2 (independent of ε) so that

$$|f(\varepsilon)| \leq \delta |\varphi(\varepsilon)| \quad \text{for} \quad \varepsilon_0 < \varepsilon < \varepsilon_2.$$

We say that 'f is little oh of φ' as $\varepsilon \downarrow \varepsilon_0$.

Sometimes $f = o(\phi)$ is written as $f \ll \varphi$.

THEOREM 1.2.
1. If

$$\lim_{\varepsilon \downarrow \varepsilon_0} \frac{f(\varepsilon)}{\varphi(\varepsilon)} = L,$$

where $-\infty < L < \infty$, then $f = O(\varphi)$ as $\varepsilon \downarrow \varepsilon_0$.
2. If

$$\lim_{\varepsilon \downarrow \varepsilon_0} \frac{f(\varepsilon)}{\varphi(\varepsilon)} = 0,$$

then $f = o(\varphi)$ as $\varepsilon \downarrow \varepsilon_0$.

This theorem follows directly from the definition of a limit. The following properties are clear from the definitions, but since they are often used, we state them explicitly:

(1) $f = O(1)$ as $\varepsilon \downarrow \varepsilon_0$ if and only if f is bounded as $\varepsilon \downarrow \varepsilon_0$.
(2) $f = o(1)$ as $\varepsilon \downarrow \varepsilon_0$ if and only if $f \to 0$ as $\varepsilon \downarrow \varepsilon_0$.
(3) $f = o(\varphi)$ as $\varepsilon \downarrow \varepsilon_0$ implies $f = O(\varphi)$ as $\varepsilon \downarrow \varepsilon_0$ (but not necessarily vice versa).

In this thesis we only use $\varepsilon_0 = 0$. Therefore, if it is stated that something is $O(1)$ or $O(\varepsilon)$ it is always meant in the limit $\varepsilon \downarrow 0$.

As mentioned before, in this study we want to approximate solutions to partial differential equations. An important question is what we mean by an approximation in this respect. For example, one approach is saying that a series which converges to a function is an approximation of that function. A Taylor expansion is an example of this. However, another possibility is to demand that the error of the approximation should be of a smaller order than the approximation itself. We take the latter approach in this study.

DEFINITION 1.3. Given $f(\varepsilon)$ and $g(\varepsilon)$, we say that $g(\varepsilon)$ is an *asymptotic approximation* to $f(\varepsilon)$ as $\varepsilon \downarrow \varepsilon_0$ whenever $f = g + o(g)$ as $\varepsilon \downarrow \varepsilon_0$. In this case we write $f \sim g$ as $\varepsilon \downarrow \varepsilon_0$.

An asymptotic approximation to a function is not necessarily unique. To create some structure in this non uniqueness, we will define so called asymptotic sequences and asymptotic expansions.

DEFINITION 1.4. The functions $\varphi_0(\varepsilon), \varphi_1(\varepsilon), \ldots$ form an *asymptotic sequence*, or are *well ordered*, as $\varepsilon \downarrow \varepsilon_0$ if and only if $\varphi_{m+1} = o(\varphi_m)$ as $\varepsilon \downarrow \varepsilon_0$ for all m.

DEFINITION 1.5. If $\varphi_0(\varepsilon), \varphi_1(\varepsilon), \ldots$ is an asymptotic sequence, then $f(\varepsilon)$ has an *asymptotic expansion* to n terms, with respect to this sequence, if and only if

$$f = \sum_{k=0}^{m} a_k \varphi_k + o(\varphi_m) \quad \text{for} \quad m = 0, 1, \ldots, n \quad \text{as} \quad \varepsilon \downarrow \varepsilon_0,$$

where the a_k are independent of ε. In this case we write

$$f \sim a_0\varphi(\varepsilon) + a_1\varphi(\varepsilon) + \cdots + a_n\varphi_n(\varepsilon) \quad \text{as} \quad \varepsilon \downarrow \varepsilon_0. \tag{1.4}$$

The φ_k are called the *scale* or *gauge* or *basis* functions.

If the scale functions are given, the expansion is unique. To see this, assume we have

$$f \sim a_0\varphi_0(\varepsilon) + a_1\varphi_1(\varepsilon) + \cdots .$$

In particular, this means that

$$f = a_0\varphi_0 + o(\varphi_0).$$

Dividing by φ_0 gives

$$a_0 = \lim_{\varepsilon \downarrow \varepsilon_0} \frac{f}{\varphi_0}.$$

Repeating this process yields

$$a_1 = \lim_{\varepsilon \downarrow \varepsilon_0} \frac{f - a_0\varphi_0}{\varphi_1}.$$

We can repeat this to find a_i for every i. Hence, if all these limits exists, and given the scale functions, the asymptotic expansion is unique. In this study the scale functions

$$\varphi_i(\varepsilon) = \varepsilon^i$$

are used. A function f is then approximated as

$$f \sim a_0 + a_1\varepsilon + a_2\varepsilon^2 + O(\varepsilon^3).$$

An important observation is that including more terms in the asymptotic expansion does not necessarily make the approximation better, as is the case with Taylor expansions. The reason is that the asymptotic expansion only makes a statement about the approximation in the limit of $\varepsilon \downarrow \varepsilon_0$, while adding more terms says something about the limit $n \to \infty$. In fact, an asymptotic expansion of a function does not need to converge as $n \to \infty$ and if it does, it does not need to converge to the function it is representing. For examples, consider Section 3.8 in Bender and Orszag (1999).

A good thing about an asymptotic expansion is that it is possible that if only a small number of terms are included, an asymptotic expansion may produce a smaller error than a series converging to the function does. We refer to Section 1.4.2 in Holmes (2013) for an example where this is the case. Also if, for example, a solution of a partial differential equation is asymptotically approximated as in (1.4) and a_0 and a_1 can be calculated analytically, we know what the solution does in the regimes of $O(\varphi_0)$ and $O(\varphi_1)$. The availability of computing power makes numerics very powerful. It provides a manner of approximating solutions to higher order nonlinear partial differential equations. However, sometimes asymptotic approximations can give different insights in solutions. Therefore, applying both numerical and asymptotic methods to the same problem can be beneficial.

CHAPTER 2

The model

In Chapter 1 some basic terminology of coastal research and perturbation methods were introduced. In this chapter the model is described by first describing the domain and then the equations governing the model. As stated before, the model is a highly idealized one dimensional version of hydrodynamics in the tidal channel connecting the 'Marsdiep' with the 'Vlie', in the Dutch Wadden Sea. The starting point of the derivation of the model equations are the depth averaged shallow water equations derived in Appendix C.

2.1. Domain

Although the starting point of this chapter are two dimensional equations, it is useful to have the three dimensional geometry of the domain in mind. Figure 2.1 shows the geometry of the tidal channel used in this study. Figure 2.1a depicts the cross section, Figure 2.1b the along channel side view and Figure 2.1c the top view. Also, the placement of the x_1, x_2 and x_3 axis is presented in Figure 2.1. The x_1 axis is pointing in the along channel direction and is located at the undisturbed water level, the x_2 axis is in the direction of the width of the channel and the x_3 axis is pointing upwards. The origin is placed in the middle of the channel at the location of the undisturbed water level.

The width of the main channel, b_c, is taken constant. It is also possible to derive the cross sectionally averaged shallow water equations for the case where b_c may vary. This is more realistic and only a minor change in the derivation. However, as a first step in understanding the effect of the momentum sink we will consider the simple case in which b_c is constant. A trapezoidal shape is chosen for the cross section of the channel because it makes it possible to have a mass storage and momentum sink of the same order, as will be seen in Chapter 3. To shorten notation in the calculations, denote as in Figure 2.1,

$$\Omega(t) = \Omega_1(t) \cup \Omega_2 \cup \Omega_3(t),$$

with

$$\Omega_1(t) = \left[-\frac{b(t)}{2}, -\frac{b_c}{2}\right], \quad \Omega_2 = \left[-\frac{b_c}{2}, \frac{b_c}{2}\right], \Omega_3(t) = \left[\frac{b_c}{2}, \frac{b(t)}{2}\right].$$

With 'the width of the channel' we will henceforth mean 'the width of the wetted part of the channel'. The width of the channel, b, is dependent on ξ and hence on t and x_1 and reads

$$b = b_{\max} - \frac{b_{\max} - b_c}{2q}\left(1 - \frac{\xi}{d_f}\right), \tag{2.1}$$

where q is a parameter that determines the steepness of the flats (higher q means steeper flats). A derivation of equation (2.1) is given in the gray box below.

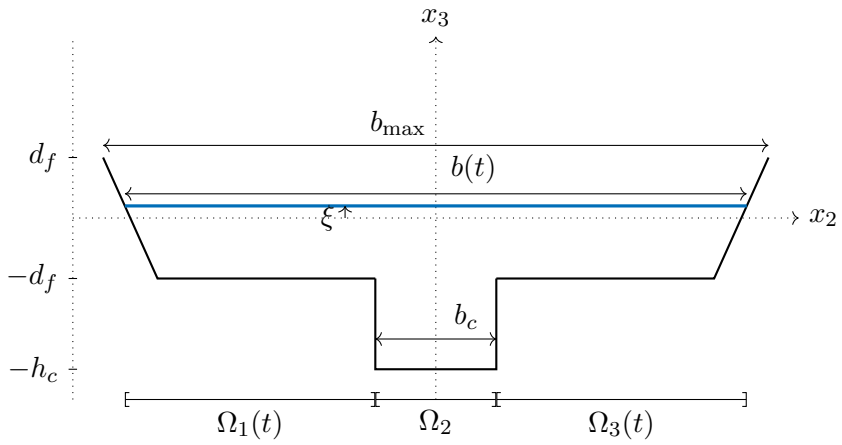

(a) Cross sectional view

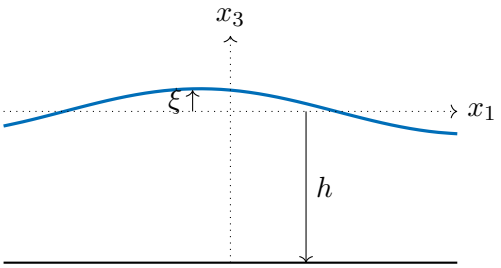

(b) Along channel view

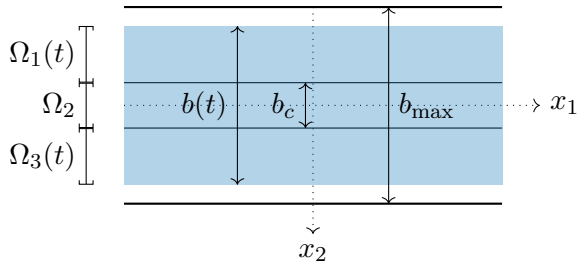

(c) Top view

Figure 2.1. The geometry of the tidal channel, where $b_{\max}$ is the maximal width of the channel, $b(t)$ is the width of the wetted part of the channel, b_c is the width of the main channel, d_f is the distance from the undisturbed water level to the bottom of the flats (which will be specified later), h is the distance from the undisturbed water level to the bottom of the channel (which equals h_c in the main channel), $\Omega_1(t)$ is the interval of the wetted part of the left tidal flat, Ω_2 is the interval of the main channel, $\Omega_3(t)$ is the interval of the wetted part of the right tidal flat and ξ is the free surface elevation.

The trapezoidal shape is an approximation of the bottom of the flats described by a exponential function. Let $q \in \mathbb{R}_{\geq 1}$ be a number greater than 1 and let

$$f : \left[\frac{b_c}{2}, \frac{b_{\max}}{2}\right] \to [-d_f, d_f], \quad x_2 \mapsto 2d_f \left(\frac{2x_2 - b_c}{b_{\max} - b_c}\right)^q - d_f,$$

be the function (dashed lines in Figure 2.2) that discribes the bottom of the tidal flat at the positive x_2 side of the channel (in the figure the right hand side). We approximate the

bottom of the flats with a trapezoidal geometry such that the slope at $x_2 = b_{\max}/2$ equals the slope of f at this point.

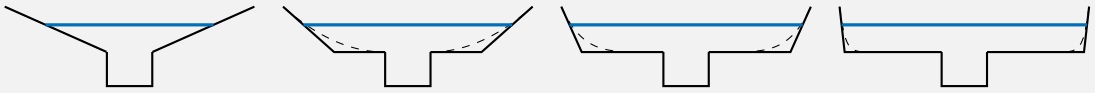

Figure 2.2. The geometry of the cross section for different values of q. Starting at the left figure the values used are $q = 1$, $q = 2$, $q = 5$ and $q = 20$ respectively.

The derivative of f at $x_2 = b_{\max}/2$ equals

$$\frac{\partial f}{\partial x_2}\left(\frac{b_{\max}}{2}\right) = \frac{4d_f q}{b_{\max} - b_c}.$$

The linear function describing the steep part of the flats becomes

$$x_2 \mapsto \frac{4d_f q}{b_{\max} - b_c} x_2 + d_f - \frac{2d_f q b_{\max}}{b_{\max} - b_c},$$

with inverse

$$x_3 \mapsto \frac{b_{\max} - b_c}{4d_f q}(x_3 - d_f) + \frac{b_{\max}}{2}. \tag{2.2}$$

The inverse of the function describing the steep part of the flats, (2.2), evaluated at $\xi(t, x)$ is half the width of the channel at (t, x). This gives equation (2.1) for the width of the channel.

2.2. The depth averaged shallow water equations

The depth averaged shallow water equations in conservative form read

$$\frac{\partial \xi}{\partial t} + \frac{\partial (\xi + h)\bar{u}_1}{\partial x_1} + \frac{\partial (\xi + h)\bar{u}_2}{\partial x_2} = 0, \tag{2.3}$$

$$\frac{\partial (\xi + h)\bar{u}_1}{\partial t} + \frac{\partial (\xi + h)\bar{u}_1\bar{u}_1}{\partial x_1} + \frac{\partial (\xi + h)\bar{u}_1\bar{u}_2}{\partial x_2} = -g(\xi + h)\frac{\partial \xi}{\partial x_1} - \frac{\tau}{\rho}, \tag{2.4}$$

$$0 = \frac{\partial \xi}{\partial x_2}, \tag{2.5}$$

where, $x = (x_1, x_2)$ is the spatial coordinate, t the time coordinate, $\bar{u}_1$ (m s^{-1}) the depth averaged horizontal velocity in the along channel direction, $\bar{u}_2$ (m s^{-1}) the depth averaged horizontal velocity in the cross section, ξ (m) the free surface elevation, ρ (kg m^{-3}) the density, g (m s^{-2}) the gravitational acceleration, f (s^{-1}) the Coriolis parameter and τ (N m^{-2}) is the bottom friction in the x_1 direction.

The assumptions made in the derivation of the depth averaged shallow water equations are as follows (see also Appendix C).

1. The density, ρ, is considered to be constant[1].
2. The depth of the channel is much smaller than both the width and length of the channel. This assumption is sometimes referred to as the shallow water approximation. Consequences of this approximation are the following.
   - The vertical momentum balance reduces to a hydrostatic equilibrium. This means that we assume a balance between the vertical pressure gradient force and gravity.
   - The only relevant stresses are those that act in the x_1 and x_2 direction. In fact, we only consider stresses at the seabed, so wind stress is also neglected.
3. The width of the channel is much smaller than its length. This implies the following.
   - The change of velocity in the x_2 direction following a particle, Du_2/Dt, is neglected.
   - The stresses that act in the x_2 direction are neglected.
   - Coriolis forces are ignored.
4. The stresses that result from averaging over depth are ignored. In this chapter also the stresses that result from averaging over the width will be ignored. This implies that boundary layers at the bottom and sides of the channel are ignored; the so called no-slip condition is not imposed.

Many of the assumptions come down to the fact that the only relevant differences occur in the horizontal directions such that it is defendable to reduce the three dimensions of the system to two. Assumptions 2 and 3 and their implications are based on Appendix A of Parker (1984) and the dimensional analysis of Winant (2007).

We impose the following conditions to the system. The boundary conditions 1 and 2 were already used in the derivation of the depth averaged shallow water equations.

1. Water particles at the free surface will stay at the free surface and particles at the seabed will stay at the seabed. These are kinematic boundary conditions. Thus, processes like evaporation, precipitation and percolation are ignored.

[1] It is possible to derive shallow water equations without this assumption, but we do not do this.

2. The pressure at the free surface, $x_3 = \xi$, equals the atmospheric pressure, p_a, that is assumed to be constant.
3. The average volume of water over one tidal period remains the same. This is a condition for the residual free surface elevation.
4. It is assumed that the water loses all its speed in the x_1 direction when it comes on the tidal flats. So specifically, if $x_2 \in \Omega(t) \backslash \Omega_2$ then $\bar{u}_1(t, x_1, x_2) = 0$ for all t and x_1. In fact, we assume that $\bar{u}_1$ is discontinuous in x_2 at $x_2 = \pm b_c/2$. This makes physically sense, since h is also discontinuous at $x_2 = \pm b_c/2$.
5. There is no tidally averaged transport of water through the channel. Also, there are no sluises or rivers connected to the channel that induce a residual current.
6. From both the right and the left a M_2 free surface elevation signal enters the channel. Internally generated overtides and additional M_2 can be decomposed in a signal traveling to the right and one traveling to the left. The signal traveling to the right is zero on the left boundary and the signal traveling to the left is zero on the right boundary. The situation is schematically depicted in Figure 2.3.

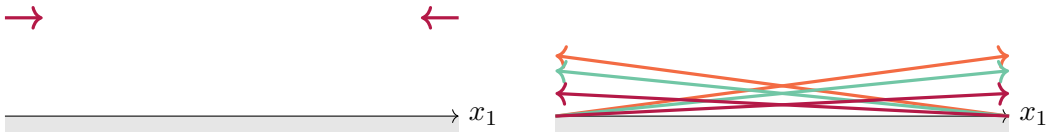

(a) Prescribed M_2

(b) Internally generated overtides and M_2

Figure 2.3. Schematic representation of the boundary conditions for: (a) incoming free surface elevation M_2 and (b) internally generated overtides and additional M_2. The arrows represent the direction the wave is propagating and the starting point of the arrow represents the amplitude of the wave. In the right figure the fact that the arrows go up represents the fact that the amplitude of those waves are zero at the boundaries but become nonzero inside the channel.

Before we proceed with the derivation of the cross sectionally averaged shallow water equations, a remark. The following two sections ignore some mathematical difficulties in order to maintain a storyline. An example of such a ignored mathematical difficulty is that h and $\bar{u}_1$ are discontinuous at the boundary of Ω_2 and hence do not have well defined derivatives in those points. The readers that are interested in the details of the calculations are invited to read Appendix A.

2.3. Cross sectionally averaged continuity equation

In the preceding section the depth averaged shallow water equations were stated together with the assumptions and conditions we impose on the model. From the depth averaged shallow water equations the cross sectionally averaged shallow water equations are derived in this and the next section. The goal of this section is deriving a continuity equation that is dependent of the cross sectionally averaged current velocity, $\hat{u}_1$, and no longer of $\bar{u}_1$. In order to achieve this we integrate equation (2.3) over the width of the main channel, Ω_2. From the lateral momentum balance (2.5), follows that ξ does not depend on x_2. Furthermore, remember that we consider b_c constant. Integrating equation (2.3) over Ω_2 yields

$$\begin{aligned} 0 &= \int_{\Omega_2} \frac{\partial \xi}{\partial t}\, dx_2 + \int_{\Omega_2} \frac{\partial (\xi + h)\bar{u}_1}{\partial x_1}\, dx_2 + \int_{\Omega_2} \frac{\partial (\xi + h)\bar{u}_2}{\partial x_2}\, dx_2 \\ &= \frac{\partial \xi}{\partial t} \int_{\Omega_2} dx_2 + \frac{\partial}{\partial x_1}\left[(\xi + h_c)\int_{\Omega_2} \bar{u}_1\, dx_2\right] + (\xi + h)\bar{u}_2(t, x_1, b_c/2) - (\xi + h)\bar{u}_2(t, x_1, -b_c/2) \\ &= b_c \frac{\partial \xi}{\partial t} + b_c \frac{\partial (\xi + h_c)\hat{u}_1}{\partial x_1} + (\xi + h)\bar{u}_2(t, x_1, b_c/2) - (\xi + h)\bar{u}_2(t, x_1, -b_c/2), \end{aligned} \tag{2.6}$$

where we denoted the cross sectionally averaged current velocity as,

$$\hat{u}_1 = \frac{1}{b_c}\int_{\Omega_2} \bar{u}_1\, dx_2,$$

where $\bar{u}_1$ still denotes the depth averaged current velocity. We wish to interpret the last two terms in (2.6). Therefore, note that

$$(\xi + h)\bar{u}_2(t, x_1, \pm b_c/2)$$

has dimension $\mathrm{m^2 s^{-1}} = \mathrm{m^3 s^{-1} m^{-1}}$. So $(\xi + h)\bar{u}_2(t, x_1, \pm b_c/2)$ is the amount of water ($\mathrm{m^3}$) that flows through the boundary per second ($\mathrm{s^{-1}}$) per unit length ($\mathrm{m^{-1}}$).

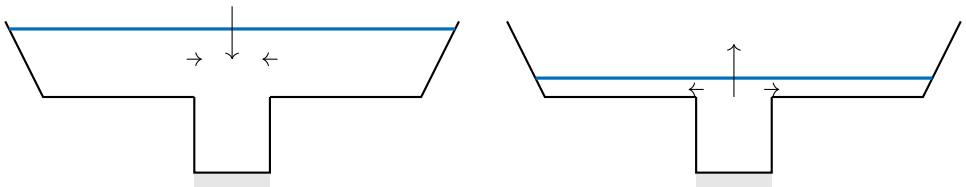

(a) Falling tide (b) Rising tide

Figure 2.4. Water flowing on and from the flats when the tide rises and falls, respectively.

In order to determine what the amount of water flowing through the boundaries is (per second per unit length), we analyse the continuity equation at the left and right tidal flat, $\Omega_1(t)$ and $\Omega_3(t)$. First, consider the right tidal flat and integrate over equation (2.3) over $\Omega_3(t)$. Since the

the length of the interval Ω_3 equals $\frac{1}{2}(b-b_c)$ this yields

$$\int_{\Omega_3} \frac{\partial \xi}{\partial t}\, dx_2 + \int_{\Omega_3} \frac{\partial (\xi+h)\bar{u}_1}{\partial x_1}\, dx_2 + \int_{\Omega_3} \frac{\partial (\xi+h)\bar{u}_2}{\partial x_2}\, dx_2 = 0,$$
$$\frac{1}{2}(b-b_c)\frac{\partial \xi}{\partial t} + 0 + (\xi+h)\bar{u}_2(t,x_1,b(t)/2) - (\xi+h)\bar{u}_2(t,x_1,b_c/2) = 0.$$

The depth, $\xi + h$, is zero at $x_2 = b(t)/2$, which gives us

$$(\xi+h)\bar{u}_2(t,x_1,b_c/2) = \frac{1}{2}(b-b_c)\frac{\partial \xi}{\partial t}. \tag{2.7}$$

Equation (2.7) makes physically sense; when water comes on the flat, water needs to be pushed up to fit on the flat. We repeat the procedure for $\Omega_1(t)$ to find

$$(\xi+h)\bar{u}_2(t,x_1,-b_c/2) = -\frac{1}{2}(b-b_c)\frac{\partial \xi}{\partial t}. \tag{2.8}$$

It also shows that $\bar{u}_2$ at $x_2 = b_c/2$ is positive if the water level rises and negative if the water level drops. The opposite is true at the other side of the main channel where $x_2 = -b_c/2$. This is depicted in Figure 2.4. Plugging equations (2.7) and (2.8) in equation (2.6) yields

$$b_c\frac{\partial \xi}{\partial t} + b_c\frac{\partial (\xi+h)\hat{u}_1}{\partial x_1} + (b-b_c)\frac{\partial \xi}{\partial t} = 0.$$

After dividing by b_c, we arrived at the cross sectionally averaged continuity equation

$$\frac{b}{b_c}\frac{\partial \xi}{\partial t} + \frac{\partial (\xi+h_c)\hat{u}_1}{\partial x_1} = 0. \tag{2.9}$$

2.4. Cross sectionally averaged momentum balance

Similar as in the previous section, the goal is to obtain a momentum balance dependent of $\hat{u}_1$ and independent of $\bar{u}_1$. For that reason we integrate equation (2.4) over the width of the main channel Ω_2.,

$$\int_{\Omega_2} \frac{\partial (\xi+h)\bar{u}_1}{\partial t}\, dx_2 + \int_{\Omega_2} \frac{\partial (\xi+h)\bar{u}_1\bar{u}_1}{\partial x_1}\, dx_2 + \int_{\Omega_2} \frac{\partial (\xi+h)\bar{u}_1\bar{u}_2}{\partial x_2}\, dx_2$$
$$+ \int_{\Omega_2} g(\xi+h)\frac{\partial \xi}{\partial x_1}\, dx_2 + \int_{\Omega_2} \frac{\tau}{\rho}\, dx_2 = 0.$$

The first term and last two terms become

$$\int_{\Omega_2} \frac{\partial (\xi+h)\bar{u}_1}{\partial t}\, dx_2 = b_c\frac{\partial (\xi+h_c)\hat{u}_1}{\partial t} = b_c(\xi+h_c)\frac{\partial \hat{u}_1}{\partial t} + b_c\hat{u}_1\frac{\partial \xi}{\partial t},$$
$$\int_{\Omega_2} g(\xi+h)\frac{\partial \xi}{\partial x_1}\, dx_2 = b_c g(\xi+h_c)\frac{\partial \xi}{\partial x_1},$$
$$\int_{\Omega_2} \frac{\tau}{\rho}\, dx_2 = b_c\frac{\hat{\tau}}{\rho},$$

where $\hat{\tau}$ is the bottom friction averaged over the width of the main channel,

$$\hat{\tau} = \frac{1}{b_c}\int_{\Omega_2} \tau\, dx_2.$$

For the second term we make an assumption similar as Assumption 4 in Section 2.2. That is, the stresses that arise from averaging over the width are neglected. To make this statement

more specific, denote $\bar{u}_\alpha = \hat{u}_\alpha + \tilde{\tilde{u}}_\alpha$, for $\alpha \in \{1, 2\}$, where $\bar{u}_\alpha$ is the depth averaged velocity, $\hat{u}_\alpha$ the cross sectionally averaged velocity and $\tilde{\tilde{u}}_\alpha$ the difference between those two. We assume[2]

$$\int_{\Omega_2} \frac{\partial(\xi + h_c)\bar{u}_1\bar{u}_1}{\partial x_1}\, dx_2 = b_c \frac{\partial(\xi + h_c)\hat{u}_1\hat{u}_1}{\partial x_1}.$$

Specifically, it is assumed that

$$\frac{\partial}{\partial x_1} \int_{\Omega_2} \tilde{\tilde{u}}_1 \tilde{\tilde{u}}_1\, dx_2 = 0. \tag{2.10}$$

Hence, using the continuity equation (2.9) the second term can be expressed as follows,

$$\begin{aligned}\int_{\Omega_2} \frac{\partial(\xi + h_c)\bar{u}_1\bar{u}_1}{\partial x_1}\, dx_2 = b_c \frac{\partial(\xi + h_c)\hat{u}_1\hat{u}_1}{\partial x_1} &= \hat{u}_1 b_c \frac{\partial(\xi + h_c)\hat{u}_1}{\partial x_1} + b_c(\xi + h_c)\hat{u}_1 \frac{\partial \hat{u}_1}{\partial x_1} \\ &= -\hat{u}_1 b \frac{\partial \xi}{\partial t} + b_c(\xi + h_c)\hat{u}_1 \frac{\partial \hat{u}_1}{\partial x_1}.\end{aligned}$$

For the third term we obtain

$$\int_{\Omega_2} \frac{\partial(\xi + h)\bar{u}_1\bar{u}_2}{\partial x_2}\, dx_2 = (\xi + h)\bar{u}_2\bar{u}_1(t, x_1, b_c/2) - (\xi + h)\bar{u}_2\bar{u}_1(t, x_1, -b_c/2).$$

What would $(\xi + h)\bar{u}_2\bar{u}_1$ be on $\partial\Omega_2$? It represents $\bar{u}_1$ times the amount of water per unit length per second transported through the boundary of the main channel. That is, the amount of momentum in the x_1 direction transported through the boundary of the main channel. The quantity of the lateral transport depends on if the water level rises or drops, as was found in equations (2.7) and (2.8). We consider the situation at the right boundary, $x_2 = b_c/2$. The same reasoning (with some additional minuses) will hold on the other side. If the water level rises, $\bar{u}_2$ is positive at $x_2 = b_c/2$; water flows towards the flats. In that case, a water column moving through $x_2 = b_c/2$, from the main channel towards the flats, still has its velocity $\bar{u}_1$ in the x_1 direction. So momentum is transported from the main channel to the flats. When the water level drops, water moves from the flats to the main channel. On the flats there is no along channel momentum, as it is dissipated due to friction. Therefore, no momentum comes back if the water level drops. So no momentum is transported from the flats to the main channel; the flats act as a momentum sink. This gives, together with equations (2.7) and (2.8), a motivation to take

$$(\xi + h)\bar{u}_2\bar{u}_1(t, x_1, \pm b_c/2) = \pm\frac{1}{2}(b - b_c)\hat{u}_1 \mathcal{H}\left(\frac{\partial \xi}{\partial t}\right)\frac{\partial \xi}{\partial t},$$

where $\mathcal{H}$ is the Heaviside (or step) function defined as[3]

$$\mathcal{H}(x) = \begin{cases} 1 & \text{if } x > 0 \\ \frac{1}{2} & \text{if } x = 0 \\ 0 & \text{if } x < 0 \end{cases}. \tag{2.11}$$

The third term thus becomes

$$\int_{\Omega_2} \frac{\partial(\xi + h)\bar{u}_1\bar{u}_2}{\partial x_2}\, dx_2 = (b - b_c)\hat{u}_1 \mathcal{H}\left(\frac{\partial \xi}{\partial t}\right)\frac{\partial \xi}{\partial t}.$$

[2]For this one time, the average of a product equals the product of the averages.

[3]Note that it does not matter what $\mathcal{H}(0)$ is since $\mathcal{H}\left(\frac{\partial \xi}{\partial t}\right)\frac{\partial \xi}{\partial t}$ vanishes when $\frac{\partial \xi}{\partial t} = 0$.

Combining all of this yields

$$b_c(\xi+h_c)\frac{\partial \hat{u}_1}{\partial t}+\left(\hat{u}_1(b_c-b)+(b-b_c)\hat{u}_1\mathcal{H}\left(\frac{\partial \xi}{\partial t}\right)\right)\frac{\partial \xi}{\partial t}+b_c(\xi+h_c)\hat{u}_1\frac{\partial \hat{u}_1}{\partial x_1}+b_c g(\xi+h_c)\frac{\partial \xi}{\partial x_1}+b_c\frac{\hat{\tau}}{\rho}=0.$$

Divide by $b_c(\xi+h_c)$ and use $1-\mathcal{H}(x)=\mathcal{H}(-x)$, to obtain

$$\frac{\partial \hat{u}_1}{\partial t}+\hat{u}_1\frac{\partial \hat{u}_1}{\partial x_1}-\frac{b-b_c}{b_c(\xi+h_c)}\hat{u}_1\mathcal{H}\left(-\frac{\partial \xi}{\partial t}\right)\frac{\partial \xi}{\partial t}+g\frac{\partial \xi}{\partial x_1}+\frac{\hat{\tau}}{\rho(\xi+h_c)}=0.$$

The term

$$-\frac{b-b_c}{b_c(\xi+h_c)}\hat{u}_1\mathcal{H}\left(-\frac{\partial \xi}{\partial t}\right)\frac{\partial \xi}{\partial t}$$

is only nonzero when the water lever drops, $\frac{\partial \xi}{\partial t}<0$. This might seem strange since the term was connected to momentum which is only transported when the water level rises, $\frac{\partial \xi}{\partial t}>0$. This asks for a somewhat different interpretation of this term. The following interpretation is based on Dronkers (1964). Consider first the case where the water level drops. Water columns on the flat move into the main channel. There they should accelerate from zero velocity to the velocity $\hat{u}_1$ in the main channel. The term we are talking about has dimension m s^{-2} and is exactly this acceleration. When the water level rises, water particles flow from the main channel towards the flats. The water particles need to 'accelerate' from their $\hat{u}_1$ velocity towards zero. The force that slows the particles down to zero is the friction and we do not need the term we were talking about and is thus put to zero. With a linear bottom friction parameterization as in, for example, Parker (1984), Zimmerman (1982) or Friedrichs and Aubrey (1994), $\hat{\tau}$ is expressed as

$$\hat{\tau}=\rho r\hat{u}_1,$$

where r (m s^{-1}) is a friction parameter. Thus the cross sectionally averaged shallow water momentum balance reads

$$\frac{\partial \hat{u}_1}{\partial t}+\hat{u}_1\frac{\partial \hat{u}_1}{\partial x_1}-\frac{b-b_c}{b_c}\frac{\hat{u}_1}{\xi+h_c}\mathcal{H}\left(-\frac{\partial \xi}{\partial t}\right)\frac{\partial \xi}{\partial t}+g\frac{\partial \xi}{\partial x_1}-\frac{r\hat{u}_1}{\xi+h_c}=0, \tag{2.12}$$

and for completeness, the continuity equation we found earlier is[4]

$$\frac{b}{b_c}\frac{\partial \xi}{\partial t}+\frac{\partial(\xi+h_c)\hat{u}_1}{\partial x_1}=0. \tag{2.13}$$

[4]Remember that b_c is taken constant. If b_c is not constant the continuity equation changes a little bit (see for example Alebregtse et al. (2015) or Parker (1984))

CHAPTER 3

Model Analysis

In Chapter 2 a model for the hydrodynamics in a tidal channel was formulated. The equations (2.12) and (2.13) governing the model are hard, if at all possible, to solve analytically. In this chapter we will use some knowledge about shallow water waves to find the dominant balances that allows us to construct approximate solutions of equations (2.12) and (2.13) by means of asymptotic methods.

3.1. Scaling

In this section we will scale the variables in equations (2.12) and (2.13). Therefor, we first introduce four, to be determined, scaling parameters $\mathcal{U}$ (m s^{-1}), $\mathcal{Z}$ (m), $\mathcal{L}$ (m), $\mathcal{T}$ (s) and four dimensionless variables,

$$\tilde{u} = \frac{u}{\mathcal{U}}, \quad \tilde{\xi} = \frac{\xi}{\mathcal{Z}}, \quad \tilde{x} = \frac{x}{\mathcal{L}} \quad \text{and} \quad \tilde{t} = \frac{t}{\mathcal{T}}.$$

The goal now is to identify a small parameter, ε, and to find expressions for the scaling parameters $\mathcal{U}$, $\mathcal{Z}$, $\mathcal{L}$ and $\mathcal{T}$. Substituting the scaling parameters in the momentum balance, (2.12), and the continuity equation, (2.13), yields

$$\frac{\mathcal{U}}{\mathcal{T}}\frac{\partial \tilde{u}}{\partial \tilde{t}} + \frac{\mathcal{U}^2}{\mathcal{L}}\tilde{u}\frac{\partial \tilde{u}}{\partial \tilde{x}} - \frac{\mathcal{U}\mathcal{Z}}{\mathcal{T}}\frac{b-b_c}{b_c}\frac{\tilde{u}}{h_c\left(1+\frac{\mathcal{Z}}{h_c}\tilde{\xi}\right)}\mathcal{H}\left(-\frac{\partial \tilde{\xi}}{\partial \tilde{t}}\right)\frac{\partial \tilde{\xi}}{\partial \tilde{t}} + \frac{g\mathcal{Z}}{\mathcal{L}}\frac{\partial \tilde{\xi}}{\partial \tilde{x}} + \frac{r\mathcal{U}}{h_c}\frac{\tilde{u}}{\left(1+\frac{\mathcal{Z}}{h_c}\tilde{\xi}\right)} = 0,$$

$$\frac{\mathcal{Z}}{\mathcal{T}}\frac{b}{b_c}\frac{\partial \tilde{\xi}}{\partial \tilde{t}} + \frac{\mathcal{U}h_c}{\mathcal{L}}\frac{\partial\left(\frac{\mathcal{Z}}{h_c}\tilde{\xi}+1\right)\tilde{u}}{\partial \tilde{x}} = 0.$$

Dividing the momentum balance by $\mathcal{U}/\mathcal{T}$ and the continuity equation by $\mathcal{Z}/\mathcal{T}$ gives

$$\frac{\partial \tilde{u}}{\partial \tilde{t}} + \frac{\mathcal{T}\mathcal{U}}{\mathcal{L}}\tilde{u}\frac{\partial \tilde{u}}{\partial \tilde{x}} - \frac{\mathcal{Z}}{h_c}\frac{b-b_c}{b_c}\frac{\tilde{u}}{1+\frac{\mathcal{Z}}{h_c}\tilde{\xi}}\mathcal{H}\left(-\frac{\partial \tilde{\xi}}{\partial \tilde{t}}\right)\frac{\partial \tilde{\xi}}{\partial \tilde{t}} + \frac{\mathcal{T}g\mathcal{Z}}{\mathcal{L}\mathcal{U}}\frac{\partial \tilde{\xi}}{\partial \tilde{x}} + \frac{r\mathcal{T}}{h_c}\frac{\tilde{u}}{\left(1+\frac{\mathcal{Z}}{h_c}\tilde{\xi}\right)} = 0, \tag{3.1}$$

$$\frac{b}{b_c}\frac{\partial \tilde{\xi}}{\partial \tilde{t}} + \frac{\mathcal{T}\mathcal{U}h_c}{\mathcal{L}\mathcal{Z}}\frac{\partial\left(\frac{\mathcal{Z}}{h_c}\tilde{\xi}+1\right)\tilde{u}}{\partial \tilde{x}} = 0. \tag{3.2}$$

Define

$$\varepsilon = \frac{\mathcal{Z}}{h_c}, \tag{3.3}$$

which is assumed to be small. At the end of this section this parameter will be given a physical interpretation. With this small dimensionless parameter, ε, it is possible to use asymptotic

methods. To find expressions for the scaling parameters, $\mathcal{U}$, $\mathcal{Z}$, $\mathcal{L}$ and $\mathcal{T}$, we assume it is possible to choose these parameters such that[1]

$$\tilde{u}, \tilde{\xi}, \frac{\partial \tilde{u}}{\partial \tilde{t}}, \frac{\partial \tilde{u}}{\partial \tilde{x}}, \frac{\partial \tilde{\xi}}{\partial \tilde{t}}, \frac{\partial \tilde{\xi}}{\partial \tilde{x}}, \frac{\partial \tilde{u}\tilde{\xi}}{\partial \tilde{x}} = O(1) \text{ as } \varepsilon \downarrow 0.$$

The idea of this assumption is that it is possible to choose $\mathcal{U}$ and $\mathcal{Z}$ such that they are representable values for u and ξ and that $\mathcal{L}$ and $\mathcal{T}$ are representable values for the length and time scale on which changes in u and ξ occur. Also, we assume

$$\frac{b}{b_c} = O(1) \text{ as } \varepsilon \downarrow 0.$$

Next, let's look at the continuity equation (3.2). With the parameter ε as in (3.3), this reads

$$\underbrace{\frac{b}{b_c}\frac{\partial \tilde{\xi}}{\partial \tilde{t}}}_{O(1)} + \frac{\mathcal{T}\mathcal{U}}{\mathcal{L}} \underbrace{\frac{1}{\varepsilon}\left(\frac{\partial \tilde{u}}{\partial \tilde{x}} + \varepsilon \frac{\partial \tilde{\xi}\tilde{u}}{\partial \tilde{x}}\right)}_{O(\varepsilon^{-1})} = 0.$$

The first term is of $O(1)$ and the second term, divided by $\mathcal{T}\mathcal{U}/\mathcal{L}$, is of $O(\varepsilon^{-1})$. Since the first and second term must balance, it must be that[2]

$$\frac{\mathcal{T}\mathcal{U}}{\mathcal{L}} = O(\varepsilon).$$

We choose $\mathcal{T}\mathcal{U}/\mathcal{L} = \varepsilon$. Substituting this in the momentum balance, (3.1) we find

$$\frac{\partial \tilde{u}}{\partial \tilde{t}} + \varepsilon \tilde{u}\frac{\partial \tilde{u}}{\partial \tilde{x}} - \varepsilon \frac{b - b_c}{b_c}\frac{\tilde{u}}{1+\varepsilon\tilde{\xi}}\mathcal{H}\left(-\frac{\partial \tilde{\xi}}{\partial \tilde{t}}\right)\frac{\partial \tilde{\xi}}{\partial \tilde{t}} + \frac{\mathcal{T}g\mathcal{Z}}{\mathcal{L}\mathcal{U}}\frac{\partial \tilde{\xi}}{\partial \tilde{x}} + \frac{r\mathcal{T}}{h_c}\frac{\tilde{u}}{(1+\varepsilon\tilde{\xi})} = 0. \tag{3.4}$$

Since for $|x| \leq 1$,

$$\frac{1}{1+x} = \sum_{n=0}^{\infty}(-x)^n, \tag{3.5}$$

the last term reads, for $|\varepsilon\tilde{\xi}| < 1$,

$$\frac{r\mathcal{T}}{h_c}\frac{\tilde{u}}{(1+\varepsilon\tilde{\xi})} = \frac{r\mathcal{T}}{h_c}\tilde{u}\left(1 - \varepsilon\tilde{\xi} + O(\varepsilon^2)\right). \tag{3.6}$$

The terms that are (potentially) $O(1)$ in equation (3.4) must balance and therefore, using the expression (3.6),

$$\underbrace{\frac{\partial \tilde{u}}{\partial \tilde{t}}}_{O(1)} + \frac{\mathcal{T}g\mathcal{Z}}{\mathcal{L}\mathcal{U}}\frac{\partial \tilde{\xi}}{\partial \tilde{x}} + \frac{r\mathcal{T}}{h_c}\tilde{u} = 0. \tag{3.7}$$

The first term is $O(1)$. At least one of the other terms must be balanced with the first one since otherwise Equation (3.7) would reduce to

$$\frac{\partial \tilde{u}}{\partial \tilde{t}} = 0,$$

[1]Note that this implies that ε goes to zero by $h_c \to \infty$ and retaining $\mathcal{Z}$ bounded. Because otherwise, if $\varepsilon \downarrow 0$ by $\mathcal{Z} \downarrow 0$, $\tilde{\xi} = \xi/\mathcal{Z} \neq O(1)$ as $\varepsilon \downarrow 0$.

[2]Since $O(f)O(g) = O(fg)$.

which would mean that $\tilde{u}$ hardly changes in time. If one of the two terms is of lower order that $O(1)$, for example $O(\varepsilon^{-1})$, it can not be balanced by something else and must equal zero. It follows that for the second and third terms there remain three options. The first option is that the second term is $O(1)$ and the third term $O(\varepsilon)$. The second option is that the second term is $O(\varepsilon)$ and the third term $O(1)$ and the third option is that they are both $O(1)$. In the first (second) option the change in $\tilde{u}$ is mainly due to the pressure gradient (friction). We take the third option and thus consider a tidal channel where the pressure gradient and the friction are of equal order. In fact we choose:

$$\frac{\mathcal{T}g\mathcal{Z}}{\mathcal{L}\mathcal{U}} = 1 \quad \text{and} \quad \tilde{r} = \frac{r\mathcal{T}}{h_c} = O(1).$$

Substituting this in (3.4) yields

$$\frac{\partial \tilde{u}}{\partial \tilde{t}} + \varepsilon \tilde{u}\frac{\partial \tilde{u}}{\partial \tilde{x}} - \varepsilon \frac{b-b_c}{b_c}\frac{\tilde{u}}{1+\varepsilon\tilde{\xi}}\mathcal{H}\left(-\frac{\partial \tilde{\xi}}{\partial \tilde{t}}\right)\frac{\partial \tilde{\xi}}{\partial \tilde{t}} + \frac{\partial \tilde{\xi}}{\partial \tilde{x}} + \frac{\tilde{r}\tilde{u}}{(1+\varepsilon\tilde{\xi})} = 0. \tag{3.8}$$

We still need to do something with

$$\frac{b-b_c}{b_c} = O(1).$$

The total the term is chosen[3] to be $O(1)$, however, we did not specify any possible $O(\varepsilon)$ terms inside it. Recall from Chapter 2, that

$$b = b_{\max} - \frac{b_{\max}-b_c}{2q}\left(1 - \frac{\mathcal{Z}}{d_f}\tilde{\xi}\right),$$

and thus

$$\frac{b-b_c}{b_c} = \frac{b_{\max}-b_c}{b_c} - \frac{b_{\max}-b_c}{b_c}\frac{1}{2q}\left(1 - \frac{\mathcal{Z}}{d_f}\tilde{\xi}\right).$$

The ratio of the width of the tidal flats and width of the main channel is denoted by β. We assume this to be of $O(1)$, that is,

$$\beta = \frac{b_{\max}-b_c}{b_c} = O(1).$$

Furthermore, the part of the flats where the depth decreases is assumed to be narrow and steep (large q, see Figure 2.2),

$$\frac{1}{2q} = O(\varepsilon).$$

In fact, we assume

$$\frac{1}{2q} = \alpha\varepsilon,$$

for some $\alpha = O(1)$. With the parameters α and β we find

$$\frac{b-b_c}{b_c} = \beta - \beta\alpha\varepsilon\left(1 - \frac{\mathcal{Z}}{d_f}\tilde{\xi}\right),$$

and thus

$$\frac{b}{b_c} = 1 + \beta - \beta\alpha\varepsilon\left(1 - \frac{\mathcal{Z}}{d_f}\tilde{\xi}\right).$$

[3] $\frac{b-b_c}{b_c} = \frac{b}{b_c} - 1 = O(1)$ as $O(f) + O(g) = O(|f| + |g|)$.

Lastly, we choose $\mathcal{Z}/d_f = O(1)$ and in fact,

$$\frac{\mathcal{Z}}{d_f} = 1.$$

In the rest of this chapter only terms up to $O(\varepsilon)$ are considered. For that reason terms that are $O(\varepsilon^2)$ are already neglected. The scaled momentum balance and continuity equation now read

$$\frac{\partial u}{\partial t} + \varepsilon u \frac{\partial u}{\partial x} - \varepsilon\beta \frac{u}{1+\varepsilon\xi} \mathcal{H}\left(-\frac{\partial \xi}{\partial t}\right) \frac{\partial \xi}{\partial t} + \frac{\partial \xi}{\partial x} + \frac{ru}{1+\varepsilon\xi} = 0, \tag{3.9}$$

$$(1 + \beta - \beta\alpha\varepsilon(1-\xi))\frac{\partial \xi}{\partial t} + \frac{\partial}{\partial x}\left[(1+\varepsilon\xi)u\right] = 0, \tag{3.10}$$

where all variables and parameters are dimensionless and tildes are omitted in the notation. In the next section we approximate solutions of these equations. Note that a part of the mass storage, $\frac{b}{b_c}\frac{\partial \xi}{\partial t}$, and the momentum sink term are both $O(\varepsilon)$. If $1/2q$ was $O(1)$ it is was not possible. This is the motivation for the trapezoidal cross section chosen in Chapter 2.

When interpreting solutions, it is useful to be able transform the scaled dimensionless variables back to there original dimensional form. For this we need actual values for $\mathcal{U}$, $\mathcal{Z}$, $\mathcal{L}$ and $\mathcal{T}$. Up to now only some ratios between them are chosen. Remember we chose

$$\frac{\mathcal{T} g \mathcal{Z}}{\mathcal{L}\mathcal{U}} = \frac{\mathcal{T}\mathcal{U} h_c}{\mathcal{L}\mathcal{Z}} = 1, \tag{3.11}$$

from which it follows that

$$\mathcal{U} = \mathcal{Z}\sqrt{\frac{g}{h_c}}. \tag{3.12}$$

So choosing a value for $\mathcal{Z}$ or $\mathcal{U}$ fixes the other. Now, we choose $\mathcal{Z}$ to be a typical value for the tidal amplitude in the western parts of the Wadden Sea,

$$\mathcal{Z} = 1 \text{ m}.$$

This makes $\mathcal{U}$ to be close to 1 m s^{-1}, which seems representable for current velocities in the Wadden Sea. Furthermore, we already chose

$$\frac{\mathcal{T}\mathcal{U}}{\mathcal{L}} = \frac{\mathcal{Z}}{h_c} = \varepsilon$$

and therefore, substituting (3.12),

$$\frac{\mathcal{T}}{\mathcal{L}} = \frac{1}{\sqrt{g h_c}}.$$

From which it follows that when we choose $\mathcal{T}$ or $\mathcal{L}$ the other one is determined. The typical velocity of a shallow water wave is $\sqrt{g h_c}$ m s^{-1}. This equals the wavelength times the frequency of the wave. Therefore, when we choose

$$\mathcal{T} = \frac{1}{\sigma},$$

that is, the period divided by 2π, it follows that

$$\mathcal{L} = \frac{\sqrt{g h_c}}{\sigma},$$

that is, wavelength divided by 2π. These seem representable values for the time and length scale on which changes in u and ξ occur. Note that

$$\varepsilon = \frac{\mathcal{T}\mathcal{U}}{\mathcal{L}} = \frac{\mathcal{U}}{\sqrt{gh_c}},$$

which is commonly known as the *Froude number*. In the Wadden Sea this number is close to 10^{-1}.

3.2. Asymptotic approximation

Equations (3.9) and (3.10) is a system of two coupled nonlinear first order partial differential equations. In this section we will find an asymptotic approximation to the solution. Each nonlinear term contains the small parameter, ε, which makes it possible to construct approximate solutions as an asymptotic expansion in the small parameter ε.

Substituting the Taylor expansion of $1/(1+\varepsilon\xi)$ as in (3.5), in equations (3.9) and (3.10) yields

$$\frac{\partial u}{\partial t} + \varepsilon u \frac{\partial u}{\partial x} - \varepsilon\beta u \sum_{n=0}^{\infty} (-\varepsilon\xi)^n \mathcal{H}\left(-\frac{\partial \xi}{\partial t}\right) \frac{\partial \xi}{\partial t} + \frac{\partial \xi}{\partial x} + ru \sum_{n=0}^{\infty} (-\varepsilon\xi)^n = 0, \tag{3.13}$$

$$(1+\beta-\beta\alpha\varepsilon(1-\xi))\frac{\partial \xi}{\partial t} + \frac{\partial}{\partial x}\left[(1+\varepsilon\xi)u\right] = 0. \tag{3.14}$$

Next, expand u and ξ asymptotically as[4]

$$u = u_0 + \varepsilon u_1 + O(\varepsilon^2) \quad \text{and} \quad \xi = \xi_0 + \varepsilon\xi_1 + O(\varepsilon^2)$$

and substitute these in (3.13) and (3.14). Then collecting terms that are $O(1)$ and not $o(1)$ gives a problem called the $O(1)$ problem. Collecting the terms that are $O(\varepsilon)$ and not $o(\varepsilon)$ gives a problem called the $O(\varepsilon)$ problem. Regarding the Heaviside function $\mathcal{H}$, note that

$$\lim_{\varepsilon\downarrow 0} \mathcal{H}\left(-\frac{\partial \xi}{\partial t}\right) = \lim_{\varepsilon\downarrow 0} \begin{cases} 1 & \text{if} \quad \frac{\partial \xi}{\partial t} \le 0 \\ 0 & \text{if} \quad \frac{\partial \xi}{\partial t} > 0 \end{cases} = \begin{cases} 1 & \text{if} \quad \frac{\partial \xi_0}{\partial t} \le 0 \\ 0 & \text{if} \quad \frac{\partial \xi_0}{\partial t} > 0 \end{cases} = \mathcal{H}\left(-\frac{\partial \xi_0}{\partial t}\right).$$

Since $\mathcal{H}\left(-\frac{\partial \xi_0}{\partial t}\right)$ is finite and nonzero,

$$\mathcal{H}\left(-\frac{\partial \xi}{\partial t}\right) = O(1) \quad \text{and} \quad \mathcal{H}\left(-\frac{\partial \xi}{\partial t}\right) \neq o(1) \quad \text{as} \quad \varepsilon \downarrow 0.$$

Therefore, $\mathcal{H}\left(-\frac{\partial \xi}{\partial t}\right)$ fits with the $O(1)$ terms and, in that regiem, equals[5] $\mathcal{H}\left(-\frac{\partial \xi_0}{\partial t}\right)$.

3.2.1. The $O(1)$ problem.

Collecting terms in (3.13) and (3.14) that are of $O(1)$ (and not $o(1)$) yield the $O(1)$ problem,

$$\frac{\partial u_0}{\partial t} + \frac{\partial \xi_0}{\partial x} + ru_0 = 0, \tag{3.15}$$

$$(1+\beta)\frac{\partial \xi_0}{\partial t} + \frac{\partial u_0}{\partial x} = 0, \tag{3.16}$$

with boundary conditions such that from both sides of the channel a free surface elevation M_2 signal propagates into the channel. The M_2 signal entering on the left and moving to the right has amplitude z_1 and phase zero. The M_2 signal entering on the right and moving to the left has amplitude z_2 and phase θ.

The solution to the $O(1)$ problem is summarized in Section 3.2.1.1. If $z_1 = z_2$ and $\theta = 0$ half of the channel represents a semi-enclosed basin and the waves coming from the other half represent

[4] Apologies for reintroducing the subscript notation; u_1 is no longer the velocity in the x_1 direction.

[5] This is an approximation. We neglect the $O(\varepsilon)$ contribution of ξ to the Heaviside function.

the reflected waves. To find the solutions, first an equation for ξ_0 is derived. This is done by differentiating the first equation with respect to x and the second one with respect to t,

$$\frac{\partial^2 u_0}{\partial x \partial t} + \frac{\partial^2 \xi_0}{\partial x^2} + r\frac{\partial u_0}{\partial x} = 0,$$
$$(1+\beta)\frac{\partial^2 \xi_0}{\partial t^2} + \frac{\partial^2 u_0}{\partial t \partial x} = 0.$$

Substituting the first one into the second one and using equation (3.19) yields

$$(1+\beta)\frac{\partial^2 \xi_0}{\partial t^2} - \frac{\partial^2 \xi_0}{\partial x^2} + (1+\beta)r\frac{\partial \xi_0}{\partial t} = 0. \tag{3.17}$$

With solutions to this equations u_0 can be obtained from equation (3.18). This is a homogenous damped wave equation and since the boundary conditions are such that only M_2 waves enter the channel, we may assume ξ_0 to be a superposition of two waves, in fact we expect ξ_0 to be of the form[6]

$$\xi_0(x,t) = |\hat{\xi}_0(x)|\cos(\phi_{\hat{\xi}_0}(x) - t) = \mathrm{Re}\left\{\hat{\xi}_0(x)e^{-it}\right\},$$

with $\hat{\xi}_0(x) = |\hat{\xi}_0(x)|e^{i\phi_{\hat{\xi}_0}(x)}$ independent of t. Substituting this in the wave equation yields

$$\mathrm{Re}\left\{-(1+\beta)\hat{\xi}_0 e^{-it}\right\} - \mathrm{Re}\left\{\frac{\partial^2 \hat{\xi}_0}{\partial x^2}e^{-it}\right\} + r\mathrm{Re}\left\{-i(1+\beta)\hat{\xi}_0 e^{-it}\right\} = 0$$

and thus

$$\mathrm{Re}\left\{-\left(\frac{\partial^2 \hat{\xi}_0}{\partial x^2} + (1+\beta)(1+ir)\hat{\xi}_0\right)e^{-it}\right\} = 0.$$

Since this holds for all $t \in [t_0, t_0 + 2\pi]$,

$$\frac{\partial^2 \hat{\xi}_0}{\partial x^2} + \underbrace{(1+\beta)(1+ir)}_{k^2}\hat{\xi}_0 = 0.$$

The general solution of this ordinary differential equation (ode) is given by

$$\hat{\xi}_0(x) = Ae^{ikx} + Be^{-ikx},$$

with $k^2 = (1+\beta)(1+ir)$ and we will determine $A, B \in \mathbb{C}$ by looking what they represent in the equation for the free surface elevation. Note,

$$\xi_0(x,t) = \mathrm{Re}\left\{\left(Ae^{ikx} + Be^{-ikx}\right)e^{-it}\right\} = \mathrm{Re}\left\{\underbrace{Ae^{i(kx-t)}}_{\text{wave to the right}} + \underbrace{Be^{-i(kx+t)}}_{\text{wave to the left}}\right\}.$$

The wave coming from the left and moving to the right is represented by $Ae^{i(kx-t)}$. To see this, choose a position on the wave to follow during some time interval (for example at the crust). This means keeping the phase, $kx-t$, constant. Then, if we let time t increase, x should become larger as well to keep $kx - t$ constant. Therefore, every fixed point on the wave will move to the right (x increases) and we say that the wave moves to the right. With the same reasoning $Be^{-i(kx+t)}$ represents the wave moving to the left. The amplitude of the wave going to the right is

$$|Ae^{i(kx-t)}| = |A|e^{-\mathrm{Im}\{kx-t\}} = |A|e^{-\mathrm{Im}\{k\}x}.$$

[6]We neglect the transient term. This is permitted since (3.17) is a damped wave equation and the tides exists longer than the period in which the transient terms are significant (few days).

We choose this to equal $z_1 \in \mathbb{R}_{>0}$ at the left boundary, $x = -L/2$. Then

$$|A|e^{\mathrm{Im}\{k\}\frac{L}{2}} = z_1.$$

We make the choice of A to be positive and its argument to be zero ($A \in \mathbb{R}$), which results in

$$A = z_1 e^{-\mathrm{Im}\{k\}\frac{L}{2}}.$$

For the wave to the left we do the same, but now forcing the amplitude at the right ($x = L/2$) to be $z_2 \in \mathbb{R}_{>0}$. This yields

$$|B|e^{\mathrm{Im}\{kx+t\}} = |B|e^{\mathrm{Im}\{k\}\frac{L}{2}} = z_2.$$

We choose B to be

$$B = z_2 e^{-\mathrm{Im}\{k\}\frac{L}{2}+i\theta}.$$

For $u_0(x,t)$ a similar form as for ξ_0 is expected,

$$u_0(x,t) = \mathrm{Re}\left\{\hat{u}_0(x)e^{-it}\right\},$$

with $\hat{u}_0(x) \in \mathbb{C}$ independent of t. Substituting this in (3.18) gives

$$\mathrm{Re}\left\{-i\hat{u}_0 e^{-it}\right\} + \mathrm{Re}\left\{\frac{\partial\hat{\xi}_0}{\partial x}e^{-it}\right\} + r\mathrm{Re}\left\{\hat{u}_0 e^{-it}\right\} = \mathrm{Re}\left\{\left(\hat{u}_0(r-i) + \frac{\partial\hat{\xi}_0}{\partial x}\right)e^{-it}\right\} = 0.$$

Again this must hold for every $t \in [t_0, t_0+T]$. Hence, using the expression found for $\hat{\xi}_0$,

$$\hat{u}_0(x) = \frac{1}{i-r}\frac{\partial\hat{\xi}_0}{\partial x} = \frac{ik}{i-r}\left(Ae^{ikx} - Be^{-ikx}\right) = \gamma\left(Ae^{ikx} - Be^{-ikx}\right),$$

with $\gamma = \frac{ik}{i-r}$. This solves the $O(1)$ problem.

3.2.1.1. *Summary.*
To summarize, the $O(1)$ problem is

$$\frac{\partial u_0}{\partial t} + \frac{\partial\xi_0}{\partial x} + ru_0 = 0, \tag{3.18}$$

$$(1+\beta)\frac{\partial\xi_0}{\partial t} + \frac{\partial u_0}{\partial x} = 0, \tag{3.19}$$

with boundary conditions such that from both sides of the channel a free surface elevation M_2 signal propagates into the channel. The M_2 signal entering on the left and moving to the right has amplitude z_1 and phase zero. The M_2 signal entering on the right and moving to the left has amplitude z_2 and phase θ. The solution found to this problem is

$$\xi_0(x,t) = \mathrm{Re}\left\{\hat{\xi}_0(x)e^{-it}\right\} \quad \text{with} \quad \hat{\xi}_0(x) = Ae^{ikx} + Be^{-ikx},$$
$$u_0(x,t) = \mathrm{Re}\left\{\hat{u}_0(x)e^{-it}\right\} \quad \text{with} \quad \hat{u}_0(x) = \gamma\left(Ae^{ikx} - Be^{-ikx}\right),$$

with

$$A = z_1 e^{-\mathrm{Im}\{k\}\frac{L}{2}}, \qquad B = z_2 e^{-\mathrm{Im}\{k\}\frac{L}{2}+i\theta},$$
$$k^2 = (1+\beta)(1+ir), \quad \gamma = \frac{ik}{i-r}.$$

3.2.2. The $O(\varepsilon)$ problem.

Collecting terms in (3.13) and (3.14) that are of $O(\varepsilon)$ (and not $o(\varepsilon)$) yield the $O(\varepsilon)$ problem,

$$\frac{\partial u_1}{\partial t} + \frac{\partial \xi_1}{\partial x} + r u_1 = \underbrace{-u_0 \frac{\partial u_0}{\partial x}}_{\text{I}} \underbrace{+ r u_0 \xi_0}_{\text{II}} \underbrace{+ \beta u_0 \frac{\partial \xi_0}{\partial t} \mathcal{H}\left(-\frac{\partial \xi_0}{\partial t}\right)}_{\text{III}}, \tag{3.20}$$

$$(1+\beta)\frac{\partial \xi_1}{\partial t} + \frac{\partial u_1}{\partial x} = \underbrace{-\frac{\partial}{\partial x}(u_0 \xi_0)}_{\text{IV}} \underbrace{+ \beta\alpha(1-\xi_0)\frac{\partial \xi_0}{\partial t}}_{\text{V}}. \tag{3.21}$$

The boundary conditions of the $O(\varepsilon)$ problem are such that for every individual M_{2m} ($m \geq 1$) signal of ξ_1, the amplitude of the part that is propagating to the left is zero on the right boundary and the amplitude of the part propagating to the right is zero on the left boundary. These internally generated overtides may radiate freely at the boundaries.

The $O(\varepsilon)$ problem is the same as the $O(1)$ problem but inhomogeneous. Every term in the inhomogeneity (forcing) comes from nonlinear terms in equations (3.13) and (3.14). In Table 3.1 the physical origin of every nonlinear term is presented. In this study we are mainly concerned about the effects of the momentum sink, term III.

Term	Origin
I	advection of momentum
II	bottom friction
III	**momentum sink**
IV	divergence of mass
V	mass storage

Table 3.1. Origin of inhomogeneous (forcing) terms.

The solution to the $O(\varepsilon)$ problem is summarized in Section 3.2.2.1. To find the solutions, we take the same route as we did in the $O(1)$ problem. That is, derive from equations (3.35) and (3.36) a single second order damped wave equation for ξ_1 by differentiating equation (3.35) and (3.36) with respect to x and t respectively:

$$\frac{\partial^2 u_1}{\partial t \partial x} + \frac{\partial^2 \xi_1}{\partial x^2} + r\frac{\partial u_1}{\partial x} = -\frac{1}{2}\frac{\partial^2}{\partial x^2}\left(u_0^2\right) + r\frac{\partial}{\partial x}\left(u_0\xi_0\right) + \frac{\partial}{\partial x}\left(\beta u_0 \frac{\partial \xi_0}{\partial t}\mathcal{H}\left(-\frac{\partial \xi_0}{\partial t}\right)\right),$$

$$(1+\beta)\frac{\partial^2 \xi_1}{\partial t^2} + \frac{\partial^2 u_1}{\partial x \partial t} = -\frac{\partial^2}{\partial x \partial t}(u_0\xi_0) + \beta\alpha\frac{\partial^2 \xi_0}{\partial t^2} - \frac{\beta\alpha}{2}\frac{\partial^2}{\partial t^2}\left(\xi_0^2\right).$$

Substituting into each other and using (3.36) gives a pde for ξ_1,

$$(1+\beta)\frac{\partial^2 \xi_1}{\partial t^2} - \frac{\partial^2 \xi_1}{\partial x^2} + (1+\beta)r\frac{\partial \xi_1}{\partial t} = \underbrace{-\frac{\partial^2}{\partial x \partial t}\left(u_0\xi_0\right)}_{\text{IV}} \underbrace{+ 2\beta\alpha\frac{\partial^2 \xi_0}{\partial t^2} - \beta\alpha\frac{\partial^2}{\partial t^2}\left(\xi_0^2\right)}_{\text{V}} \underbrace{+ \frac{1}{2}\frac{\partial^2}{\partial x^2}\left(u_0^2\right)}_{\text{I}}$$
$$\underbrace{- 2r\frac{\partial}{\partial x}\left(u_0\xi_0\right)}_{\text{II}} \underbrace{- \frac{\partial}{\partial x}\left(\beta u_0 \frac{\partial \xi_0}{\partial t}\mathcal{H}\left(-\frac{\partial \xi_0}{\partial t}\right)\right)}_{\text{III}}. \tag{3.22}$$

The origin of the terms are as in Table 3.1. This is the same wave equation as arose in the $O(1)$ problem but now inhomogeneous. In the derivation of the $O(1)$ problem we argued that because of the boundary conditions ξ_0 must have a particular form. When we substituted this form in the damped wave equation an ode arose for $\hat{\xi}_0$. Solving this ode gave us ξ_0, which in turn allowed us to solve $\hat{u}_0$ and hence u_0. So to do the same, the question is now what form to choose for ξ_1 to substitute in (3.22). In order to decide this, let's take a closer look at the inhomogeneity of the wave equation. The first thing to notice is that, by the choice of the boundary conditions of the $O(1)$ problem, every term is periodic in time. Therefore, it must be possible to write the inhomogeneity as a Fourier series. Term III consists of the discontinuous Heaviside function, $\mathcal{H}$. Hence, the Fourier series must contain an infinite amount of terms[7]. As the inhomogeneity can be written as Fourier series containing every harmonic, we may assume ξ_1 to be of the form

$$\xi_1(x,t) = \sum_{m=0}^{\infty} \mathrm{Re}\left\{\hat{\xi}_{1,m}(x)e^{-imt}\right\}. \tag{3.23}$$

It is now our goal to find $\hat{\xi}_{1,m}$ for every m. The term for $m = 0$ is special in the sense that it is time independent. Moreover, it represents the average value of ξ_1 over one tidal period, denoted by $\bar{\xi}_1$ and also called the residual or M_0 component. Concretely, since, for $m \neq 0$,

$$\frac{1}{2\pi}\int_{t_0}^{t_0+2\pi} \mathrm{Re}\left\{\hat{\xi}_{1,m}e^{-imt}\right\}\, dt = 0,$$

we have

$$\bar{\xi}_1 = \frac{1}{2\pi}\int_{t_0}^{t_0+2\pi} \sum_{m=0}^{\infty} \mathrm{Re}\left\{\hat{\xi}_{1,m}e^{-imt}\right\}\, dt = \mathrm{Re}\left\{\hat{\xi}_{1,0}\right\}.$$

From equations (3.35) and (3.36) it is clear that if ξ_1 contains every harmonic, u_1 also does. Therefore, u_1 is assumed to be of the form

$$u_1(x,t) = \sum_{m=1}^{\infty} \mathrm{Re}\left\{\hat{u}_{1,m}(x)e^{-imt}\right\} + \bar{u}_1(x). \tag{3.24}$$

By the observation that $\bar{\xi}_1$ and $\bar{u}_1$ are the average values of ξ_1 and u_1 over a tidal period, they can already be calculated. Integrating equation (3.36) over one tidal period yields

$$\frac{1}{2\pi}\int_{t_0}^{t_0+2\pi} \left[(1+\beta)\frac{\partial \xi_1}{\partial t} + \frac{\partial u_1}{\partial x} + \frac{\partial}{\partial x}(u_0\xi_0) - \beta\alpha\frac{\partial \xi_0}{\partial t} + \frac{\beta\alpha}{2}\frac{\partial \xi_0^2}{\partial t}\right] dt = 0. \tag{3.25}$$

Since ξ_0, ξ_1 and ξ_0^2 have period 2π, this reduces to

$$\frac{\partial \bar{u}_1}{\partial x} = -\frac{1}{2\pi}\int_{t_0}^{t_0+2\pi} \frac{\partial}{\partial x}(u_0\xi_0)\, dt = -\frac{\partial}{\partial x}(\overline{u_0\xi_0}).$$

Hence, there is a constant $\nu \in \mathbb{C}$ such that $\bar{u}_1 = -\overline{u_0\xi_0} + \nu$. We take the constant $\nu = 0$. That is, we choose, as stated in Section 2.2, that there is no external residual flow due to, for example, a river or sluises. Therefore, after some algebraic manipulations (see Calculation 1 in Appendix B),

$$\bar{u}_1 = -\overline{u_0\xi_0} = \underbrace{-\frac{1}{2}|\hat{u}_0||\hat{\xi}_0|\cos(\phi_{\hat{u}_0} - \phi_{\hat{\xi}_0})}_{\text{IV}}. \tag{3.26}$$

[7]Since a finite sum of continuous functions is continuous.

The residual free surface elevation, $\bar{\xi}_1$, is found with the same method. Integrating (3.35) over one tidal period yields

$$\int_{t_0}^{t_0+2\pi} \left[\frac{\partial u_1}{\partial t} + \frac{\partial \xi_1}{\partial x} + r u_1 + u_0 \frac{\partial u_0}{\partial x} - r u_0 \xi_0 - \beta u_0 \frac{\partial \xi_0}{\partial t} \mathcal{H}\left(-\frac{\partial \xi_0}{\partial t} \right) \right] dt = 0. \tag{3.27}$$

After writing the Heaviside function as a Fourier series (see Calculation 2 in Appendix B) and some algebraic manipulations (see Calculations 3 in Appendix B) this reduces to

$$\frac{\partial \bar{\xi}_1}{\partial x} = -\frac{1}{4} \frac{\partial |\hat{u}_0|^2}{\partial x} + |\hat{u}_0||\hat{\xi}_0| \left(r \cos(\phi_{\hat{u}_0} - \phi_{\hat{\xi}_0}) - \frac{\beta}{4} \sin(\phi_{\hat{u}_0} - \phi_{\hat{\xi}_0}) \right). \tag{3.28}$$

Integrating gives,

(3.29)

$$\begin{aligned} \bar{\xi}_1(x) &= a_3 + \int_{a_4}^{x} \left[-\frac{1}{4} \frac{\partial |\hat{u}_0|^2}{\partial x} + |\hat{u}_0||\hat{\xi}_0| \left(r \cos(\phi_{\hat{u}_0} - \phi_{\hat{\xi}_0}) - \frac{\beta}{4} \sin(\phi_{\hat{u}_0} - \phi_{\hat{\xi}_0}) \right) \right] ds \\ &= a_3 - \underbrace{\frac{1}{4} \left(|\hat{u}_0(x)|^2 - |\hat{u}_0(a_4)|^2 \right)}_{\text{I}} + \int_{a_4}^{x} \Big[|\hat{u}_0||\hat{\xi}_0| \Big(\underbrace{r \cos(\phi_{\hat{u}_0} - \phi_{\hat{\xi}_0})}_{\text{II}} \underbrace{- \frac{\beta}{4} \sin(\phi_{\hat{u}_0} - \phi_{\hat{\xi}_0})}_{\text{III}} \Big) \Big] ds, \end{aligned}$$

for a_3 and $a_4 \in \mathbb{C}$. We know found both $\bar{\xi}_1$ and $\bar{u}_1$. We proceed with finding $\hat{\xi}_{1,m}$ for $m \neq 0$. Writing $\mathcal{H}$ as a Fourier series (see Calculation 2 of Appendix B), substituting (3.23) and the solutions of ξ_0 and u_0 in equation (3.22) and preforming some algebraic manipulations (see Calculation 4 of Appendix B), the result is

(3.30)

$$\begin{aligned} &\sum_{m=0}^{\infty} \mathrm{Re} \left\{ - \left(\frac{\partial^2 \hat{\xi}_{1,m}}{\partial x^2} + (1+\beta) m (m + ri) \hat{\xi}_{1,m} \right) e^{-imt} \right\} \\ &\quad = \mathrm{Re} \left\{ \underbrace{- 2\beta\alpha \hat{\xi}_0}_{\text{V}} e^{-it} \right\} + \mathrm{Re} \left\{ \Big(\underbrace{i \frac{\partial}{\partial x} (\hat{u}_0 \hat{\xi}_0)}_{\text{IV}} \underbrace{+ \frac{1}{4} \frac{\partial^2}{\partial x^2} (\hat{u}_0^2)}_{\text{I}} \underbrace{- r \frac{\partial}{\partial x} (\hat{u}_0 \hat{\xi}_0)}_{\text{II}} \underbrace{+ 2\beta\alpha \hat{\xi}_0^2}_{\text{V}} \Big) e^{-i2t} \right\} \\ &\qquad \underbrace{+ \frac{1}{4} \frac{\partial^2}{\partial x^2} (|\hat{u}_0|^2)}_{\text{I}} \underbrace{- r \mathrm{Re} \left\{ \frac{\partial}{\partial x} (\hat{u}_0 \hat{\xi}_0^*) \right\}}_{\text{II}} \underbrace{- \frac{\beta}{4} \mathrm{Re} \left\{ \frac{\partial}{\partial x} (i \hat{u}_0 \hat{\xi}_0^*) \right\} - \sum_{m=1}^{\infty} \mathrm{Re} \left\{ \frac{\partial p_m}{\partial x} e^{-imt} \right\}}_{\text{III}}, \end{aligned}$$

where

$$p_m = \frac{i\beta}{2} \left(c_{2+m}^* \hat{u}_0^* \hat{\xi}_0^* - c_{2-m} \hat{u}_0 \hat{\xi}_0 \right) - c_m^* \beta |\hat{u}_0||\hat{\xi}_0| \sin(\phi_{\hat{u}_0} - \phi_{\hat{\xi}_0})$$

and

$$c_m = \begin{cases} \dfrac{1}{2} & \text{if } m = 0 \\ \dfrac{-i}{m2\pi} \left(1 - e^{-im\pi} \right) e^{-im\phi_{\hat{\xi}_0}} & \text{if } m \neq 0. \end{cases}$$

The (Fourier) coefficients c_m and p_m are such that

$$\mathcal{H}\left(-\frac{\partial \xi_0}{\partial t} \right) = \sum_{m \in \mathbb{Z}} c_m e^{imt} \quad \text{and} \quad \beta u_0 \frac{\partial \xi_0}{\partial t} \mathcal{H}\left(-\frac{\partial \xi_0}{\partial t} \right) = \frac{1}{2} \sum_{m \in \mathbb{Z}} p_m e^{-imt}.$$

For $m = 1$, from equation (3.30) we obtain an ode for $\hat{\xi}_{1,1}$,

$$\frac{\partial^2 \hat{\xi}_{1,1}}{\partial x^2} + \underbrace{(1+\beta)(1+ri)}_{(k_1)^2}\,\hat{\xi}_{1,1} = \underbrace{\underbrace{2\beta\alpha\hat{\xi}_0}_{\text{V}} + \underbrace{\frac{\partial p_1}{\partial x}}_{\text{III}}}_{f_1(x)}.$$

For $m = 2$, we obtain the ode for $\hat{\xi}_{1,2}$,

$$\frac{\partial^2 \hat{\xi}_{1,2}}{\partial x^2} + \underbrace{(1+\beta)2(2+ri)}_{(k_2)^2}\,\hat{\xi}_{1,2} = \underbrace{\underbrace{-i\frac{\partial}{\partial x}(\hat{u}_0\hat{\xi}_0)}_{\text{IV}} \underbrace{-\frac{1}{4}\frac{\partial^2}{\partial x^2}(\hat{u}_0^2)}_{\text{I}} \underbrace{+r\frac{\partial}{\partial x}(\hat{u}_0\hat{\xi}_0)}_{\text{II}} \underbrace{-2\beta\alpha\hat{\xi}_0^2}_{\text{V}} + \underbrace{\frac{\partial p_2}{\partial x}}_{\text{III}}}_{f_2(x)}.$$

For the other m's, $m \geq 3$, we find

$$\frac{\partial^2 \hat{\xi}_{1,m}}{\partial x^2} + \underbrace{(1+\beta)m(m+ri)}_{(k_m)^2}\,\hat{\xi}_{1,m} = \underbrace{\underbrace{\frac{\partial p_m}{\partial x}}_{\text{III}}}_{f_m(x)}.$$

In every case the ode is of the form

$$\frac{\partial^2 \hat{\xi}_{1,m}}{\partial x^2} + (k_m)^2 \hat{\xi}_{1,m} = f_m(x). \tag{3.31}$$

Note that this is of the same form as the ode we found for $\hat{\xi}_0$ but now inhomogeneous. The solution to (3.31) is (see Calculation 5 of Appendix B),

(3.32)

$$\hat{\xi}_{1,m}(x) = \left(C_m + \frac{1}{2ik_m}\int_{a_1}^{x} e^{-ik_m s} f_m(s)\,ds\right) e^{ik_m x} + \left(D_m - \frac{1}{2ik_m}\int_{a_2}^{x} e^{ik_m s} f_m(s)\,ds\right) e^{-ik_m x},$$

with a_1, a_2, C_m, D_m constants such that ξ_1 obeys the boundary conditions specified in the beginning of this section.

The first step in letting the solution of ξ_1 obey the boundary conditions is identifying signals of M_{2m} propagating to the right and left.

$$\sum_{m=1}^{\infty} \text{Re}\left\{\hat{\xi}_{1,m} e^{-imt}\right\} = \sum_{m=1}^{\infty} \text{Re}\Bigg\{ \underbrace{\left(C_m + \frac{1}{2ik_m}\int_{a_1}^{x} e^{-ik_m s} f_m(s)\,ds\right) e^{i(k_m x - mt)}}_{M_{2m} \text{ moving to the right}}$$
$$+ \underbrace{\left(D_m + \frac{1}{2ik_m}\int_{a_2}^{x} e^{i\alpha s} f_m(s)\,ds\right) e^{-i(k_m x + mt)}}_{M_{2m} \text{ moving to the left}} \Bigg\}.$$

The amplitude of the M_{2m} signal propagating to the right is

$$\left| C_m + \frac{1}{2ik_m}\int_{a_1}^{x} e^{-ik_m s} f_m(s)\,ds \right| e^{-\text{Im}\{k_m\}x}.$$

We choose this to be zero at the left boundary, $x = -L/2$. This can be achieved by letting $a_1 = -L/2$ and $C_m = 0$ for all m. Furthermore, we choose the amplitude of the M_{2m} wave

going to the left to be zero at the right boundary $x = L/2$. This happens if $a_2 = L/2$ and $D_m = 0$ for all m. Note that the homogeneous solution of ξ_1 is now the trivial one. We proceed with the residual free surface elevation $\bar{\xi}_1$. The average volume of water in the channel over one tidal period is

$$\int_{-L/2}^{L/2} \left[h + \bar{\xi}_1\right] dx = hL + \int_{-L/2}^{L/2} \bar{\xi}_1 dx.$$

If

$$\int_{-L/2}^{L/2} \bar{\xi}_1 dx \neq 0,$$

the average water level will increase or decrease each tidal period. In the real world there might be mechanisms that can cause an alternation between $\int \bar{\xi}_1 dx > 0$ and $\int \bar{\xi}_1 dx < 0$. However, since in our model ξ and u are assumed to have a period of one tidal period these mechanisms are not possible. A natural assumption is than that the average volume of water over one tidal period remains the same,

$$\int_{-L/2}^{L/2} \bar{\xi}_1 \, dx = 0.$$

To reduce notation, denote

$$E(x) = -\frac{1}{4}\frac{\partial |\hat{u}_0|^2}{\partial x} + |\hat{u}_0||\hat{\xi}_0| \left(r\cos(\phi_{\hat{u}_0} - \phi_{\hat{\xi}_0}) - \frac{\beta}{4}\sin(\phi_{\hat{u}_0} - \phi_{\hat{\xi}_0}) \right).$$

Expression (3.29) then reads

$$\bar{\xi}_1(x) = a_3 + \int_{a_4}^{x} E(s)\, ds.$$

We like to have

$$0 = \int_{-L/2}^{L/2} \bar{\xi}_1 \, dx = \int_{-L/2}^{L/2} a_3 \, dx + \int_{-L/2}^{L/2}\int_{a_4}^{x} E(s)\, ds\, dx = a_3 L + \int_{-L/2}^{L/2}\int_{a_4}^{x} E(s)\, ds\, dx,$$

which happens if

$$a_3 = -\frac{1}{L}\int_{-L/2}^{L/2}\int_{a_4}^{x} E(s)\, ds\, dx.$$

Choosing $a_4 = 0$, gives

$$\bar{\xi}_1(x) = -\frac{1}{L}\int_{-L/2}^{L/2}\int_{0}^{x} E(s)\, ds\, dx + \int_{0}^{x} E(s)\, ds.$$

We now solved

$$\xi_1 = \sum_{m=1}^{\infty} \mathrm{Re}\left\{\hat{\xi}_{1,m} e^{-imt}\right\} + \bar{\xi}_1.$$

The $O(\varepsilon)$ current velocity, u_1, now follows from (3.35). Moving $\frac{\partial \xi_1}{\partial x}$ to the other side,

$$\frac{\partial u_1}{\partial t} + r u_1 = \underbrace{-\frac{1}{2}\frac{\partial}{\partial x}(u_0^2)}_{\text{I}} \underbrace{-\frac{\partial \xi_1}{\partial x}}_{} \underbrace{+ r u_0 \xi_0}_{\text{II}} \underbrace{+ \beta u_0 \frac{\partial \xi_0}{\partial t}\mathcal{H}\left(-\frac{\partial \xi_0}{\partial t}\right)}_{\text{III}}, \tag{3.33}$$

and by substituting (3.24) in equation (3.33) we obtain (see Calculation 6 in Appendix B)
(3.34)

$$\sum_{m=1}^{\infty} \mathrm{Re}\left\{\hat{u}_{1,m}(r-im)e^{-imt}\right\} + r\bar{u}_1$$
$$= \mathrm{Re}\left\{ -\Big(\underbrace{\frac{1}{4}\frac{\partial \hat{u}_0^2}{\partial x}}_{\mathrm{I}} + \frac{\partial \hat{\xi}_{1,2}}{\partial x} \underbrace{-\frac{r}{2}\hat{u}_0\hat{\xi}_0}_{\mathrm{II}} \underbrace{-p_2}_{\mathrm{III}} \Big) e^{-i2t} \right\} + \sum_{\substack{m=1 \\ m\neq 2}}^{\infty} \mathrm{Re}\left\{ -\Big(\frac{\partial \hat{\xi}_{1,m}}{\partial x} \underbrace{-p_m}_{\mathrm{III}} \Big) e^{-imt} \right\} \underbrace{-\frac{r}{2}\mathrm{Re}\left\{\hat{u}_0\hat{\xi}_0^*\right\}}_{\mathrm{II}}.$$

For $m = 2$ we find

$$\hat{u}_{1,2}(r - i2) = -\left(\frac{1}{4}\frac{\partial \hat{u}_0^2}{\partial x} + \frac{\partial \hat{\xi}_{1,2}}{\partial x} - \frac{r}{2}\hat{u}_0\hat{\xi}_0 - p_2 \right),$$

and thus

$$\hat{u}_{1,2} = \frac{1}{2i - r}\Big(\underbrace{\frac{1}{4}\frac{\partial \hat{u}_0^2}{\partial x}}_{\mathrm{I}} + \frac{\partial \hat{\xi}_{1,2}}{\partial x} \underbrace{-\frac{r}{2}\hat{u}_0\hat{\xi}_0}_{\mathrm{II}} \underbrace{-p_2}_{\mathrm{III}} \Big).$$

For the other m's, $m \in \{1, 3, 4, \dots\}$, we find

$$\hat{u}_{1,m} = \frac{1}{im - r}\left(\frac{\partial \hat{\xi}_{1,m}}{\partial x} \underbrace{-p_m}_{\mathrm{III}} \right).$$

This solves the rest of the $O(\varepsilon)$ problem.

We now have an asymptotic approximation to ξ and u from which we can identify an approximation for the overtides, $M_2, M_4, \dots$ and the residual M_0. For example for ξ,

$$\begin{aligned}
\xi &= \xi_0 + \varepsilon\xi_1 + O(\varepsilon^2) \\
&= \mathrm{Re}\left\{\hat{\xi}_0 e^{-it}\right\} + \varepsilon \sum_{m=1}^{\infty} \mathrm{Re}\left\{\hat{\xi}_{1,m} e^{-imt}\right\} + \varepsilon\bar{\xi}_1 + O(\varepsilon^2) \\
&= \underbrace{\mathrm{Re}\left\{ \left(\hat{\xi}_0 + \varepsilon\hat{\xi}_{1,1}\right) e^{-it} \right\}}_{M_2} + \underbrace{\varepsilon \sum_{m=2}^{\infty} \mathrm{Re}\left\{\hat{\xi}_{1,m} e^{-imt}\right\}}_{M_4,\, M_6,\, M_8,\, \dots} + \underbrace{\varepsilon\bar{\xi}_1}_{M_0} + O(\varepsilon^2).
\end{aligned}$$

3.2.2.1. *Summary.*
The $O(\varepsilon)$ problem is

$$\frac{\partial u_1}{\partial t}+\frac{\partial \xi_1}{\partial x}+ru_1=\underbrace{-u_0\frac{\partial u_0}{\partial x}}_{\text{I}}\underbrace{+ru_0\xi_0}_{\text{II}}\underbrace{+\beta u_0\frac{\partial \xi_0}{\partial t}\mathcal{H}\left(-\frac{\partial \xi_0}{\partial t}\right)}_{\text{III}}, \tag{3.35}$$

$$(1+\beta)\frac{\partial \xi_1}{\partial t}+\frac{\partial u_1}{\partial x}=\underbrace{-\frac{\partial}{\partial x}(u_0\xi_0)}_{\text{IV}}\underbrace{+\beta\alpha(1-\xi_0)\frac{\partial \xi_0}{\partial t}}_{\text{V}}, \tag{3.36}$$

with boundary conditions such that for every individual M_{2m} ($m>0$) signal of ξ_1, the amplitude of the part that is propagating to the left is zero on the right boundary and the amplitude of the part propagating to the right is zero on the left boundary. These internally generated overtides may radiate freely at the boundaries.

The non transient solution of this problem is found to be

$$\xi_1(x,t)=\sum_{m=0}^{\infty}\operatorname{Re}\left\{\hat{\xi}_{1,m}(x)e^{-imt}\right\}\quad\text{and}\quad u_1(x,t)=\sum_{m=0}^{\infty}\operatorname{Re}\left\{\hat{u}_{1,m}(x)e^{-imt}\right\}, \tag{3.37}$$

where

$$\hat{\xi}_{1,m}(x)=\frac{e^{ik_mx}}{2ik_m}\int_{-L/2}^{x}e^{-ik_ms}f_m(s)\,ds-\frac{e^{-ik_mx}}{2ik_m}\int_{L/2}^{x}e^{ik_ms}f_m(s)\,ds,$$

$$\hat{u}_{1,m}(x)=\begin{cases}\dfrac{1}{2i-r}\Big(\underbrace{\dfrac{1}{4}\dfrac{\partial \hat{u}_0^2}{\partial x}}_{\text{I}}+\dfrac{\partial \hat{\xi}_{1,2}}{\partial x}\underbrace{-\dfrac{r}{2}\hat{u}_0\hat{\xi}_0}_{\text{II}}\underbrace{-p_2}_{\text{III}}\Big) & \text{if } m=2\\ \dfrac{1}{im-r}\Big(\dfrac{\partial \hat{\xi}_{1,m}}{\partial x}-\underbrace{p_m}_{\text{III}}\Big) & \text{otherwise,}\end{cases}$$

$$\bar{\xi}_1(x)=-\frac{1}{L}\int_{-L/2}^{L/2}\int_0^x E(s)\,ds\,dx+\int_0^x E(s)\,ds,$$

$$\bar{u}_1(x)=\underbrace{-\frac{1}{2}|\hat{u}_0||\hat{\xi}_0|\cos(\phi_{\hat{u}_0}-\phi_{\hat{\xi}_0})}_{\text{IV}},$$

with

$$E(x)=\underbrace{-\frac{1}{4}\frac{\partial|\hat{u}_0|^2}{\partial x}}_{\text{I}}+|\hat{u}_0||\hat{\xi}_0|\Big(\underbrace{r\cos(\phi_{\hat{u}_0}-\phi_{\hat{\xi}_0})}_{\text{II}}-\underbrace{\frac{\beta}{4}\sin(\phi_{\hat{u}_0}-\phi_{\hat{\xi}_0})}_{\text{III}}\Big),$$

$$f_m(x)=\begin{cases}\underbrace{2\beta\alpha\hat{\xi}_0}_{\text{V}}\underbrace{+\dfrac{\partial p_1}{\partial x}}_{\text{III}} & \text{for } m=1\\ \underbrace{-i\dfrac{\partial}{\partial x}(\hat{u}_0\hat{\xi}_0)}_{\text{IV}}\underbrace{-\dfrac{1}{4}\dfrac{\partial^2}{\partial x^2}(\hat{u}_0^2)}_{\text{I}}\underbrace{+r\dfrac{\partial}{\partial x}(\hat{u}_0\hat{\xi}_0)}_{\text{II}}\underbrace{-2\beta\alpha\hat{\xi}_0^2}_{\text{V}}\underbrace{+\dfrac{\partial p_2}{\partial x}}_{\text{III}} & \text{for } m=2\\ \underbrace{\dfrac{\partial p_m}{\partial x}}_{\text{III}} & \text{otherwise}\end{cases}$$

and

$$(k_m)^2 = (1+\beta)m(m+ri),$$
$$p_m(x) = \frac{i\beta}{2}\left(c^*_{2+m}\hat{u}^*_0\hat{\xi}^*_0 - c_{2-m}\hat{u}_0\hat{\xi}_0\right) - c^*_m\beta|\hat{u}_0||\hat{\xi}_0|\sin(\phi_{\hat{u}_0} - \phi_{\hat{\xi}_0}),$$
$$c_m(x) = \frac{-i}{m2\pi}\left(1 - e^{-im\pi}\right)e^{-im\phi_{\hat{\xi}_0}},$$

where the origin of the terms are as in Table 3.2 (same as Table 3.1).

Term	Origin
I	advection of momentum
II	bottom friction
III	**momentum sink**
IV	divergence of mass
V	mass storage

Table 3.2. Origin of inhomogeneous (forcing) terms.

CHAPTER 4

Results

With the solution obtained in Chapter 3 we will investigate the effect of the momentum sink on the distortion characteristics of the free surface elevation and the velocity. First the the solutions for ξ and u are investigated for parameters representable for the Marsdiep-Vlie system (the default model) because from the equations in Sections 3.2.1.1 and 3.2.2.1 it is not directly clear how the solutions for ξ and u look like. Then, we will focus on the contribution of the momentum sink to the solutions. This is done by first calculating the analytical expression for the difference between the solution where the momentum sink is taken into account and the one where it is not. Then, multiple effects of the momentum sink on the hydrodynamics in a tidal channel are presented. This gives an indication of the features that are absent when the momentum sink term is neglected.

4.1. Default configuration

The goal of this section is to explore the approximate solution of ξ and u for a fixed set of parameters. This set of parameters is representable for the Marsdiep-Vlie system, except for the phase difference between the incoming M_2 signals, θ. A value of $\pi/4$ is more realistic than 0. However, the results with $\theta = 0$ are easier to interpret and to compare with literature. The reason for this is that if $\theta = 0$ the channel represents such a semi-enclosed basin as is often used in literature. This is because if $\theta = 0$ the waves coming from the right and left cancel in the middle and hence the current velocity will be zero in the middle of the channel. The middle of the channel then represents the closed boundary of the semi-enclosed basin. The waves coming from behind this closed boundary are then interpreted as the waves reflected on the boundary. Therefore, in the default model $\theta = 0$.

When thinking about 'tidal curves', people often think of a plot with the height of the water on the horizontal axis and the time on the vertical axis. This motivates to first show how the approximations of u and ξ, that is, $u = u_0 + \varepsilon u_1$ and $\xi = \xi_0 + \varepsilon\xi_1$, change at certain locations through time. Since $\theta = 0$, the free surface elevation, ξ, and the current velocity, u, are symmetric around $x = 0$ km.

	dimensionless	dimensional
Length of channel	$\frac{2\pi}{7.8}$	57 km
Time interval	2π	12 h 25 m
Friction coefficient	1	$1.4 \cdot 10^{-3}$ m s^{-1}
Amplitude incoming M_2 at boundaries, z_1, z_2	1	1 m
The phase difference between incoming M_2, θ	0	0 h
Typical tidal amplitude, $\mathcal{Z}$		1 m
Depth of flats, d_f		1 m
Depth main channel, h_c		10 m
Froude Number, $\varepsilon = \frac{\mathcal{Z}}{h_c}$	10^{-1}	
Relative flat width, $\beta = \frac{b_{\max} - b_c}{b_c}$	8	
Inversely proportional to slope of the flats, $\alpha = \frac{1}{2q\varepsilon}$	1	

Table 4.1. Parameters used in default configuration, representative for the Marsdiep-Vlie system (except for θ).

In Figure 4.1, ξ and u are plotted at $x = -28, -14$ km and $x = 0$ km. The first observation is that the curves are far from sinusoidal. Also, as expected, the velocity is zero in the middle of the channel. Furthermore, notice that at the middle of the channel, $x = 0$ km, the falling of the tide is longer than the rising of the tide. At $x = -14$ km this is still the case but the difference between the falling and rising tide is smaller. At $x = -28$ km, the rising is slightly longer than the falling of the tide. Furthermore, In Figure 4.1 it is seen that at $x = -28$ km the average water free surface elevation is below 0 m while at $x = 0$ km it is above 0 m. At both $x = -28$ km and $x = -14$ km the absolute values of u are higher at the maximum than at the minimum, that is, the system is + dominant (as defined in Section 1.2.1).

The curves in Figure 4.1 are a superposition of different constituents. In the approximation we only consider the constituents M_2, M_4, M_6 and M_0 as these four constituents are the main cause of tidal distortion. In Figure 4.2 the constituents of ξ and u at $x = -28, -14$ km and $x = 0$ km are shown. The M_6 is multiplied by ten to make its curve visible. In Figure 4.1 it was seen that the average free surface elevation at $x = -28$ km is negative while at $x = 0$ it is positive, in Figure 4.2 this is again seen as the residual free surface elevation, M_0, is negative at $x = -28$ km and positive at $x = 0$ km. This implies that the relation (see Chapter 1) between the relative phase and the difference in absolute value of high and low water as in Figure 1.4 is invalid and will therefore not be used in the remaining of this study. In Figure 4.2e we see that the M_4 and M_6 are relatively large compared to the M_2. This was to be expected since the sinusoidal shape of the curve in Figure 4.1e is strongly distorted. Figure 4.2 also reveals that the residual current velocity is very small at all three locations. This implies that the relation (see Chapter 1) between the system being + or − dominant and the relative phase of the M_4 and M_2 as in Figure 1.5 is valid.

$x = -28$ km	$x = -14$ km	$x = 0$ km

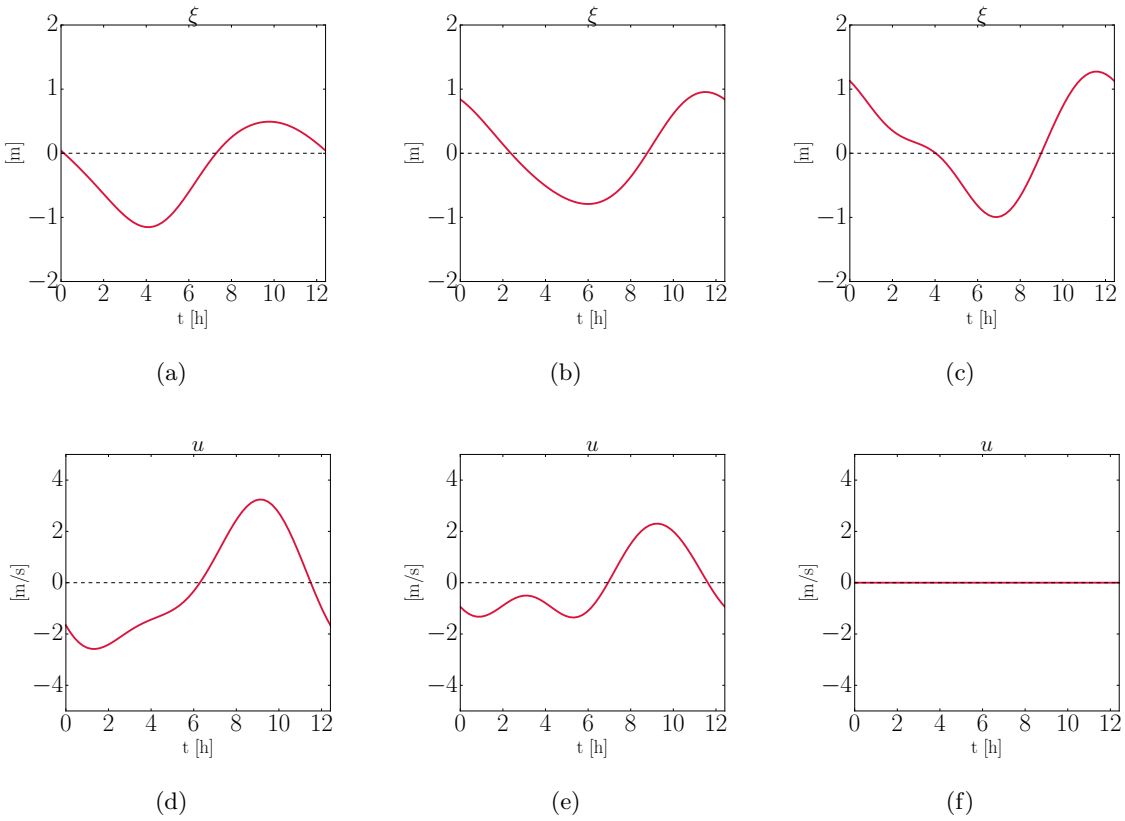

Figure 4.1. The free surface elevation, ξ, and the current velocity, u, versus time at $x = -28, -14$ km and $x = 0$ km. Parameters are as in the default configuration.

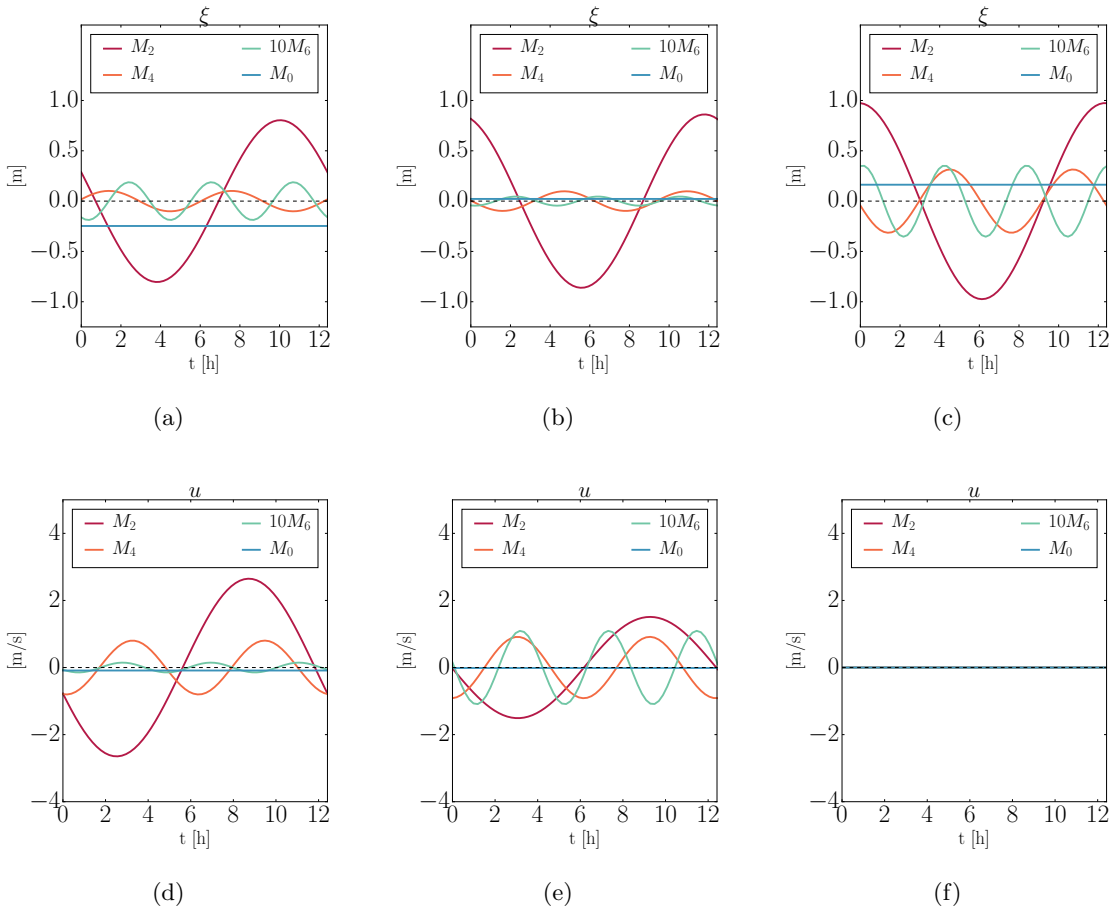

Figure 4.2. The constituents, M_2, M_4, M_6 and M_0 of ξ and u versus time at $x = -28, -14$ km and $x = 0$ km. The M_6 is multiplied by ten to make its curve visible. Parameters are as in the default configuration.

In Figures 4.1 and 4.2 it is clear that ξ and u are strongly dependent on x. Therefore, it is worthwhile to add the spatial dimension to the plots. However, 3d plots are almost never clear. An other possibility of presenting ξ and u is plotting their complex amplitudes. The norm of the complex amplitude of, for example, the M_2 is the (real) amplitude of the M_2 and the argument of the complex amplitude is the phase of the M_2. So continuing the example of the M_2, the M_2 component of ξ reads

$$\mathrm{Re}\Big\{ \underbrace{(\hat{\xi}_0 + \hat{\xi}_{1,1})}_{\text{complex amplitude of } M_2} e^{-it} \Big\}.$$

The M_2 amplitude and phase are

$$|\hat{\xi}_0 + \hat{\xi}_{1,1}| \quad \text{and} \quad \arg(\hat{\xi}_0 + \hat{\xi}_{1,1}).$$

In Figure 4.3 the amplitudes and phases of ξ and u are plotted as functions of x. To avoid that the computer choses some random phase for complex numbers with small amplitudes, the

phases are only plotted at the points in space where the amplitude is larger than 0.05 m. The amplitude of every constituent of ξ has a maximum in the middle of the channel. The free surface elevation M_2 amplitude has a minimum close to (but not at) the boundaries of the channel. The free surface elevation M_4 and M_6 amplitude also have a minimum but further away from the boundary. The M_6 has a amplitude smaller than 0.05 m everywhere in the channel and does therefore not show up in the plot with the phases. The residual free surface elevation is positive in the middle of the channel, zero somewhere at one (and at three) quarter(s) and negative at the boundaries of the channel. The amplitude of the current velocity of every constituent is zero where the waves coming from the left and right meet, that is, in the middle of the channel. The M_4 decreases after having a maximum at somewhere around one (and three) quarter(s) of the channel. The M_6 has a maximum closer to the middle than the M_4 and decreases rather fast. At every point in the channel is the residual current oriented towards the closest boundary. That is, positive on the right hand side of the channel and negative on the left hand side of the channel. The phases of the velocity are rather flat in x and indicate that the tidal wave has a standing wave character.

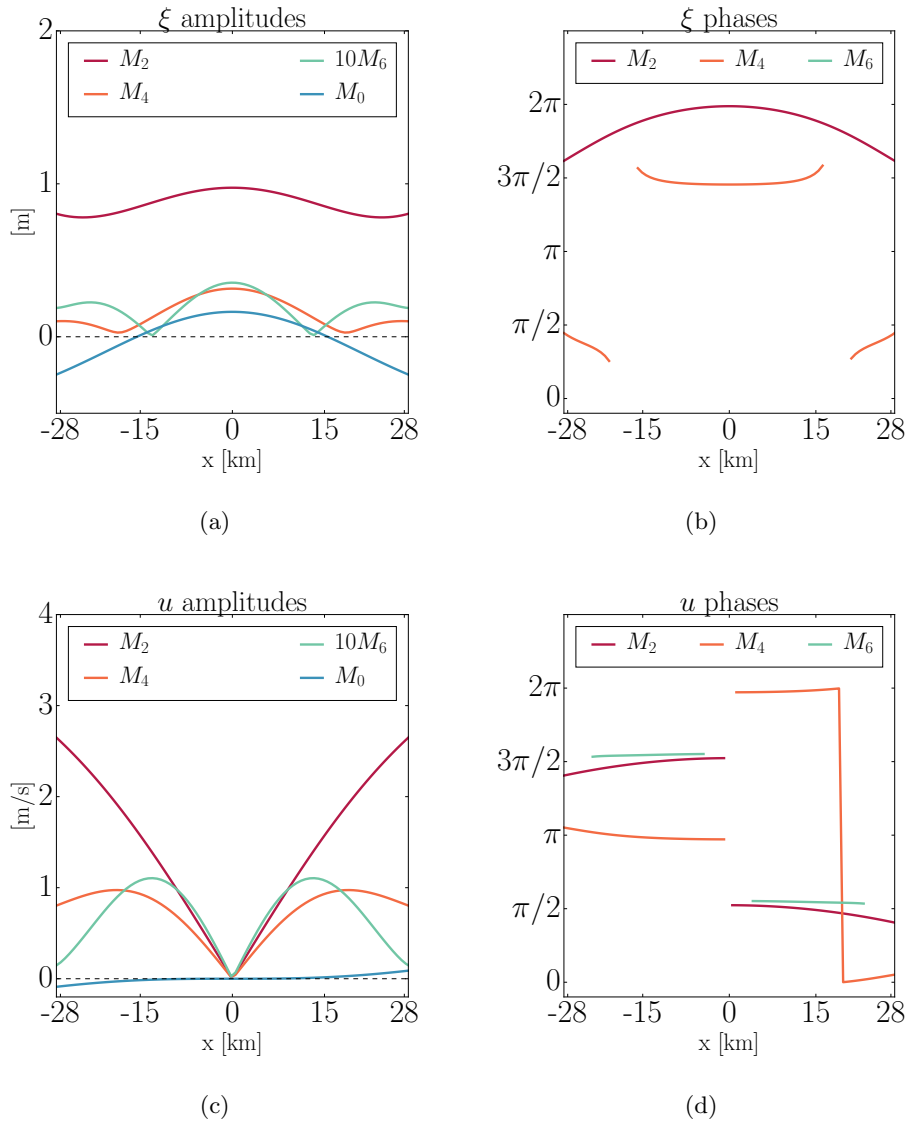

Figure 4.3. The amplitudes (norms) and phases of the complex amplitudes of the constituents M_2, M_4, M_6 and M_0 of both ξ and u versus x. Like in Figure 4.2 is the amplitude of M_6 multiplied by ten. Parameters are as in the default configuration.

On the boundaries, $x = \pm L/2$, we impose incoming free surface elevation M_2 tidal waves. That is, on the left (right) boundary, $x = -L/2$ ($x = L/2$), we impose a M_2 propagating to the right (left). It would therefore be interesting to see the parts of ξ moving to the right and to the left separately. Figure 4.4 shows the amplitudes and phases of the different constituents of ξ of both the part moving to the right and left. We see that we successfully choose the constants such that ξ obeys the boundary conditions. That is, the M_2 amplitude of the wave propagating to the right (left) is $z_1 = 1$ ($z_2 = 1$) on the left (right) boundary. The amplitude of the M_2 waves decreases as they propagate through the channel. The amplitude of the M_4 and M_6 propagating to the right (left) is zero on the left (right) boundary and increases as it moves to the right (left). Remarkable is the nonlinear structure of the M_4 amplitude in x.

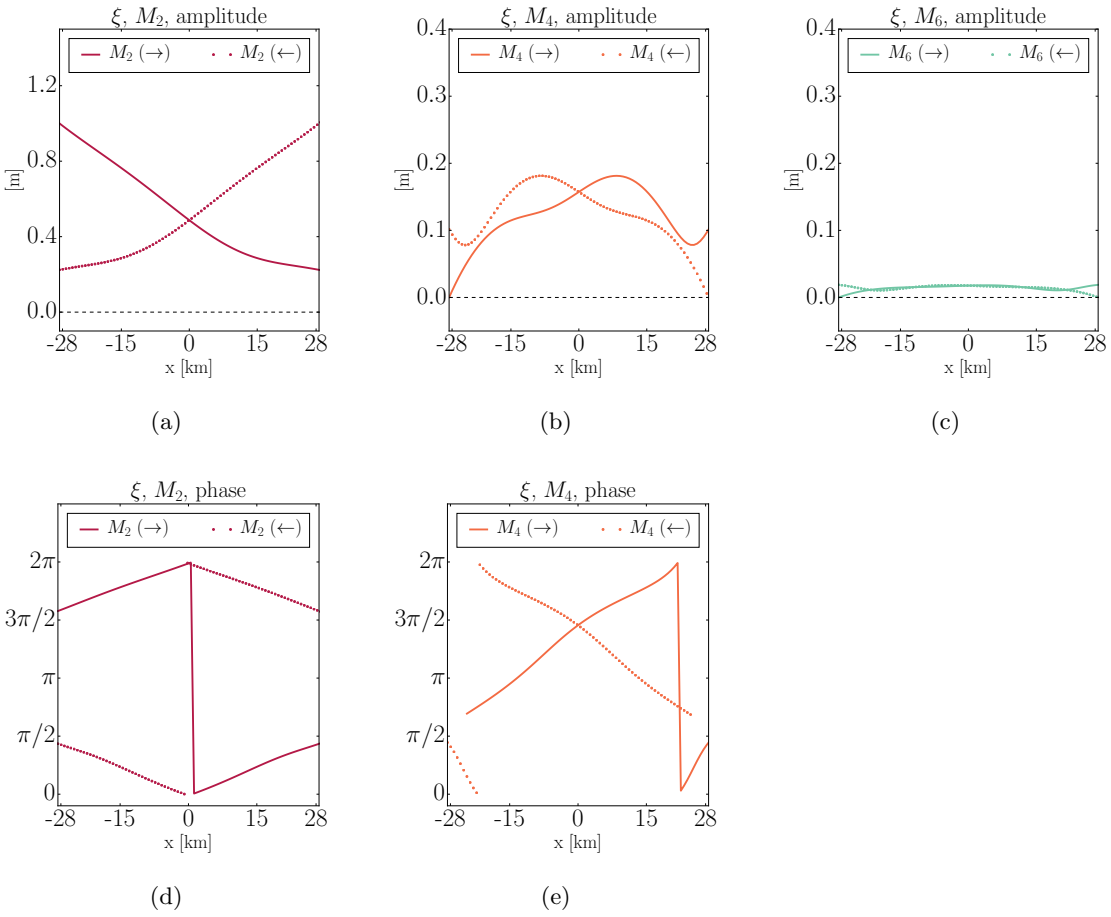

Figure 4.4. The amplitudes (norms) and phases of the complex amplitudes of ξ of the constituents M_2, M_4 and M_6 propagating to the right(solid) and left(dotted) versus x. Parameters are as in the default configuration.

4.2. Analytical difference

In Chapter 3 we derived analytical solutions to the $O(1)$ and $O(\varepsilon)$ problems. In these solutions the terms that arose due to the momentum sink term were marked by the roman number III. One of the aims of the present study is to quantify the effects of this term on the hydrodynamics in the tidal channel. One of the approaches is to calculate the analytical difference between the solutions of the $O(1)$ and $O(\varepsilon)$ problems with the momentum sink taken into account and the solutions where is it not, that is, where every term marked by III is put to zero.

The first order solutions ξ_0 and u_0 are independent of the momentum sink as they describe the primary M_2 tide that is forced by the boundary conditions. Next we consider the $O(\varepsilon)$ solutions ξ_1 and u_1. We denote with the superscript '$(-)$' the $O(\varepsilon)$ solution where the momentum sink is neglected. Since all other nonlinear terms (I, II, IV, V in (3.35) and (3.36)) are at most quadratic, they only generate M_0 ($m = 0$), M_2 ($m = 1$) and M_4 ($m = 2$) in the $O(\varepsilon)$ solutions. Therefore, without term III reduces the equations in (3.37) to

$$\xi_1^{(-)}(x,t) = \sum_{m=1}^{2} \mathrm{Re}\left\{\hat{\xi}_{1,m}^{(-)} e^{-imt}\right\} + \bar{\xi}_1^{(-)} \quad \text{and} \quad u_1^{(-)}(x,t) = \sum_{m=1}^{2} \mathrm{Re}\left\{\hat{u}_{1,m}^{(-)} e^{-imt}\right\} + \bar{u}_1^{(-)},$$

with, for $m \neq 0$,

$$\hat{\xi}_{1,m}^{(-)}(x) = \frac{e^{ik_m x}}{2ik_m}\int_{-L/2}^{x} e^{-ik_m s} f_m^{(-)}(s)\,ds - \frac{e^{-ik_m x}}{2ik_m}\int_{L/2}^{x} e^{ik_m s} f_m^{(-)}(s)\,ds,$$

$$\hat{u}_{1,m}^{(-)}(x) = \begin{cases} \dfrac{1}{im - r}\left(\dfrac{\partial \hat{\xi}_{1,m}^{(-)}}{\partial x}\right) & \text{if } m = 1 \\ \dfrac{1}{2i - r}\left(\underbrace{\dfrac{1}{4}\dfrac{\partial \hat{u}_0^2}{\partial x}}_{\text{I}} + \dfrac{\partial \hat{\xi}_{1,2}^{(-)}}{\partial x} \underbrace{- \dfrac{r}{2}\hat{u}_0\hat{\xi}_0}_{\text{II}}\right) & \text{if } m = 2 \end{cases}$$

$$\bar{\xi}_1^{(-)}(x) = -\frac{1}{L}\int_{-L/2}^{L/2}\int_0^x E^{(-)}(s)\,ds\,dx + \int_0^x E^{(-)}(s)\,ds,$$

$$\bar{u}_1^{(-)}(x) = \underbrace{-\frac{1}{2}|\hat{u}_0||\hat{\xi}_0|\cos(\phi_{\hat{u}_0} - \phi_{\hat{\xi}_0})}_{\text{IV}},$$

$$E^{(-)}(x) = \underbrace{-\frac{1}{4}\frac{\partial |\hat{u}_0|^2}{\partial x}}_{\text{I}} + \underbrace{|\hat{u}_0||\hat{\xi}_0|\left(r\cos(\phi_{\hat{u}_0} - \phi_{\hat{\xi}_0})\right)}_{\text{II}},$$

$$f_m^{(-)}(x) = \begin{cases} \underbrace{2\beta\alpha\hat{\xi}_0}_{\text{V}} & \text{for } m = 1 \\ \underbrace{-i\dfrac{\partial}{\partial x}(\hat{u}_0\hat{\xi}_0)}_{\text{IV}} \underbrace{-\dfrac{1}{4}\dfrac{\partial^2}{\partial x^2}(\hat{u}_0^2)}_{\text{I}} \underbrace{+ r\dfrac{\partial}{\partial x}(\hat{u}_0\hat{\xi}_0)}_{\text{II}} \underbrace{- 2\beta\alpha\hat{\xi}_0^2}_{\text{V}} & \text{for } m = 2 \end{cases}$$

$$(k_m)^2 = (1+\beta)m(m + ri),$$

The origin of the terms are as in Table 3.1.

Thus, the difference between the solutions with and without the momentum sink term is[1]

$$\xi_0 + \varepsilon\xi_1 - (\xi_0 + \varepsilon\xi_1^{(-)}) = \varepsilon\xi_1^{(\sim)},$$
$$u_0 + \varepsilon u_1 - (u_0 + \varepsilon u_1^{(-)}) = \varepsilon u_1^{(\sim)},$$

where,

$$\xi_1^{(\sim)}(x,t) = \xi_1(x,t) - \xi_1^{(-)}(x,t) = \sum_{m=1}^{\infty} \mathrm{Re}\left\{\hat{\xi}_{1,m}^{(\sim)} e^{-imt}\right\} + \bar{\xi}_1^{(\sim)}, \tag{4.1}$$

$$u_1^{(\sim)}(x,t) = u_1(x,t) - u_1^{(-)}(x,t) = \sum_{m=1}^{\infty} \mathrm{Re}\left\{\hat{u}_{1,m}^{(\sim)} e^{-imt}\right\} + \bar{u}_1^{(\sim)}, \tag{4.2}$$

with for $m \neq 0$,

$$\hat{\xi}_{1,m}^{(\sim)}(x) = \frac{e^{ik_m x}}{2ik_m}\int_{-L/2}^{x} e^{-ik_m s}\frac{\partial p_m}{\partial x}\,ds - \frac{e^{-ik_m x}}{2ik_m}\int_{L/2}^{x} e^{ik_m s}\frac{\partial p_m}{\partial x}\,ds,$$
$$\hat{u}_{1,m}^{(\sim)} = \frac{1}{2i - r}\left(\frac{\partial \hat{\xi}_{1,m}^{(\sim)}}{\partial x} - p_m\right)$$
$$\bar{\xi}_1^{(\sim)}(x) = -\frac{1}{L}\int_{-L/2}^{L/2}\int_0^x E^{(\sim)}(s)\,ds\,dx + \int_0^x E^{(\sim)}(s)\,ds,$$
$$\bar{u}_1^{(\sim)}(x) = 0,$$
$$E^{(\sim)}(x) = -\frac{\beta}{4}|\hat{u}_0||\hat{\xi}_0\sin(\phi_{\hat{u}_0} - \phi_{\hat{\xi}_0}),$$
$$(k_m)^2 = (1+\beta)m(m+ri),$$
$$p_m(x) = \frac{i\beta}{2}\left(c_{2+m}^{*}\hat{u}_0^{*}\hat{\xi}_0^{*} - c_{2-m}\hat{u}_0\hat{\xi}_0\right) - c_m^{*}\beta|\hat{u}_0||\hat{\xi}_0|\sin(\phi_{\hat{u}_0} - \phi_{\hat{\xi}_0}),$$
$$c_m(x) = \frac{-i}{m2\pi}\left(1 - e^{im\pi}\right)e^{-im\phi_{\hat{\xi}_0}}.$$

The expressions above will be used in the next section. Notice that $\xi_1^{(\sim)}$ and $u_1^{(\sim)}$ are nonlinear in β because of the dependence of wavenumber k_m on β. This is interesting; if one tidal channel has twice as wide tidal flats as another tidal channel, this does not imply that the effect of the momentum sink on the hydrodynamics is two times larger in the first channel than in the second. The term $(1+\beta)$ comes in k_m via the $O(1)$ effect of the mass storage. The relation between β and the by the momentum sink generated M_2 and M_4 amplitude is depicted in Figures 4.5 and 4.6. It is seen that in as β increases, the amplitudes of the overtides generated by the momentum sink increase faster in the middle of the channel than in the end of the channel. Both the M_2 and the M_4 increase as β to a power smaller than 1.

[1]Note that, when looking at amplitudes of u and/or ξ, the difference in amplitude is not the same as the amplitude of the difference (triangle inequality).

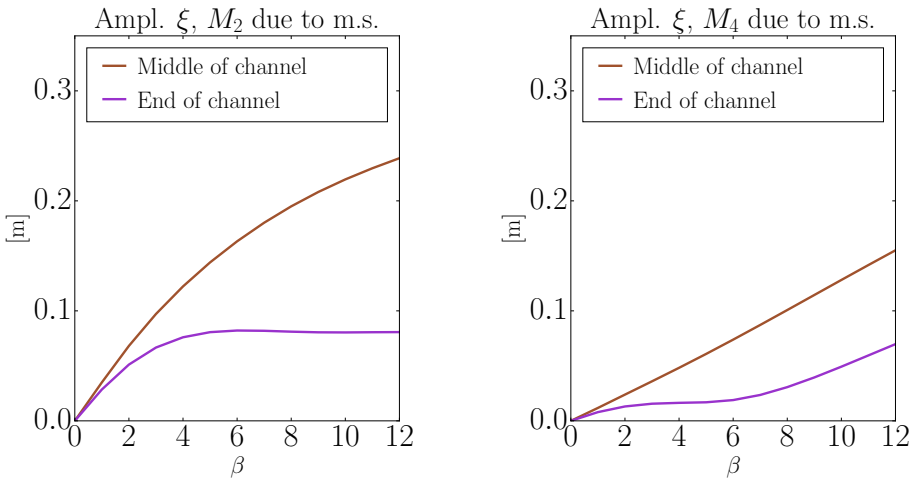

(a) (b)

Figure 4.5. The free surface elevation M_2 (panel a) and M_4 (panel b) amplitude generated by the momentum sink (m.s.) versus the relative tidal flat width, β at the middle of the channel (brown) and at the end of the channel (purple). Parameters are as in the default configuration.

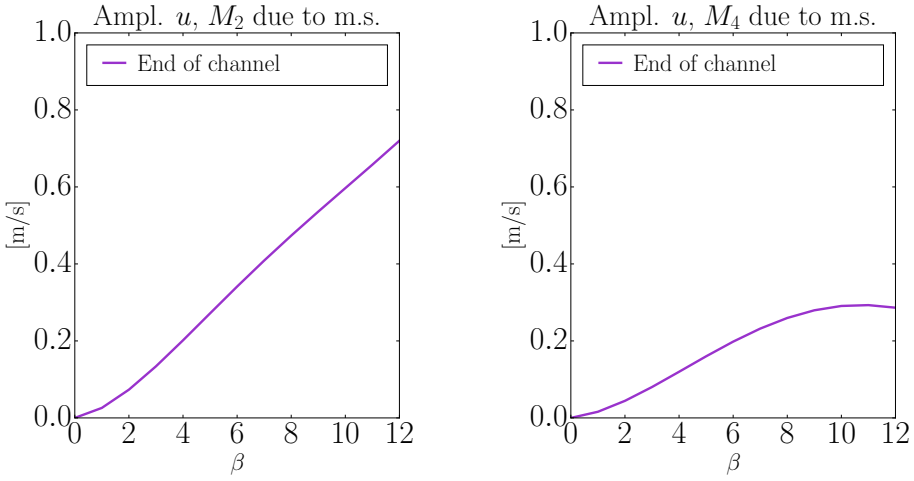

(a) (b)

Figure 4.6. Same as Figure 4.5 but for the current velocity, u. In the middle of the channel the velocity is zero and is therefore left out.

4.3. Effects of the momentum sink on hydrodynamics

In this section multiple effects of the momentum sink on the hydrodynamics in a tidal channel are presented. In the analysis the analytical difference derived in Section 4.2 is occasionally used. The parameters used, are the same as in the default model (see Table 4.1). We vary the ratio of the width of the tidal flats and the width of the main channel, β, and the phase difference between the incoming M_2 signals, θ. Most runs are done for three different values of β. In the Marsdiep-Vlie system a tidal flat that is four or eight times as wide as the main channel ($\beta = 4, 8$) is reasonable. As the effect of the momentum sink are expected to be larger when the tidal flats are wider, the results are included for $\beta = 12$, which is a large but not unrealistic value. The case where the width of the tidal flats is the same as the width of the main channel, $\beta = 1$, is only included in the first effect. The reason it is not included in the other effects becomes apparent in the demonstration of Effect 1. Furthermore, we consider the case where the phase difference between the incoming M_2 signals, θ, is zero and $\pi/4$. The phase difference of $\theta = \pi/4$ represents 1,5 hours and is based on the time difference between high tide in Den Helder (south coast of the Marsdiep) and high tide in West-Terschelling (north coast of the Vlie).

In the rest of this section multiple effect of the momentum sink on the hydrodynamics are presented.

Effect 1. The momentum sink generates, for both ξ and u, M_4 and M_{2m} for $m \geq 3$ and $m \not\equiv 0 \mod 2$. The generation is less for higher overtides (larger m). For a channel where the flats are of the same width as the main channel, $\beta = 1$, the momentum sink hardly generates overtides.

Equations (4.1) and (4.2) reveal that the momentum sink generates multiple overtides of both ξ and u. To find out which overtides exactly, we need to calculate for what m the expresion for p_m is nonzero. The expression for p_m is nonzero (for every x) if either $c^*_{2+m} \neq 0$, $c^*_{2-m} \neq 0$ or $c_m \neq 0$. We know that $c_0 \neq 0$ and for the other m's that $c_m = 0$ if $m \equiv 0 \mod 2$. Therefore, $p_1, p_2 \neq 0$ and for $m \geq 3$ we find that $p_m \neq 0$ if $m \not\equiv 0 \mod 2$. This means that the momentum sink generates, for ξ, M_4 and M_{2m} for $m \geq 3$ and $m \not\equiv 0 \mod 2$. That is, it generates every overtide except $M_8, M_{12}, M_{16}, \ldots$. Furthermore, notice that $|c_m|$ decreases if m increases because of the factor $-i/(m2\pi)$. This implies that the generation of M_{2m} decreases as m increases. To quantify the generation of M_2, M_4 and M_6 due to the momentum sink the amplitudes of M_2, M_4 and M_6 of both ξ and u are presented in Figures 4.7 and 4.8. That is, the amplitudes of the M_2, $|\varepsilon\hat{\xi}^{(\sim)}_{1,1}|$, the M_4, $|\varepsilon\hat{\xi}^{(\sim)}_{1,2}|$ and the M_6, $|\varepsilon\hat{\xi}^{(\sim)}_{1,3}|$ from equations (4.1) and (4.2). The colors of the lines indicate the ratio of the width of the tidal flats and the width of the main channel, β. Figure 4.7 represents the case of no phase difference, $\theta = 0$ and Figure 4.8 the case where $\theta = \pi/4$. Figures 4.7 and 4.8 reveal that the momentum sink has a noticeable effect on the hydrodynamics for $\beta \geq 4$. For $\beta = 1$ the effect is very small and hence the case of $\beta = 1$ is excluded from the following results.

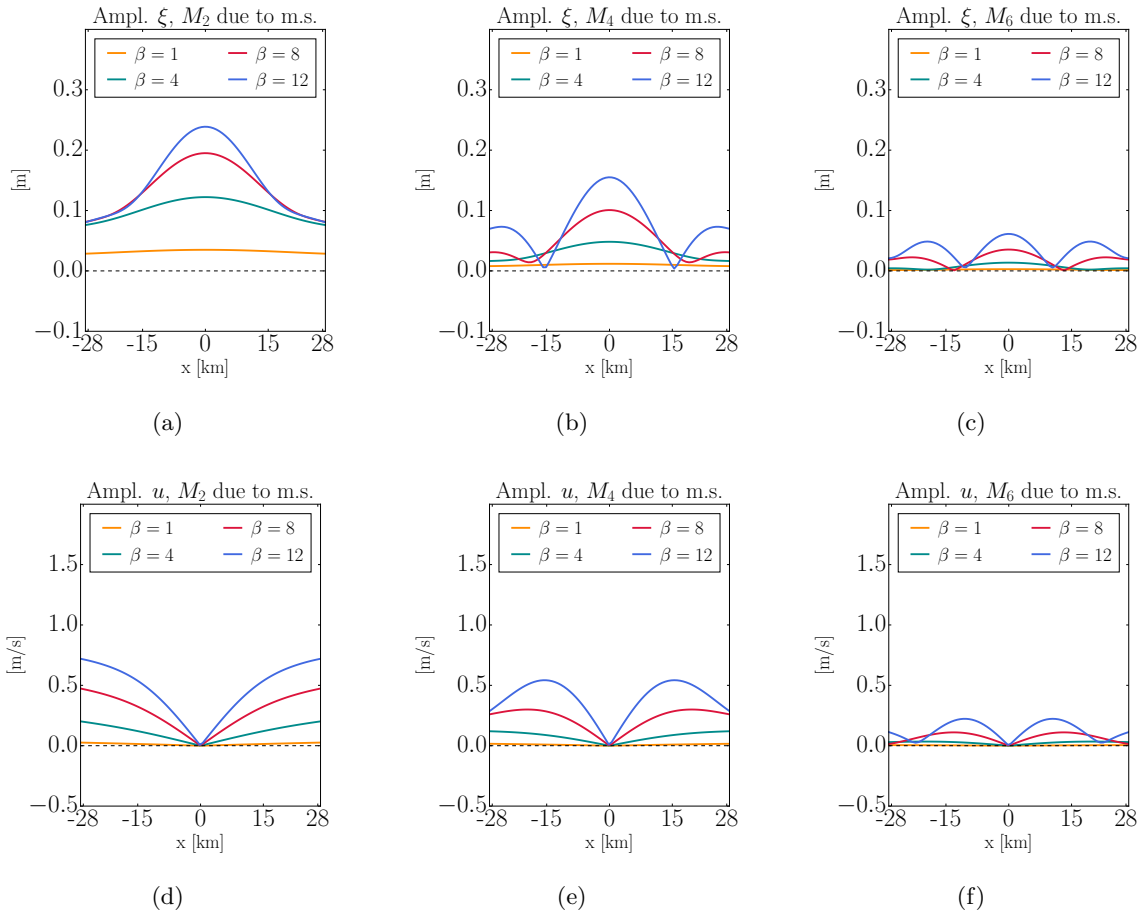

Figure 4.7. Amplitudes of M_2, M_4 and M_6 of both the free surface elevation, ξ, and the current velocity, u due to the momentum sink (m.s.) versus x. The colors of the lines indicate the ratio of the width of the tidal flats and the width of the main channel, β. In this run there is no phase difference between the incoming M_2 waves, $\theta = 0$.

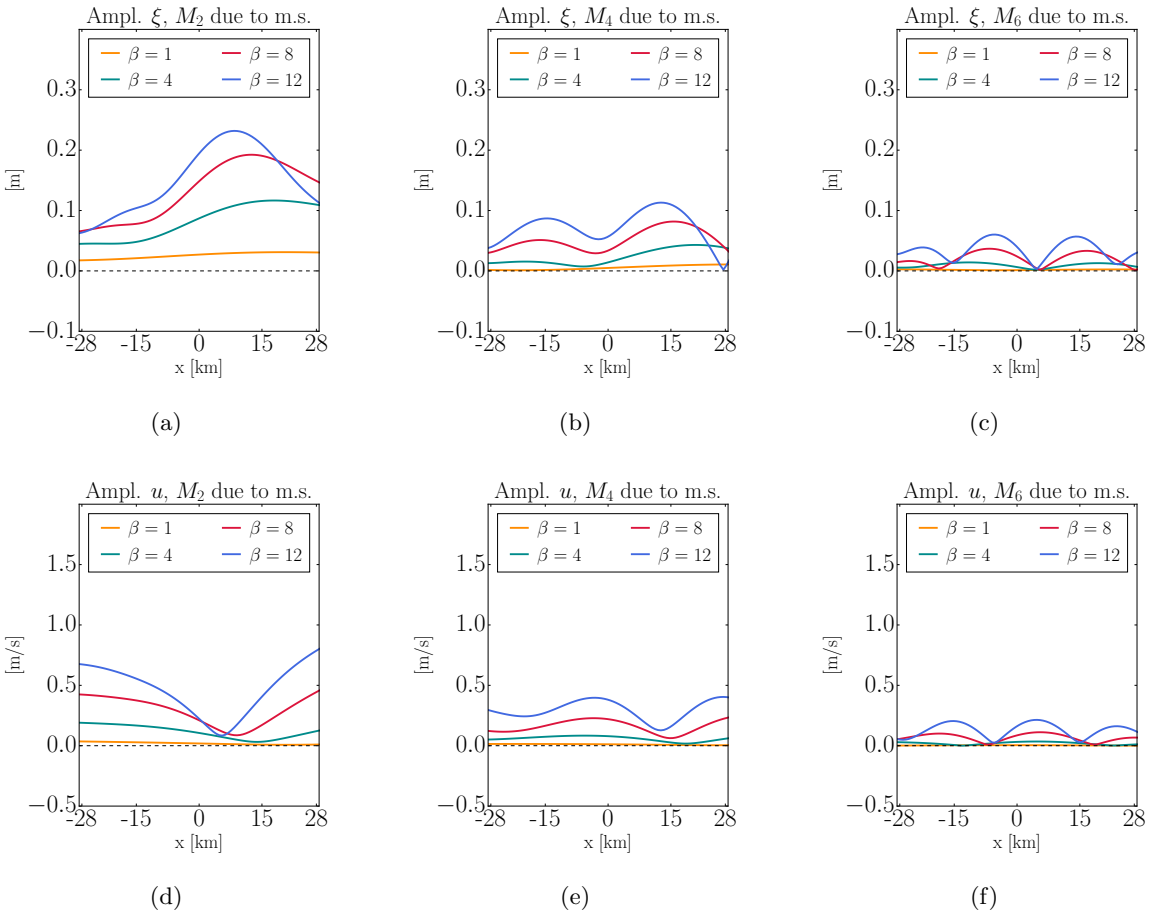

Figure 4.8. Same as Figure 4.7 but with $\theta = \pi/4$.

Effect 2. The momentum sink has no influence on the residual current velocity, but increases the absolute value of the residual free surface elevation.

The fact that the momentum sink has no influence on the residual current velocity is directly clear from the analytical difference in Section 4.2 since $\bar{u}_1^{(\sim)} = 0$. Figure 4.9 reveals that when the residual free surface elevation is positive it becomes larger and when it is negative it becomes smaller. The upper panels show two curves for each value of β (color), one for the situation where the momentum sink is taken into account (solid) and one where it is not (dashed). The difference between the two is depicted in the lower panels. Henceforth, 'the difference' refers to the difference between the cases with and without the momentum sink taken into account. When this difference equals zero, the momentum sink has no effect. When $\theta = \pi/4$ the curves are shifted to the right.

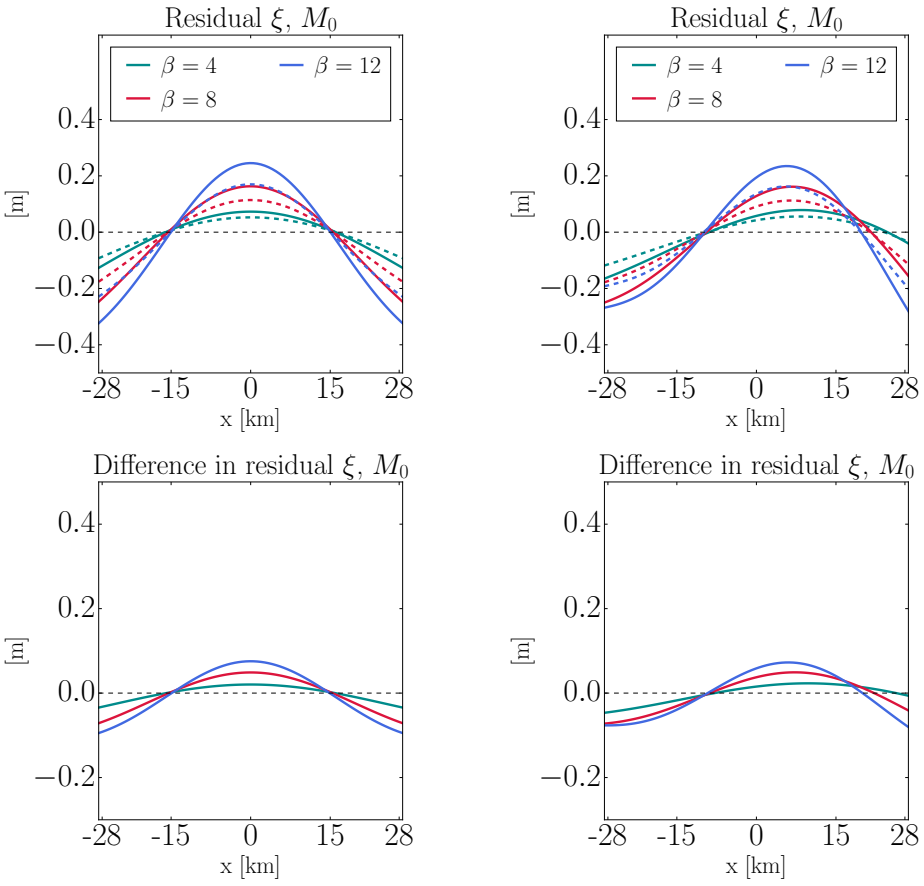

(a) $\theta = 0$.

(b) $\theta = \pi/4$.

Figure 4.9. Residual free surface elevation versus x. In the upper panels are two curves for each β (color), one for the situation where the momentum sink is taken into account (solid) and one where it is not (dashed). The difference between the two is depicted in the lower panels. (a) is with no phase difference between the incoming M_2 waves, $\theta = 0$, and (b) with a phase difference of $\theta = \pi/4$.

Effect 3. When the momentum sink is taken into account, the amplitude of the M_2 constituent of ξ strongly decreases in the middle of the channel and increases at other places in the channel. For u the amplitude of the M_2 is decreased everywhere in the channel. The amplitude of the M_4 increases everywhere for both ξ and u. This occurs for both $\theta = 0$ and $\theta = \pi/4$. Also, the dependence on x of the difference between the solutions where the momentum sink is taken into account and the solutions where it is not increases as β increases.

In Figure 4.10 and 4.11 the free surface elevation and current velocities amplitudes of the M_2 and M_4 are plotted. Like in Figure 4.9 of Effect 2, in the upper panels are two curves for each value of β (color), one for the situation where the momentum sink is taken into account (solid) and one where it is not (dashed). Note that the difference between the case where the momentum sink is taken into account and the case where it is not is different from the generated M_2 and M_4 as in Effect 1. Now, the fact that these signals are in or out of phase with other M_2 and M_4 signals is taken into account.

Figure 4.10a reveals that at the middle of the channel the the momentum sink decreases the M_2 amplitude of ξ, while it increases the amplitude of the M_2 at the boundaries. It follows that in the middle of the channel, the M_2 generated by the momentum sink, $\mathrm{Re}\left\{\varepsilon\hat{\xi}^{(\sim)}_{1,1}e^{-it}\right\}$, and the forced (incoming) M_2, $\mathrm{Re}\left\{\hat{\xi}_0 e^{-it}\right\}$, are almost out of phase. This is confirmed by Figures 4.12a and 4.7a. In the middle of the channel the phase difference between the M_2 generated by the momentum sink and the forced M_2 is almost π; $\arg(\hat{\xi}_0) - \arg(\hat{\xi}^{(\sim)}_{1,1}) \approx \pi$. This is confirmed by the fact that the amplitude of the M_2 generated by the momentum sink, $|\hat{\xi}^{(\sim)}_{1,1}|$ is slightly more than 0.2 m in the middle of the channel and that this is close to the value of the difference in amplitude in the middle of the channel (but in that case negative). On the other hand, on the boundaries of the channel the phase difference is almost 0. So, here the M_2 generated by the momentum sink is almost in phase with the forced M_2. Hence, the amplitudes are adding up there. Indeed, on the boundary the amplitude of the by the momentum sink generated M_2 is around 0.1 m, which is close to the value of the difference on the boundaries. Figure 4.10b reveals that the amplitude of the M_4 of ξ is increased everywhere in the channel. Furthermore, note that for wider flats, (higher β), the difference in the amplitude of ξ for both the M_2 and the M_4 amplitude, is stronger dependent on x.

Figures 4.11a, 4.11b and 4.12b show the same plots as Figures 4.10a, 4.10b and 4.12a, but now for the current velocity u. In this case the amplitude of M_2 is everywhere in the channel decreased by the momentum sink. The M_4 is, just as for ξ, increased everywhere in the channel. Figure 4.12b shows that the M_2 generated by the momentum sink is almost everywhere in opposite phase with the forced M_2 as the phase difference is approximately π.

Figures 4.13, 4.14 and 4.15 show the same plots as Figures 4.10, 4.14 and 4.12, but now for the case that the incoming M_2 waves at the left and right boundary have a phase difference of approximately one and a half hour, that is, $\theta = \pi/4$. Although the symmetry around $x = 0$ is broken, the conclusions remain unaltered; due to the momentum sink, the amplitude of the M_2 constituent ξ decreases around the middle and increases at other places in the channel. For u the M_2 decreases everywhere. Furthermore, due to the momentum sink, the amplitude of the M_4 amplitude increases everywhere in the channel for both ξ and u. However, when $\theta = \pi/4$, the M_4 amplitude of ξ is significantly smaller then when $\theta = 0$ and its dependency on x is less; the curves are rather flat.

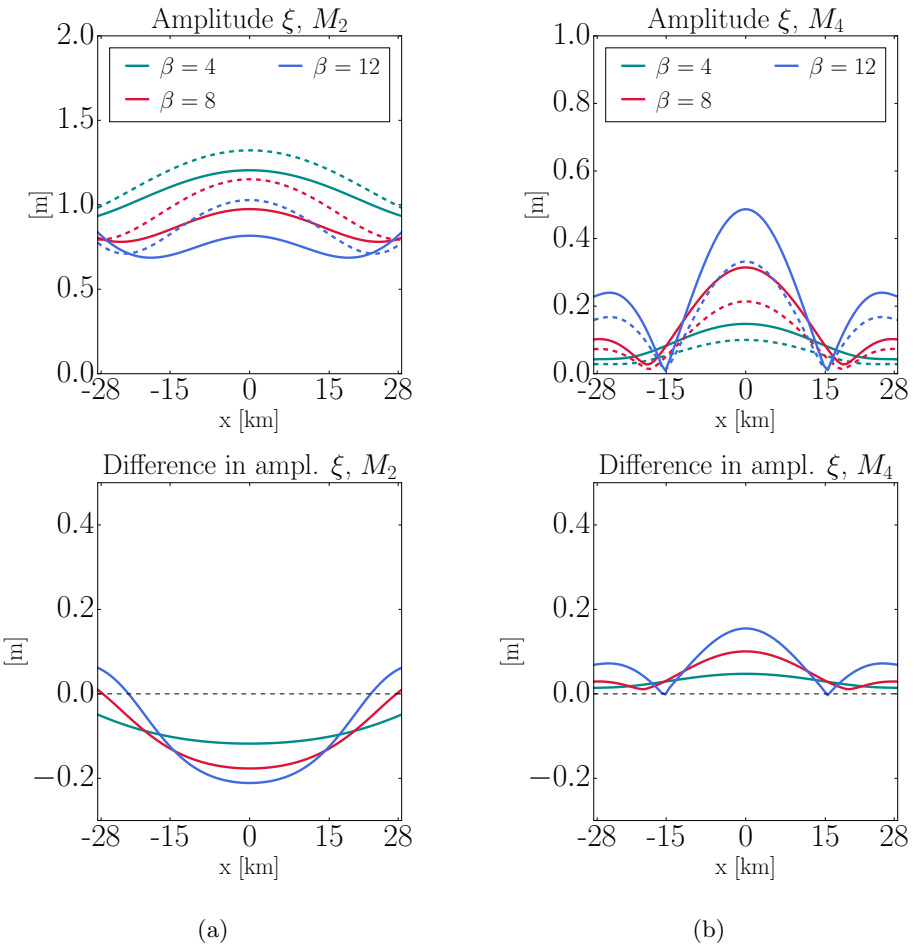

Figure 4.10. The upper panels show the amplitudes of M_2 and M_4 of free surface elevation, ξ versus x. The dashed lines are without the momentum sink term and the solid lines are with the momentum sink term. The lower panels show the differences between the amplitudes with and without the momentum sink term taken into account. The colors are as in Figure 4.7. In this case there is no phase difference between the right and left incoming M_2 waves, $\theta = 0$.

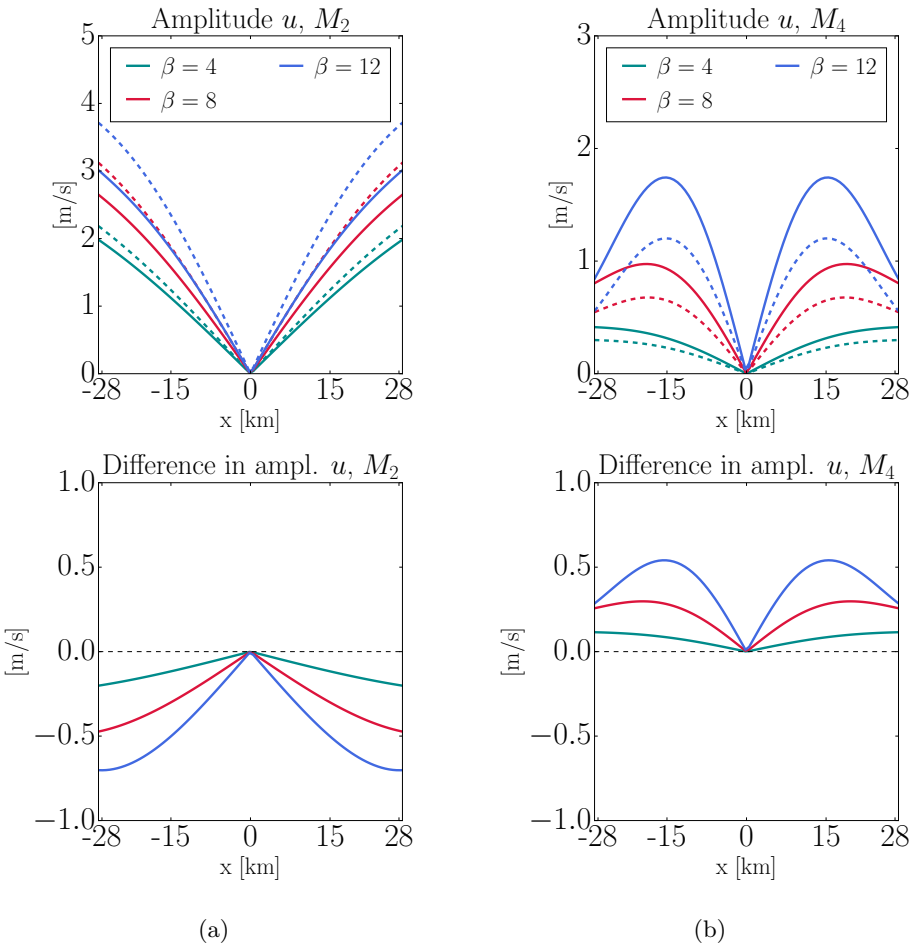

Figure 4.11. Same as Figure 4.10 but for the current velocity, u.

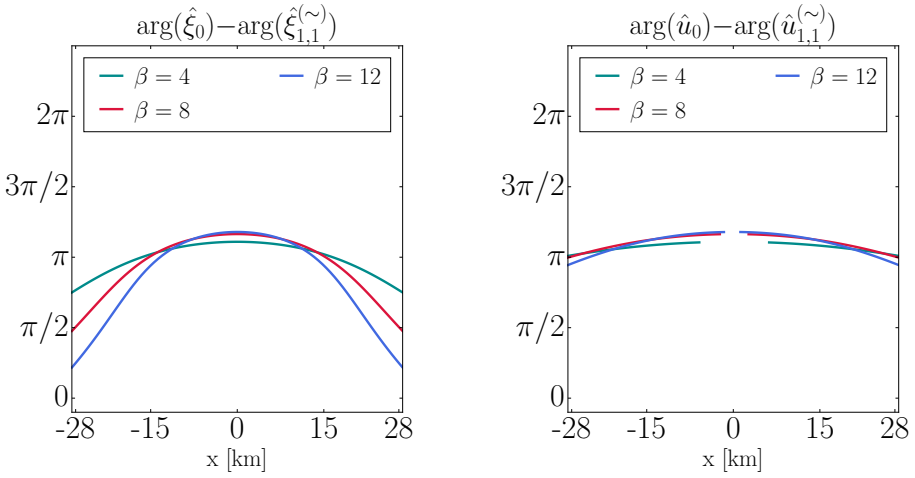

(a) (b)

Figure 4.12. The difference between the phase of the forced M_2 and the phase of the M_2 generated by the momentum sink versus x. This is the case where there is no phase difference between the right and left incoming M_2 waves, $\theta = 0$. The colors are as in Figure 4.7.

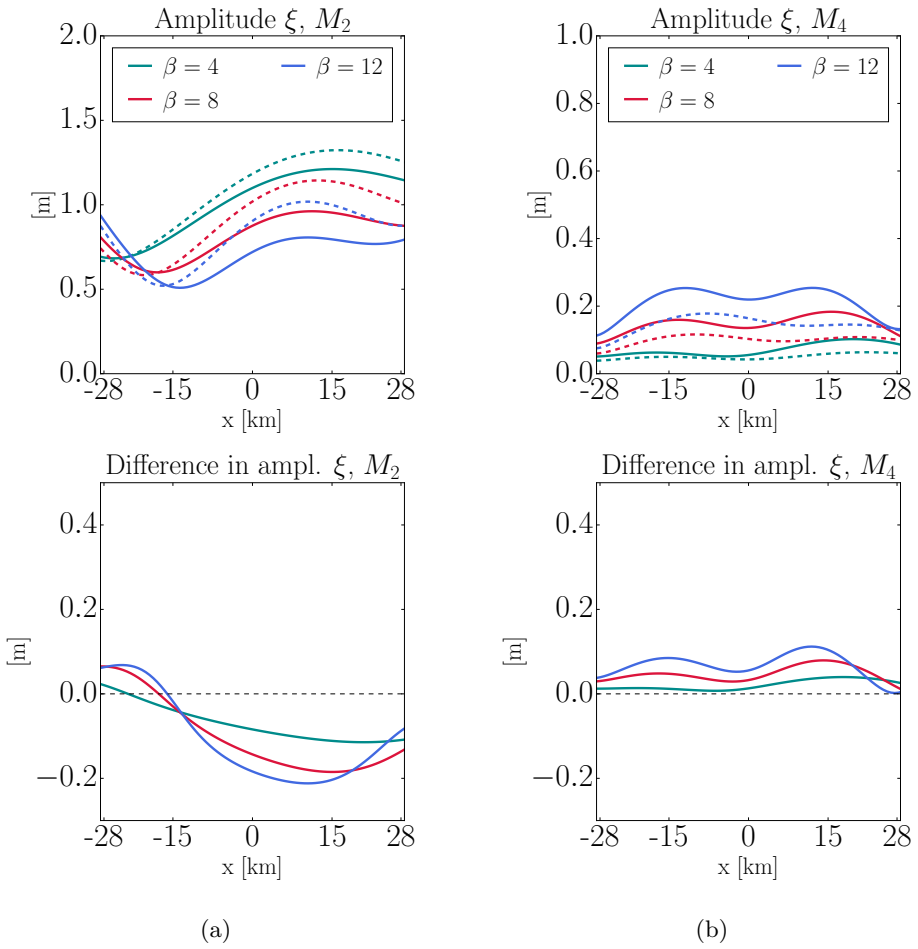

Figure 4.13. Same as Figure 4.10, but now a phase difference of $\theta = \pi/4$ is imposed between the right and left incoming M_2 waves at $x = -L/2$ and $x = L/2$, respectively.

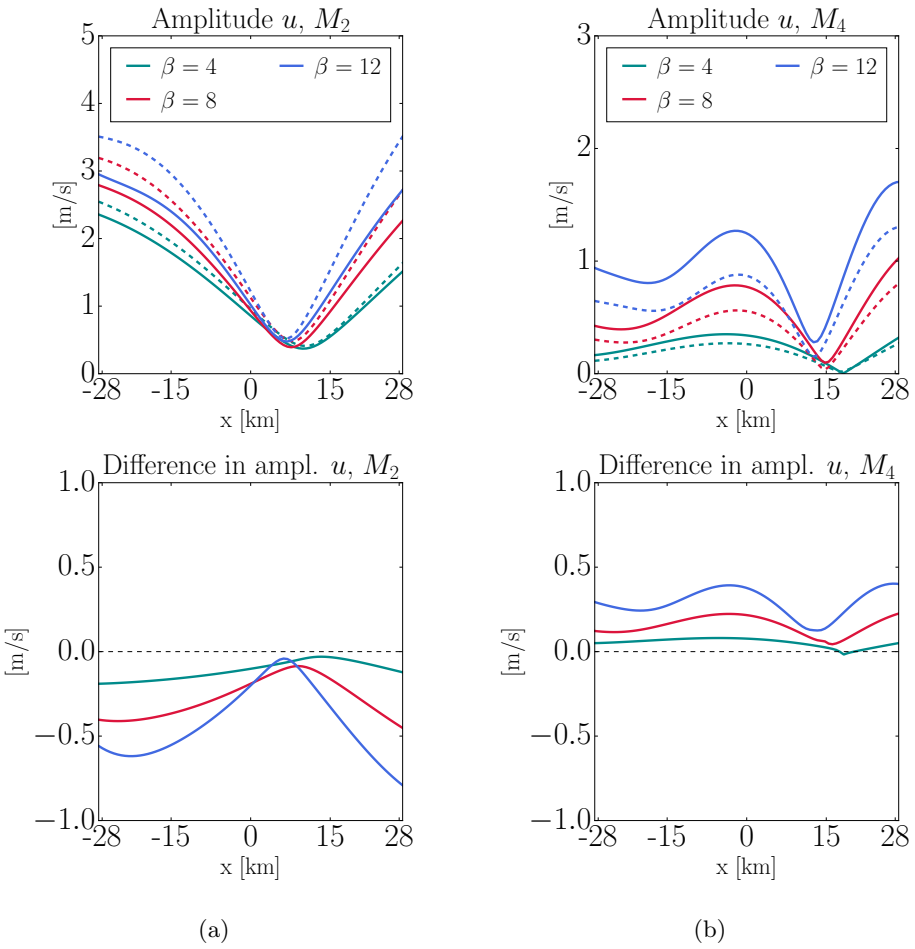

Figure 4.14. Same as Figure 4.11, but now a phase difference of $\theta = \pi/4$ is imposed between the right and left incoming M_2 waves at $x = -L/2$ and $x = L/2$, respectively.

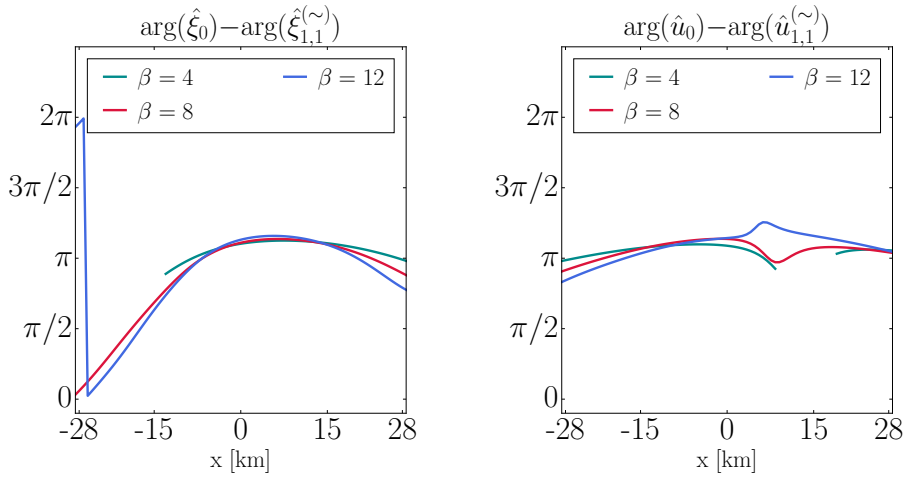

(a) (b)

Figure 4.15. Same as Figure 4.12, but now a phase difference of $\theta = \pi/4$ is imposed between the right and left incoming M_2 waves at $x = -L/2$ and $x = L/2$, respectively.

EFFECT 4. The momentum sink has significant effects on the tidal distortion of the free surface elevation. Especially in the middle of the channel the falling of the tide is longer than the rising. The momentum sink increases this distortion. For $\theta = 0$, in the middle of the channel, where the difference is the maximal, shoulder behavior, i.e., a second high and low water, are possible when the tidal flats are relatively wide compared to the main channel.

As explained in Chapter 1 the relative phase of the M_2 and M_4 characterizes the nature of the distortion of the sinusoidal shape of ξ. That is, if for the free surface elevation

$$0 < 2\phi_{\xi,M_2} - \phi_{\xi,M_4} < \pi,$$

the falling of the tide takes longer than the rising of the tide and if

$$\pi < 2\phi_{\xi,M_2} - \phi_{\xi,M_4} < 2\pi,$$

the rising of the tide takes longer than the falling of the tide. The relative phase for the free surface elevation is defined as

$$2\phi_{\xi,M_2} - \phi_{\xi,M_4} = 2\arg(\hat{\xi}_0 + \varepsilon\hat{\xi}_{1,1}) - \arg(\hat{\xi}_{1,2}).$$

It was also explained in Chapter 1 that the ratio of the M_4 and M_2 amplitude is a measure of how strong the tidal distortion is. Since Effect 3 implies that this ratio increases, the tidal distortion should also increase. The ratio in amplitude and the relative phase are depicted in Figure 4.16. Especially in the middle of the channel the momentum sink causes a strong increase the M_4, M_2 amplitude ratio and therefore increases the difference between the falling and rising of the tide. In the middle of the channel the relative phase also increases due to the momentum sink. Therefore, a large effect of the momentum sink is expected in the middle of the channel. In Figure 4.17, ξ is plotted in the middle of the channel over time for three different values of the relative tidal width, β. In the top panels the total signal ($M_0 + M_2 + M_4 + M_6$) is plotted and in the lower panels the individual constituents are plotted. For the $\beta = 4$ the tidal distortion due to the momentum sink is small, for $\beta = 8$ it is noticeable but for $\beta = 12$ the distortion is large. A clear extra 'high water' occurs; the so called 'shoulder behavior'. Note that the change in ξ is mostly when the tide is falling. This makes sense as the momentum sink term is only nonzero when $\frac{\partial \xi}{\partial t} < 0$.

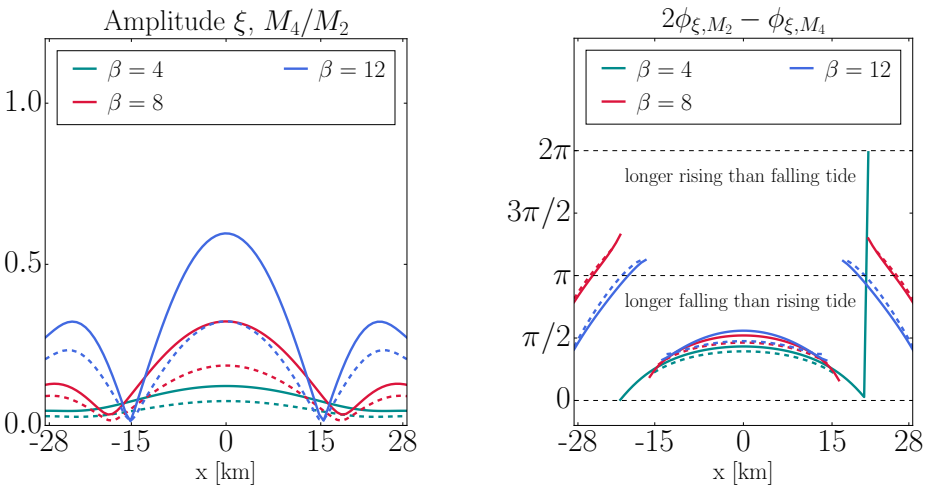

Figure 4.16. (a) The ratio of the amplitude of M_4 and M_2 of the free surface elevation, ξ versus x. (b) The relative phase, $2\phi_{\xi,M_2} - \phi_{\xi,M_4}$, of the free surface elevation versus x. As before, the solid lines are the cases where momentum sink is taken into account and the dashed lines where it is not. The colors are as in Figure 4.7.

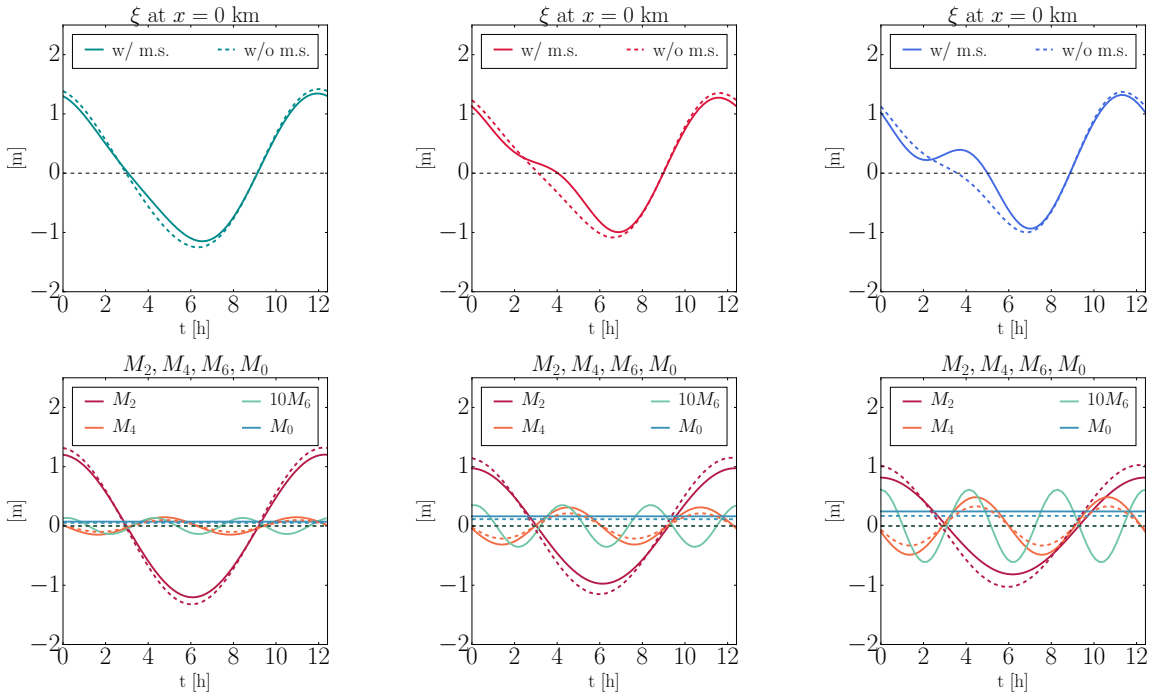

Figure 4.17. The free surface elevation, ξ, in the middle of the channel versus time. (a) is for $\beta = 4$, (b) for $\beta = 8$ and (c) for $\beta = 12$. The upper figures shows the total signal of ξ and the lower figures show the individual constituents M_2, M_4, M_6 and M_0. The M_6 is multiplied by ten to make the curve visible. As before, the solid lines are the cases where momentum sink is taken into account (w/ m.s.) and the dashed lines where it is not (w/o m.s.).

EFFECT 5. The momentum sink has significant effects on the tidal distortion of the current velocity. The momentum sink slightly increases the $+/-$ dominant character of the system and the difference in slack after positive velocities and the slack after negative velocities (as defined in Chapter 1). However, the momentum sink does not causes qualitative changes. Furthermore, increases the momentum sink extra nonlinear effects in the current velocity.

The $+$ or $-$ dominance of the system (as defined in Chapter 1) is often used as indicator for the direction of net transport of coarse sediment. Therefore, it is interesting to see what the effect of the momentum sink is on the $+/-$ dominance. As explained in Chapter 1, the system is $+$ dominant corresponds with a relative phase between the M_2 and M_4 of the current velocity such that

$$-\pi/2 < 2\phi_{u,M_2} - \phi_{u,M_4} < \pi/2,$$

and $-$ dominance corresponds with a relative phase such that

$$\pi/2 < 2\phi_{u,M_2} - \phi_{u,M_4} < 3\pi/2,$$

where the relative phase for the current velocity is defined as

$$2\phi_{u,M_2} - \phi_{u,M_4} = 2\arg(\hat{u}_0 + \varepsilon\hat{u}_{1,1}) - \arg(\hat{u}_{1,2}).$$

On the other hand, the difference between the slack after positive velocities and the slack after negative velocities is an indicator for the net transport of fine sediment. As explained in Chapter 1, the slack after positive velocities is longer than the slack after negative velocities if

$$0 < 2\phi_{u,M_2} - \phi_{u,M_4} < \pi$$

and the slack after positive velocities is shorter than slack after negative velocities if

$$\pi < 2\phi_{u,M_2} - \phi_{u,M_4} < 2\pi.$$

The spatial structure of the relative phases is shown in Figure 4.18b. Like before, the ratio of the M_4 and M_2 amplitude determines the size of the tidal distortion. This is plotted in Figure 4.18a. In the middle of the channel both the M_2 (as well as the M_4) amplitude approaches zero and makes the ratio meaningless.

Figure 4.18a reveals that the momentum sink increases the tidal distortion of in the current velocity, u. Figure 4.18b shows that no clear qualitative changes occur due to the momentum sink. Both the $+/-$ dominance of the system and the difference in slack after positive velocities and slack after negative velocities do not change significantly.

Figure 4.18a and 4.18b show that at $x = -14$ km the sinusoidal shape of u is strongly distorted towards $+$ dominance. However, more is going on. In Figure 4.19 the current velocity, u, at $x = -14$ km is plotted versus time. In the upper panels the total signal of u is plotted and in the lower figures the individual constituents are depicted. From Figure 4.18 we expect to see $+$ dominance as the relative phase is close to zero. This is the case, but also an effect not accounted for in the characterization of the $+/-$ dominance is visible. An extra local maximum in the velocity occurs. This effect is already there when the momentum sink is neglected for $\beta = 12$, but is strongly enhanced by the momentum sink. For $\beta = 8$ this is hardly visible without the momentum sink, while with the momentum sink it is clearly visible. Note that the change occurs when $u < 0$. Figure 4.20 shows that this more or less coincides with $\frac{\partial \xi}{\partial t} < 0$ and hence with the time term III, which is related to the momentum sink, is nonzero.

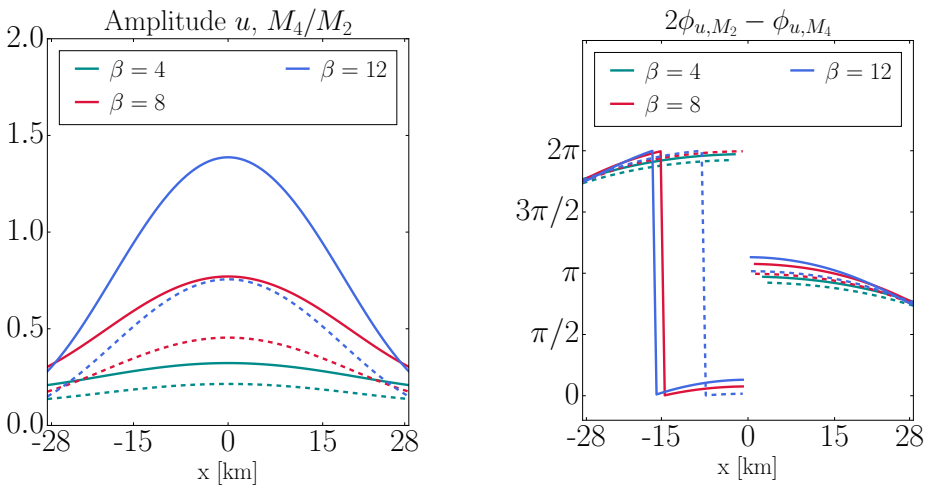

(a) (b)

Figure 4.18. (a) The ratio of the amplitude of M_4 and M_2 of the current velocity, u versus x. (b) The relative phase, $2\phi_{u,M_2} - \phi_{u,M_4}$, of the current velocity versus x. Figure 1.5 shows the interpretation of the relative phase. As before, the solid lines are the cases where momentum sink is taken into account and the dashed lines where it is not. The colors are as in Figure 4.7.

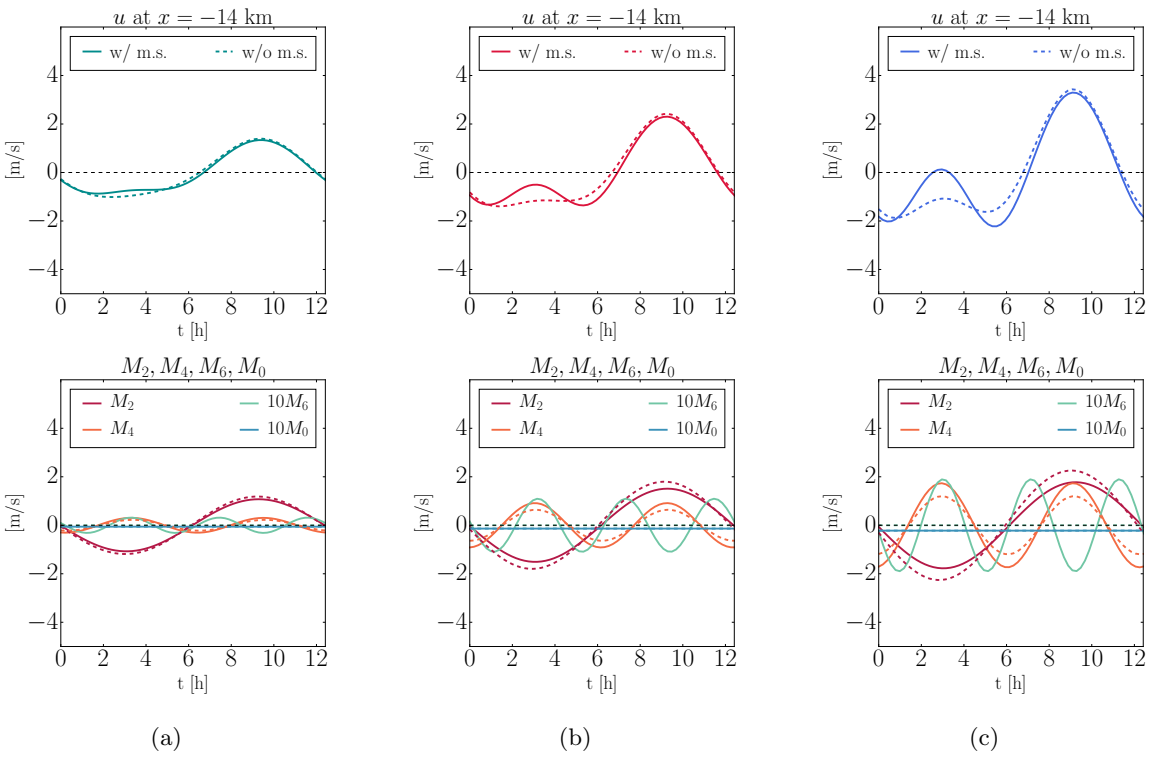

Figure 4.19. The current velocity, u, at $x = -14$ km versus time. (a) is for $\beta = 4$, (b) for $\beta = 8$ and (c) for $\beta = 12$. The upper panels show the total signal of ξ and the lower figures show the individual constituents M_2, M_4, M_6 and M_0. The M_6 and M_0 are multiplied by a factor 10 to make the curves visible. As before, the solid lines are the cases where momentum sink is taken into account (w/ m.s.) and the dashed lines where it is not (w/o m.s.).

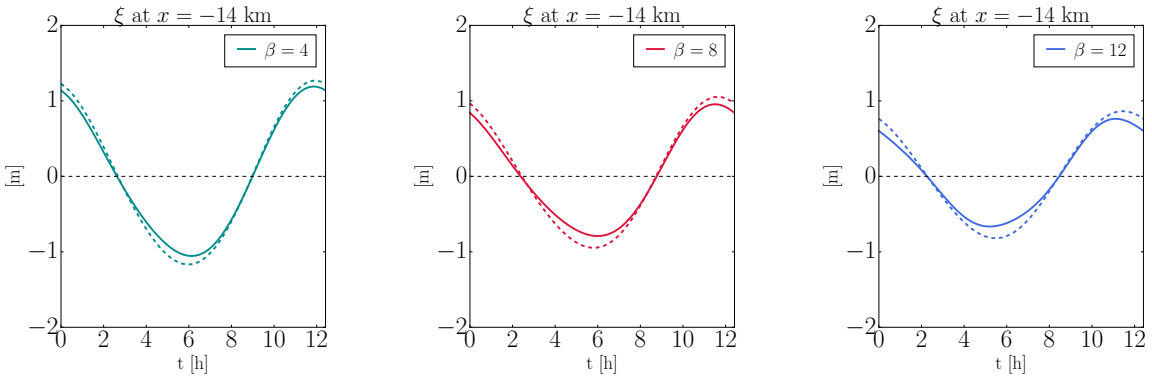

(a) (b) (c)

Figure 4.20. The free surface elevation, ξ, at $x = -14$ km versus time. (a) is for $\beta = 4$, (b) for $\beta = 8$ and (c) for $\beta = 12$. As before, the solid lines are the cases where momentum sink is taken into account and the dashed lines where it is not.

4.4. Additional remarks on results of the model

In this section we make some additional remarks on the results that do not necessarily have a link to the momentum sink. The first remark is that in Figure 4.10a it seems that two local minima in the amplitude of the M_2 of ξ move toward the middle as β increases. This means that the wavelength decreases as β increases. The complex wavenumber is $k = k_1 = \sqrt{(1+\beta)(1+ri)}$. Therefore, when β increases the real part of the complex wavenumber increases and hence the wavelength decreases.The second remark is that for every β the residual current is oriented towards the closest boundary of the channel. Around the middle of the channel there is no to a very small residual current. This follows from the phase difference between the velocity, $\hat{u}_0$, and free surface elevation, $\hat{\xi}_0$ of the forced tide. The residual current velocity is (as in Equation (3.26))

$$\bar{u}_1 = -\overline{u_0\xi_0} = -\frac{1}{2}|\hat{u}_0||\hat{\xi}_0|\cos(\phi_{\hat{u}_0} - \phi_{\hat{\xi}_0}).$$

Figure 4.21c reveals that $\phi_{\hat{u}_0} - \phi_{\hat{\xi}_0} \in (3\pi/2, 2\pi] \cup [2\pi, \pi/2)$ on the left side of the channel and $\phi_{\hat{u}_0} - \phi_{\hat{\xi}_0} \in (\pi/2, 3\pi/2)$ on the right side of the channel. Hence the cosine of this phase difference is positive on the left and negative on the right. With the minus sign this gives a residual current oriented toward the closest boundary. When $\theta = \pi/4$ there are more places in the channel such that $\phi_{\hat{u}_0} - \phi_{\hat{\xi}_0} \in (\pi/2, 3\pi/2)$, as is seen in Figure 4.21d. Therefore the residual current is oriented towards the right boundary at more places than it is to the left boundary as is seen in Figure 4.21b. The 'flat' part of the curves is not at 0 m/s anymore like in 4.21a, but slightly positive. Note that compared to the other constituents the residual current velocity is very small. The third remark is that the point in the middle of the channel, where $u = 0$, disappeared when changing θ to $\pi/4$. Now, both the M_2 and M_4 have a minimum on the right side of the channel. The location of these minima is dependent on β. The fourth remark is that in Figure 4.14b, at approximately $x = 15$ km a sudden drop in M_4 amplitude is found. This is preceded by a small increase that is larger for larger β.

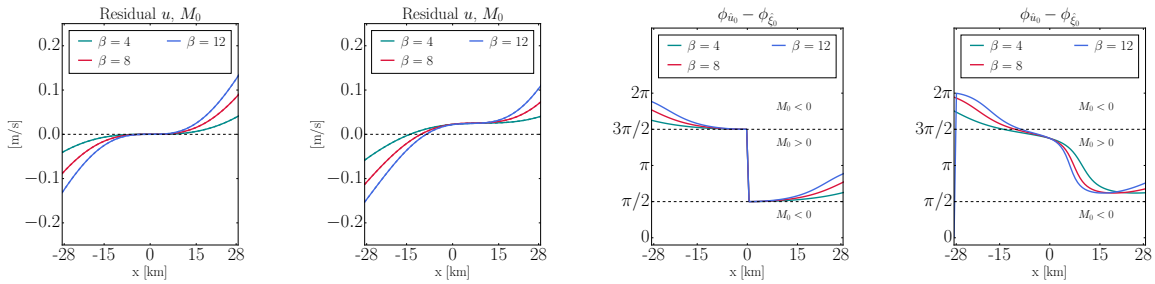

(a) $\theta = 0$ (b) $\theta = \pi/4$ (c) $\theta = 0$ (d) $\theta = \pi/4$

Figure 4.21. (a) and (b) depict the residual current velocity for the case where there is no phase difference between the incoming M_2 waves ($\theta = 0$) and the case where there is a phase difference ($\theta = \pi/4$). (c) and (d) depict the phase difference between the $O(1)$ solution of the free surface elevation, ξ, and the current velocity, u.

CHAPTER 5

Discussion

In Chapter 2 a model was made, in Chapter 3 the model was analyzed and in Chapter 4 the results were presented. These results revealed that for certain parameter settings the effects of the momentum sink are noticeable. In this chapter some remarks on the process of obtaining the results are presented and the results are placed into context with literature.

5.1. On the model

While making a model, one always needs to make assumptions. Some are more drastic than others. In this thesis the goal was to find a simple model such that it is possible to analyze it in detail but at the same time represents reality close enough such that conclusions about the model may be transferred to conclusions about reality. This section summarizes some weak points or strong assumptions of the model that need to be kept in mind.

First of all, the specific one dimensional straight shape of the channel is a simplification of reality. Natural tidal channels are not straight but are curved with large differences between the right and left tidal flats. Furthermore, in systems like the Wadden Sea, neither the width nor the height of the seabed is constant in time and/or space as is assumed in this model. These geometric properties are known to have an influence on the hydrodynamics (see for example Speer and Aubrey (1985) or Prandle and Rahman (1980)). Second, the assumption of $\bar{u}_1 = 0$ on the flats is a strong assumption. In the real world water does flow over the flats but at a smaller speed than in the main channel. The idea behind this assumption is that if the momentum sink does not have any significant effect in this setting, it will probably also not have a significant effect when $\bar{u}_1$ is small instead of zero. However, we did find significant effects and therefore it might be interesting to see what happens if $\bar{u}_1$ is assumed to be small instead of zero. In a two or three dimensional model also $\bar{u}_2$ could be restricted to be smaller on the flats than in the main channel. The third remark on the model is the choice that the momentum sink and (part of the) mass storage are both small, i.e. $O(\varepsilon)$. It might be interesting to investigate the sensitivity of the conclusions to different choices in the scaling of the equations. For example, it would be interesting to see what happens if $\beta = O(\varepsilon^{-1})$ and/or $1/2q = O(1)$. The fourth remark is that at the boundaries we choose to let M_2 signals come in at both sides of the channel. The boundaries of the Marsdiep-Vlie system are connected to the North Sea. In the North Sea it is known that there is a M_4 component present and that this M_4 component in the boundary conditions can cause large changes in the results of the model (see for example Ridderinkhof et al. (2014)).

5.2. On the model analysis

We proceed the discussion with remarks on the asymptotic approximation. An asymptotic approximation is only 'good' if ε is 'small' and the values for ε in the Wadden Sea of about 10^{-1}

are not very small. In particular, at places where the Froude number is higher, (for example around 0.3 as reasonable in the inlet of Ameland) the approximation might less good. In fact, the approximation does not tells us anything about the absolute error of the approximation. The only thing we know is that the error is $O(\varepsilon^2)$ as $\varepsilon \downarrow 0$, that is, if $\varepsilon \downarrow 0$ then the error goes to zero just as fast as ε^2 does. However, as shown in Friedrichs and Aubrey (1994) asymptotic approximations, with the Froude number as small parameter, of solutions to the shallow water equations are often consistent with observations.

A second remark is on a secular term in the solution. In Chapter 3 the ode (3.31) arose,

$$\frac{\partial^2 \hat{\xi}_{1,m}}{\partial x^2} + (k_m)^2 \hat{\xi}_{1,m} = f_m(x). \tag{5.1}$$

Section 3.2.2 in Holmes (2013) states that the solution to the differential equation of a frictionless harmonic oscillator as Equation (5.1), where $k_m > 0$, has a secular term if the forcing, $f_m(x)$, contains part of a solution of the associated homogeneous equations. Now observe that the momentum sink term,

$$\beta u_0 \frac{\partial \xi_0}{\partial t} \mathcal{H}\left(-\frac{\partial \xi_0}{\partial t}\right) = \frac{\beta}{4} \mathrm{Re}\left\{ i \hat{u}_0 \hat{\xi}_0^* \right\} + \sum_{m=1}^{\infty} \mathrm{Re}\left\{ p_m e^{-imt} \right\}$$

has an M_2 forcing in it. And that the $O(1)$ solution (i.e. the the solution of the associated homogeneous equations) only consists of an M_2. Hence, seculair terms must be appearing in the $O(\varepsilon)$ solutions and multiple scale analysis might be needed to obtain a good approximation. The reason we did not see any of these seculair terms (something like $x\varepsilon$) appearing is that they are hidden in the integrals of $\hat{\xi}_{1,m}$. But the fact remains that the solution becomes useless if $x \to \infty$. However, our channel is not very long and in fact $|x| < 1$. But, if the same model is used for very long channels the approximation becomes unreliable and multiple scale analysis is needed. Note that if we were to include a M_4 signal in incoming waves at the boundaries (and with that in the $O(1)$ problem), many more secular terms appear since all forcing terms have a M_4 component.

5.3. On context with literature

In this section results are placed in context with the results found in literature. As stated in the introduction, the momentum sink was recently studied by Alebregtse et al. (2015). There the momentum sink was model the same way as in this study; with the use of the Heaviside function. However, there are three major differences between the model (analysis) in Alebregtse et al. (2015) and this study. The first is that in Alebregtse et al. (2015) a numerical method is used instead of the asymptotic approach used in this study. Second, Alebregtse et al. (2015) considers a semi-enclosed basin instead of a tidal channel that is connected to a open sea on both sides. Third, Alebregtse et al. (2015) only investigates the effect of the momentum sink on the current velocity instead of both the current velocity and the free surface elevation.

Alebregtse et al. (2015) found that, with exponentially decreasing tidal flat width, the momentum sink slightly lowers M_2 and M_6 velocity amplitudes. In this study we also found that the momentum sink lowers the M_2 amplitude of u. However, for the free surface elevation the amplitude of the M_2 is, at some places in the channel, enhanced while at other places it is decreased. Since in this study the friction is linearized, the only M_6 signal is generated by the

momentum sink. We can therefore not comment on an increase or decrease of the M_6 amplitude due to phase differences between the M_6 signal generated by the momentum sink and M_6 signals generated by other sources. Alebregtse et al. (2015) also found that the M_4 velocity amplitude is enhanced by the momentum sink. This is in agreement with our results. Furthermore, Alebregtse et al. (2015) found that the residual velocity slightly decreases for smaller β while for larger ones it increases. In our study it was found that the momentum sink had zero effect on the residual current velocity. This is because the averaged tidal transport that induced the residual current, $\overline{u_0\xi_0}$, only consists of $O(1)$ terms on which the momentum sink has no influence. The numerical method used in Alebregtse et al. (2015) does not make the distinction between $O(1)$ or $O(\varepsilon)$ terms and shows that the momentum sink does have a small effect on the averaged tidal transport and hence on the residual current. This suggests that there is a reason to question our model for the parameter values such that the difference in residual current velocity found in Alebregtse et al. (2015) is not (close to) zero. However, as Alebregtse et al. (2015) considered smaller values for q (steepness of tidal flats) than we did, the values for β where the difference in residual current becomes large (for our choice of q) can not be seen from his figures. Lastly, Alebregtse et al. (2015) showed the dependence of the difference in velocity amplitude on q and β at $x = 0$. Our results revealed that the dependence of x increases as β increases. It might therefore be interesting to see his numerical results at different locations in the channel.

CHAPTER 6

Conclusions

This study aimed to quantify the effects of the dissipation of momentum on shallow tidal flats on the hydrodynamics in a tidal channel. This was done is by formulating a cross sectionally averaged shallow water model where the term representing the momentum sink is not neglected. Approximate solutions to the equations governing the model were constructed by means of a regular asymptotic expansion in a small parameter, ε, which is the ratio of typical tidal amplitude and channel depth.

The first conclusion is that the momentum sink generates overtides of the semi-diurnal lunar constituent, M_2. For both the free surface elevation, ξ, and the current velocity u, a signal of M_2, M_4, M_6, M_{10}, M_{14}, etc. is generated. That is, the momentum sink generates a M_{2m} signal for $m \geq 3$ and $m \not\equiv 0 \mod 2$. The generation is less for higher overtides (larger m) and for that reason only the overtides up to the M_6 were considered. For channels where the tidal flats have the same width as that of the main channel, the generation of overtides due to the momentum sink is small. Therefore, in such channels there is little harm in neglecting the momentum sink.

The second conclusion is that the momentum sink has no influence on the residual current velocity, but the momentum sink increases the absolute value of the residual free surface elevation.

The third conclusion is that when the momentum sink is taken into account, the amplitude of the M_2 constituent of the free surface elevation, ξ, strongly decreases in the middle of the channel and increases at other locations in the channel. For the current velocity, u, the amplitude of the M_2 is decreased everywhere in the channel. The amplitude of the M_4 increases everywhere for both ξ and u. This happens for both the case without a phase difference between the incoming M_2 signals as the case with a phase difference between the incoming M_2 signals at the two boundaries of the channel. Also, the dependence on x of the difference between the solutions including and excluding momentum sink increases as β increases.

The fourth conclusion is that, especially in the middle of the channel, the momentum sink increases the distortion of the sinusoidal shape of the free surface elevation, ξ. The momentum sink increases the characteristic of a longer falling of the tide than the rising. For the case without a phase difference between the incoming M_2 signals at the two boundaries of the channel, in the middle of the channel, the place with the maximal increase in amplitude of the M_4 and M_6, shoulder behavior, i.e., a second high and low water, are possible when the tidal flats are relatively wide compared to the main channel.

A fifth conclusion is that the momentum sink increases the distortion of the sinusoidal shape of the current velocity. In particular increases the momentum sink the difference between the absolute value of the maximum (positive) currents and the absolute value of the minimum (negative) currents. However, it does not causes qualitative changes. Also increases the momentum sink extra nonlinear effects in the current velocity, such as the enlargement of a local maxima in the tidal curve.

Lastly, the expression representing the difference between the solutions of the problems including and excluding the momentum sink are nonlinear in the ratio of the width of the tidal flats and the width of the main channel, β. Hence, the amplitudes of the overtides generated by the momentum sink are nonlinear in β. In fact, the amplitudes of the overtides generated by the momentum sink increase as a β to a power lower than 1. The exact relation between β and the overtides generated by the momentum sink is strongly dependent on the location in the channel.

APPENDIX A

Details on the cross sectionally averaging

The goal of this appendix chapter is to present further details about the calculations made in Chapter 2. If the reader was totally fine with all the calculations made in Chapter 2, this chapter can be skipped. If however, the reader is interested in the details of the calculations this chapter might be worth reading.

1.1. Cross sectionally averaged continuity equation

In this section we take more detailed look at the derivation of the cross sectionally averaged continuity equation starting from the depth averaged continuity equation,

$$\frac{\partial \xi}{\partial t} + \frac{\partial (\xi + h)\bar{u}_1}{\partial x_1} + \frac{\partial (\xi + h)\bar{u}_2}{\partial x_2} = 0.$$

Note that h is discontinuous in x_2 at the boundary of the main channel, $\partial\Omega_2 = \{-b_c/2, b_c/2\}$. This means that its derivative with respect to x_2 is not defined at those points. The term

$$\frac{\partial (\xi + h)\bar{u}_2}{\partial x_2}$$

is therefore potentially undefined at $\partial\Omega_2$. However, as stated in Chapter 2, $(\xi+h)\bar{u}_2$ at a certain x_2 represents the amount of water flowing through the vertical plane at this x_2 (per second per unit length). It would be physically strange if this is not continuous since this would imply that water is torn apart. It thus follows from continuity of the water. If the physical intuition is correct, it should also follow from the continuity equation. Let's check this. The discontinuities of h are at the boundary of Ω_2, therefore define,

$$\Omega_{2,\kappa} = \left[-\left(\frac{b_c}{2} - \kappa \right), \frac{b_c}{2} - \kappa \right], \tag{A.1}$$

where κ is a small parameter. For $\kappa > 0$ we have $\Omega_{2,\kappa} \subsetneq \Omega_2$ and that h is continuous on $\Omega_{2,\kappa}$. We integrate (2.3) over $\Omega_{2,\kappa}$ and take the limit of $\kappa \downarrow 0$,

$$\lim_{\kappa \downarrow 0} \left[\int_{\Omega_{2,\kappa}} \frac{\partial \xi}{\partial t}\, dx_2 + \int_{\Omega_{2,\kappa}} \frac{\partial (\xi + h)\bar{u}_1}{\partial x_1}\, dx_2 + \int_{\Omega_{2,\kappa}} \frac{\partial (\xi + h)\bar{u}_2}{\partial x_2}\, dx_2 \right] = 0. \tag{A.2}$$

The free surface ξ is differentiable with respect to t and also $(\xi + h)\bar{u}_1$ has no reason not to be differentiable with respect to x_1. So, there derivatives with respect to t and x_1, respectively, are bounded. Therefore,

$$\lim_{\kappa \downarrow 0} \int_{\Omega_{2,\kappa}} \frac{\partial \xi}{\partial t}\, dx_2 = 0 \quad \text{and} \quad \lim_{\kappa \downarrow 0} \int_{\Omega_{2,\kappa}} \frac{\partial (\xi + h)\bar{u}_1}{\partial x_1}\, dx_2 = 0. \tag{A.3}$$

Substituting Equations (A.3) in Equation (A.2) leaves

$$\lim_{\kappa \downarrow 0} \int_{\Omega_{2,\kappa}} \frac{\partial(\xi + h)\bar{u}_2}{\partial x_2}\, dx_2 = 0.$$

This can only be zero if

$$\frac{\partial(\xi + h)\bar{u}_2}{\partial x_2}$$

remains bounded. So although h is not continuous in x_2, $(\xi + h)\bar{u}_2$ must indeed be continuous in x_2. Therefore, $\bar{u}_2$ must either be zero at the discontinuities of h or also be discontinuous at those points. This means that although h is discontinuous at $\partial\Omega_2$,

$$\int_{\Omega(t)} \frac{\partial(\xi + h)\bar{u}_2}{\partial x_2}\, dx_2 = (\xi + h)\bar{u}_2(t, x_1, b_c/2) - (\xi + h)\bar{u}_2(t, x_1, -b_c/2)$$

is valid.

One last detail to be said about the derivation of the cross sectionally averaged continuity equation is the following. A integral does not change if its integrand is changed at finitely many points while remaining bounded. On Ω_2, h is constant, h_c, except at the boundaries where it is discontinuous, the integral does not change if we change h to h_c on the boundaries. Although not stated explicitly in Chapter 2 the following calculation is made with this idea in mind,

$$\int_{\Omega_2} \frac{\partial(\xi + h)\bar{u}_1}{\partial x_1}\, dx_2 = \int_{\Omega_2} \frac{\partial(\xi + h_c)\bar{u}_1}{\partial x_1}\, dx_2 = \frac{\partial}{\partial x_1}\left[(\xi + h_c)\int_{\Omega_2} \bar{u}_1\, dx_2\right] = b_c \frac{\partial(\xi + h_c)\hat{u}_1}{\partial x_1}.$$

We can now confidently state that the cross sectionally averaged continuity equation reads

$$b(t)\frac{\partial \xi}{\partial t} + b_c \frac{\partial(\xi + h_c)\hat{u}_1}{\partial x_1} = 0.$$

1.2. Cross sectionally averaged momentum balance

In this section we will clean up the calculations made in the derivation of the cross sectionally averaged momentum balance in Chapter 2. The first depth averaged momentum equation (2.4) reads

$$\frac{\partial(\xi + h)\bar{u}_1}{\partial t} + \frac{\partial(\xi + h)\bar{u}_1\bar{u}_1}{\partial x_1} + \frac{\partial(\xi + h)\bar{u}_1\bar{u}_2}{\partial x_2} = -g(\xi + h)\frac{\partial \xi}{\partial x_1} - \frac{\tau}{\rho}.$$

We integrated this equation over Ω_2. With the idea of changing h to h_c at $\partial\Omega_2$ and the assumption of (2.10) the following calculations are fine:

$$\int_{\Omega_2} \frac{\partial(\xi + h)\bar{u}_1}{\partial t}\, dx_2 = b_c \frac{\partial(\xi + h_c)\hat{u}_1}{\partial t} = b_c(\xi + h_c)\frac{\partial \hat{u}_1}{\partial t} + b_c\hat{u}_1\frac{\partial \xi}{\partial t},$$

$$\int_{\Omega_2} g\frac{\partial \xi}{\partial x_1}\, dx_2 = b_c g \frac{\partial \xi}{\partial x_1},$$

$$\int_{\Omega_2} \frac{\partial(\xi + h)\bar{u}_1\bar{u}_1}{\partial x_1}\, dx_2 = -\hat{u}_1 b(t)\frac{\partial \xi}{\partial t} + b_c(\xi + h_c)\hat{u}_1\frac{\partial \hat{u}_1}{\partial x_1}.$$

However, the terms

$$\int_{\Omega_2} \frac{\partial(\xi + h)\bar{u}_1\bar{u}_2}{\partial x_2}\, dx_2 \quad \text{and} \quad \int_{\Omega_2} \frac{\tau}{\rho(\xi + h)}\, dx_2 \tag{A.4}$$

need extra attention. It is assumed that $\bar{u}_1$ is discontinuous at $\partial\Omega_2$. In fact we have the following (see Figure A.1):

$$\bar{u}_1 = \begin{cases} \hat{u}_1 & \text{if } x_2 \in \Omega_2 \\ 0 & \text{otherwise.} \end{cases}$$

The two terms in (A.4) are investigated in the next two subsections.

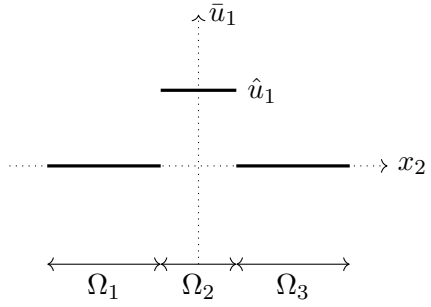

Figure A.1. Depth averaged, along channel velocity, $\bar{u}_1$.

1.2.0.1. *First term in* (A.4).
In the first term in (A.4) a derivative of $\bar{u}_1$ with respect to x_2 occurs. Again, since $\bar{u}_1$ is not continuous at $\partial\Omega_2$ its derivative is not defined in the normal sense at those two points. In the preceding section we were lucky that, before the derivative of h is taken, it is multiplied by another discontinuous function $\bar{u}_2$ such that the product became differentiable. Something similar is not going to happen with the term

$$\frac{\partial(\xi + h)\bar{u}_1\bar{u}_2}{\partial x_2}, \tag{A.5}$$

because we already showed that $(\xi+h)\bar{u}_2$ is continuous in x_2. This term is therefore not defined in the usual sense of derivatives. Luckily, other people ran into similar problems. In order to be able to work with derivatives of discontinuous functions the notion of generalized functions came up. An introduction of generalized functions, also called distributions, is given in e.g. Chapter 5 of Renardy and Rogers (2004). From this book we borrow certain definitions to define the delta distribution that will turn out to be a derivative of the Heaviside function in the sense of distributions. Note that with the Heaviside function, $\mathcal{H}$, defined as in (2.11), $\bar{u}_1$ can be written as

$$\bar{u}_1 = \hat{u}_1\mathcal{H}(x_2 + b_c/2) - \hat{u}_1\mathcal{H}(x_2 - b_c/2).$$

For that reason, the delta distribution might help us make sense of the term (A.5). Looking at the Heaviside function, $\mathcal{H}(x)$, we could argue that its derivative, $\partial\mathcal{H}/\partial x$, at $x = 0$ is ∞. On the other hand, if we approximate $\mathcal{H}$ by a smooth function, $\mathcal{H}_{C\infty}$, that is 1 for $x > \kappa$ and 0 if $x < -\kappa$ for some $\kappa > 0$, the integral

$$\int_a^b \frac{\partial\mathcal{H}_{C\infty}}{\partial x}\,dx = \mathcal{H}_{C\infty}(b) - \mathcal{H}_{C\infty}(a) = 1,$$

for $a < -\kappa$ and $b > \kappa$. This motivates us to look for a function, δ, such that,

$$\delta(x) = \begin{cases} \infty & \text{if } x = 0 \\ 0 & \text{otherwise} \end{cases} \quad \text{and} \quad \int_{-\infty}^{\infty} \delta(x)\,dx = 1.$$

Sadly in the space of 'normal' functions such a function does not exists. One space in which a function somewhat similar to this one does exists, is in the space of distributions. Since the goal of this study is to understand the effect of the momentum sink and not that of discontinuities in the variables, we will not go into the details of the topological space of distributions. However, we introduce distributions (in a not so precise manner) to gain more confidence in the calculations in Chapter 2.

Let $V \subset \mathbb{R}^n$ be a non empty subset and let $C_0^\infty(V)$ be set of compactly supported smooth functions on V, also called test functions. Consider a differentiable function $f \in C^1(V)$ and a test function $\phi \in C_0^\infty(V)$, integration by parts tells us, for every j that

$$\int_V \frac{\partial f}{\partial x_j}\phi \, dx = -\int_V f\frac{\partial \phi}{\partial x_j} \, dx.$$

Next, assume f is not differentiable (but still integrable), the integral

$$-\int_V f\frac{\partial \phi}{\partial x_j} \, dx,$$

must nontheless have similar properties as what would have been

$$\int_V \frac{\partial f}{\partial x_j}\phi \, dx,$$

if it existed. The idea of distributions and their derivatives is closely related to this. We generalize a function by saying, not by what it does with elements in V, but what the integral of its the product with a test function is. So the distribution takes a test function as argument and sends it linearly to $\mathbb{R}$. To reduce notation we write

$$(f, g) = \int_V fg \, dx.$$

A distribution is a linear mapping[1], $(f, \cdot)$,

$$\phi \mapsto (f, \phi) = \int_V f\phi \, dx.$$

Then, based on integration by parts, its derivative, $(\frac{\partial f}{\partial x_j}, \cdot)$ is defined as

$$\phi \mapsto -(f, \frac{\partial \phi}{\partial x_j}) = -\int_V f\frac{\partial \phi}{\partial x_j} \, dx,$$

which does not asks for f to be differentiable. This creates the freedom we need to 'take the derivative' of a discontinuous function. We are now ready to define the delta distribution, δ. The delta distribution, $(\delta, \cdot)$, is defined as

$$(\delta, \phi) = \phi(0).$$

The distributional derivative of the Heaviside function, $\mathcal{H}$, is the delta distribution since

$$(\frac{\partial \mathcal{H}}{\partial x}, \phi) = -(\mathcal{H}, \frac{\partial \phi}{\partial x}) = -\int_0^\infty \frac{\partial \phi}{\partial x}(x) \, dx = \phi(0) = (\delta, \phi).$$

[1] that is continuous is some topology that we will not specify.

Clearly we can still not take the derivative of $\bar{u}_1$ since that is just not possible. However, for $\phi \in C_0^\infty(\mathbb{R})$,

$$\begin{aligned}
\int_{-\infty}^{\infty} \frac{\partial \bar{u}_1}{\partial x_2}\phi \, dx_2 &= \int_{-\infty}^{\infty} \frac{\partial \hat{u}_1 \mathcal{H}(x_2 + b_c/2) - \hat{u}_1 \mathcal{H}(x_2 - b_c/2)}{\partial x_2}\phi \, dx_2 \\
&= \hat{u}_1 \int_{-\infty}^{\infty} \frac{\partial \mathcal{H}(x_2 + b_c/2)}{\partial x_2}\phi \, dx_2 - \hat{u}_1 \int_{-\infty}^{\infty} \frac{\partial \mathcal{H}(x_2 - b_c/2)}{\partial x_2}\phi \, dx_2 \\
&\overset{(!)}{=} -\hat{u}_1 \int_{-\infty}^{\infty} \mathcal{H}(x_2 + b_c/2)\frac{\partial \phi}{\partial x_2} \, dx_2 + \hat{u}_1 \int_{-\infty}^{\infty} \mathcal{H}(x_2 - b_c/2)\frac{\partial \phi}{\partial x_2} \, dx_2 \\
&= -\hat{u}_1 \int_{-b_c/2}^{\infty} \frac{\partial \phi}{\partial x_2} \, dx_2 + \hat{u}_1 \int_{b_c/2}^{\infty} \frac{\partial \phi}{\partial x_2} \, dx_2 \\
&= \hat{u}_1 \phi(-b_c/2) - \hat{u}_1 \phi(b_c/2) \\
&= -\hat{u}_1 \left[\phi(b_c/2) - \phi(-b_c/2)\right].
\end{aligned} \tag{A.6}$$

Where the domain of $\bar{u}_1$ is extended to $\mathbb{R}$ in such a way that it is zero outside $\mathbb{R}\backslash\Omega_2$. In the third row (where '(!)' is placed above the equal sign) we used the distributional derivative of $(\mathcal{H}(x_2 + b_c/2), \cdot)$. Let's take another look at the first term of (A.4) and see if we can clean up the calculation with the help of the delta distribution. Remember the definition of $\Omega_{2,\kappa}$ as in (A.1). For $\kappa \downarrow 0$, the boundary of $\Omega_{2,\kappa}$ approaches the boundary of Ω_2 from the inside. On $\Omega_{2,\kappa}$ for $\kappa > 0$ is $\bar{u}_1$ continuous. Therefore,

$$\begin{aligned}
\lim_{\kappa \downarrow 0} \int_{\Omega_{2,\kappa}} \frac{\partial(\xi + h)\bar{u}_1\bar{u}_2}{\partial x_2} \, dx_2 &= \lim_{\kappa \downarrow 0} \left[(\xi + h)\bar{u}_2\bar{u}_1(b_c/2 - \kappa) - (\xi + h)\bar{u}_2\bar{u}_1(-(b_c/2 - \kappa))\right] \\
&= \lim_{\kappa \downarrow 0} |\Omega_3| \frac{\partial \xi}{\partial t} \left[\bar{u}_1(b_c/2 - \kappa) + \bar{u}_1(-(b_c/2 - \kappa))\right] \\
&= |\Omega_3| \frac{\partial \xi}{\partial t} 2\hat{u}_1.
\end{aligned}$$

For $\kappa < 0$, $\Omega_{2,\kappa}$ is bigger than Ω_2 and includes the boundary of Ω_2 and thus the discontinuities of $\bar{u}_1$. If $\kappa \uparrow 0$ the boundary of $\Omega_{2,\kappa}$ approaches Ω_2 from the outside. We split the term with the product rule.

$$\lim_{\kappa \uparrow 0} \int_{\Omega_{2,\kappa}} \frac{\partial(\xi + h)\bar{u}_1\bar{u}_2}{\partial x_2} \, dx_2 = \lim_{\kappa \uparrow 0} \left[\underbrace{\int_{\Omega_{2,\kappa}} \bar{u}_1 \frac{\partial(\xi + h)\bar{u}_2}{\partial x_2} \, dx_2}_{\text{I}} + \underbrace{\int_{\Omega_{2,\kappa}} (\xi + h)\bar{u}_2 \frac{\partial \bar{u}_1}{\partial x_2} \, dx_2}_{\text{II}} \right]$$

Since $\bar{u}_1 = 0$ on the flat and hence on $\Omega_{2,\kappa}\backslash\Omega_2$, the first part is no problem and equals

$$\text{I} = \int_{\Omega_{2,0}} \bar{u}_1 \frac{\partial(\xi + h)\bar{u}_2}{\partial x_2} \, dx_2 = \hat{u}_1 \left[(\xi + h)\bar{u}_2|_{x_2 = b_c/2} - (\xi + h)\bar{u}_2|_{x_2 = -b_c/2} \right]. \tag{A.7}$$

For term II we use the machinery of the delta distribution. First, we may continuously extent the domain of $\bar{u}_1$ and $(\xi + h)\bar{u}_2$ from $\Omega(t)$ to $\mathbb{R}$ such that they are zero outside $\Omega(t)$. Then since $\frac{\partial \bar{u}_1}{\partial x_2} = 0$ on $\mathbb{R}\backslash\Omega_{2,\kappa}$,

$$\text{II} = \int_{\Omega_{2,\kappa}} (\xi + h)\bar{u}_2 \frac{\partial \bar{u}_1}{\partial x_2} \, dx_2 = \int_{-\infty}^{\infty} (\xi + h)\bar{u}_2 \frac{\partial \bar{u}_1}{\partial x_2} \, dx_2.$$

Now $(\xi + h)\bar{u}_2 \in C_0^\infty(\mathbb{R})$ and can play the role of ϕ in the calculation in (A.6). Hence,

$$\mathrm{II} = \int_{-\infty}^{\infty} (\xi + h)\bar{u}_2 \frac{\partial \bar{u}_1}{\partial x_2}\, dx_2 = -\hat{u}_1 \left[(\xi + h)\bar{u}_2|_{x_2 = b_c/2} - (\xi + h)\bar{u}_2|_{x_2 = -b_c/2} \right].$$

Combining with (A.7) yields

$$\lim_{\kappa \uparrow 0} \int_{\Omega_{2,\kappa}} \frac{\partial (\xi + h)\bar{u}_1 \bar{u}_2}{\partial x_2}\, dx_2 = \lim_{\kappa \uparrow 0} [\mathrm{I} + \mathrm{II}] = 0.$$

This was as expected since the 'derivative' of $\bar{u}_1$ graphically looks like Figure A.2, and the two deltas (the arrows) should cancel each other when integrating over them.

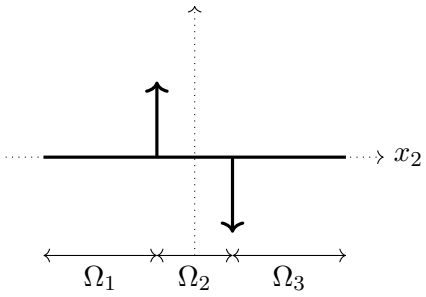

Figure A.2. 'Derivative' of $\bar{u}_1$

To summarize, the expresion for the first problematic term, dependent if $\partial\Omega_{2,\kappa}$ approaches $\partial\Omega_2$ from the in- or outside equals

$$\lim_{\kappa \downarrow 0} \int_{\Omega_{2,\kappa}} \frac{\partial (\xi + h)\bar{u}_1 \bar{u}_2}{\partial x_2}\, dx_2 = |\Omega_3| \frac{\partial \xi}{\partial t} 2\hat{u}_1,$$
$$\lim_{\kappa \uparrow 0} \int_{\Omega_{2,\kappa}} \frac{\partial (\xi + h)\bar{u}_1 \bar{u}_2}{\partial x_2}\, dx_2 = 0.$$

To arrive at

$$\int_{\Omega_2} \frac{\partial (\xi + h)\bar{u}_1 \bar{u}_2}{\partial x_2}\, dx_2 = 2\hat{u}_1 \mathcal{H}\left(\frac{\partial \xi}{\partial t}\right) |\Omega_3(t)| \frac{\partial \xi}{\partial t},$$

as in Chapter 2, we let the boundaries of $\Omega_{2,\kappa}$ follow the flow. This means that we let the boundary of $\Omega_{2,\kappa}$ approach from the inside if the water level rises, and from the outside if the water level drops[2].

1.2.0.2. *Second term in* (A.4).
Let's move to the second term in (A.4) that needed extra attention. First, we investigate what happens with τ at $\partial\Omega_2$. Therefor, define two small intervals, I_κ^+ and I_κ^-, around the discontinuities of $\bar{u}_1$,

$$I_\kappa^\pm = \left[\pm\frac{b_c}{2} - \kappa, \pm\frac{b_c}{2} + \kappa \right].$$

[2]If the reader understands why we should do this, please contact the author.

To gain inside in τ, we integrate the first depth averaged momentum equation (2.4) over I_κ^+ and I_κ^- and let $\kappa \downarrow 0$,

$$\lim_{\kappa\downarrow 0}\int_{I_\kappa^\pm}\left[\frac{1}{\xi+h}\left(\frac{\partial(\xi+h)\bar{u}_1}{\partial t}+\frac{\partial(\xi+h)\bar{u}_1\bar{u}_1}{\partial x_1}+\frac{\partial(\xi+h)\bar{u}_1\bar{u}_2}{\partial x_2}\right)\right]dx_2$$
$$=\lim_{\kappa\downarrow 0}\int_{I_\kappa^\pm}\left[-g\frac{\partial\xi}{\partial x_1}-\frac{\tau}{\rho(\xi+h)}\right]dx_2.$$

Since $(\xi+h)\bar{u}_1$ is differentiable in t, $(\xi+h)\bar{u}_1\bar{u}_1$ is differentiable in x_1 and ξ is independent of x_2, their derivatives are bounded and hence

$$\lim_{\kappa\downarrow 0}\int_{I_\kappa^\pm}\frac{\partial(\xi+h)\bar{u}_1}{\partial t}\,dx_2=0,$$
$$\lim_{\kappa\downarrow 0}\int_{I_\kappa^\pm}\frac{\partial(\xi+h)\bar{u}_1\bar{u}_1}{\partial x_1}\,dx_2=0,$$
$$\lim_{\kappa\downarrow 0}\int_{I_\kappa^\pm}-g\frac{\partial\xi}{\partial x_1}\,dx_2=0.$$

Therefore,

$$\lim_{\kappa\downarrow 0}\int_{I_\kappa^\pm}\frac{\partial(\xi+h)\bar{u}_1\bar{u}_2}{\partial x_2}\,dx_2=\lim_{\kappa\downarrow 0}\int_{I_\kappa^\pm}-\frac{\tau}{\rho(\xi+h)}\,dx_2. \tag{A.8}$$

We know the left hand side is not zero because it includes a delta distribution, hence τ must also include a delta distribution. Let's decompose τ in a part that is smooth and a part that includes the delta distribution[3],

$$\tau=\tau_{\text{smooth}}+\tau_{\text{delta}}.$$

From equation (A.8) it follows that τ_{delta} has the same form as $\bar{u}_1$ as depicted in Figure A.2. Integrating from the inside not a problem. Denote the average of τ as

$$\hat{\tau}=\frac{1}{b_c}\lim_{\kappa\downarrow 0}\int_{\Omega_{2,\kappa}}\tau\,dx_2,$$

then

$$\lim_{\kappa\downarrow 0}\int_{\Omega_{2,\kappa}}\frac{\tau}{\rho(\xi+h)}\,dx_2=\lim_{\kappa\downarrow 0}\int_{\Omega_{2,\kappa}}\frac{\tau_{\text{smooth}}}{\rho(\xi+h)}\,dx_2=b_c\frac{\hat{\tau}}{\rho(\xi+h)}.$$

For $\kappa\uparrow 0$ note that, like before, the two deltas cancel and we obtain again,

$$\lim_{\kappa\uparrow 0}\int_{\Omega_{2,\kappa}}\frac{\tau}{\rho(\xi+h)}\,dx_2=\lim_{\kappa\uparrow 0}\int_{\Omega_{2,\kappa}}\frac{\tau_{\text{smooth}}}{\rho(\xi+h)}\,dx_2=b_c\frac{\hat{\tau}}{\rho(\xi+h)}.$$

Therefore we can be confident that

$$\int_{\Omega_2}\frac{\tau}{\rho(\xi+h)}\,dx_2=b_c\frac{\hat{\tau}_{1b}}{\rho(\xi+h)}.$$

This concludes the cleaning up and we hopefully gained more confidence in the model than after Chapter 2.

[3]Of course it is not possible for a normal function as τ 'to include a delta distribution', so it is better to say the integral as in (A.4) does.

APPENDIX B

Calculations from Chapter 3

In this appendix chapter some calculations are presented, of which only the outcome was specified in the main text. Furthermore, two calculations are included that make implementation of the approximate solutions in, for example, the program language *python*, easier. The implementation is needed to obtain the plots in the main text.

A calculation step that often used is explicitly stated as the following lemma.

LEMMA B.1. Let $z, w \in \mathbb{C}$ and z^*, w^* their complex conjugates, then

$$2\mathrm{Re}\{z\}\,\mathrm{Re}\{w\} = \mathrm{Re}\{zw\} + \mathrm{Re}\{zw^*\}.$$

PROOF.

$$\begin{aligned} 2\mathrm{Re}\{z\}\,\mathrm{Re}\{w\} &= 2\frac{1}{2}(z+z^*)\frac{1}{2}(w+w^*) = \frac{1}{2}(zw + zw^* + z^*w + z^*w^*) \\ &= \frac{1}{2}(zw + (zw)^*) + \frac{1}{2}(zw^* + (zw^*)^*) = \mathrm{Re}\{zw\} + \mathrm{Re}\{zw^*\}. \end{aligned}$$

□

CALCULATION 1. The first calculation is the second equality in (3.26),

$$\bar{u}_1 = -\overline{u_0\xi_0} = -\frac{1}{2}|\hat{u}_0||\hat{\xi}_0|\cos(\phi_{\hat{u}_0} - \phi_{\hat{\xi}_0}).$$

First, note that with lemma B.1,

$$\begin{aligned} \bar{u}_1 = -\overline{u_0\xi_0} &= -\int_{t_0}^{t_0+2\pi} \frac{1}{2}\mathrm{Re}\left\{\hat{u}_0 e^{-it}\right\}\mathrm{Re}\left\{\hat{\xi}_0 e^{-it}\right\} dt \\ &= -\int_{t_0}^{t_0+2\pi} \frac{1}{2}\mathrm{Re}\left\{\hat{u}_0\hat{\xi}_0 e^{-i2t}\right\} dt - \int_{t_0}^{t_0+2\pi} \frac{1}{2}\mathrm{Re}\left\{\hat{u}_0\hat{\xi}_0^*\right\} dt \\ &= -\frac{1}{2}\mathrm{Re}\left\{\hat{u}_0\hat{\xi}_0^*\right\}. \end{aligned}$$

Furthermore,

$$\mathrm{Re}\left\{\hat{u}_0\hat{\xi}_0^*\right\} = \mathrm{Re}\left\{|\hat{u}_0|e^{i\phi_{\hat{u}_0}}|\hat{\xi}_0^*|e^{-i\phi_{\hat{\xi}_0}}\right\} = |\hat{u}_0||\hat{\xi}_0|\mathrm{Re}\left\{e^{i\left(\phi_{\hat{u}_0}-\phi_{\hat{\xi}_0}\right)}\right\} = |\hat{u}_0||\hat{\xi}_0|\cos(\phi_{\hat{u}_0} - \phi_{\hat{\xi}_0}),$$

which shows the second equality in (3.26).

CALCULATION 2. The second calculation is to write the momentum sink term

$$\beta u_0 \frac{\partial \xi_0}{\partial t}\mathcal{H}\left(-\frac{\partial \xi_0}{\partial t}\right),$$

as a Fourier series. First note that

$$-\frac{\partial \xi_0}{\partial t} = -\frac{\partial}{\partial t}\mathrm{Re}\left\{|\hat{\xi}_0|e^{i\phi_{\hat{\xi}_0}}e^{-it}\right\} = -\frac{\partial}{\partial t}|\hat{\xi}_0|\cos(\phi_{\hat{\xi}_0}-t) = |\hat{\xi}_0|\sin(t-\phi_{\hat{\xi}_0}).$$

Hence,

$$\mathcal{H}\left(-\frac{\partial \xi_0}{\partial t}\right) = \begin{cases} 1 & \text{if} \quad \phi_{\hat{\xi}_0} \le t \le \phi_{\hat{\xi}_0}+\pi \\ 0 & \text{otherwise.} \end{cases}$$

Since this is periodic in t with period 2π, there are $c_m \in \mathbb{C}$ for every $m \in \mathbb{Z}$ such that

$$\mathcal{H}\left(-\frac{\partial \xi_0}{\partial t}\right) = \sum_{m\in\mathbb{Z}} c_m e^{imt},$$

with

$$c_m = \frac{1}{2\pi}\int_0^{2\pi} \mathcal{H}\left(-\frac{\partial \xi_0}{\partial t}\right) e^{-imt}\,dt.$$

For $m = 0$,

$$c_0 = \frac{1}{2\pi}\int_0^{2\pi} \mathcal{H}\left(\sin(t-\phi_{\hat{\xi}_0})\right) e^{-imt}\,dt = \frac{1}{2\pi}\int_{\phi_{\hat{\xi}_0}}^{\phi_{\hat{\xi}_0}+\pi} 1\,dt = \frac{1}{2}.$$

For $m \neq 0$,

$$\begin{aligned} c_m &= \frac{1}{2\pi}\int_0^{2\pi} \mathcal{H}\left(\sin(t-\phi_{\hat{\xi}_0})\right) e^{-imt}\,dt = \frac{1}{2\pi}\int_{\phi_{\hat{\xi}_0}}^{\phi_{\hat{\xi}_0}+\pi} e^{-imt}\,dt \\ &= \frac{1}{-im2\pi}\left(e^{-im(\phi_{\hat{\xi}_0}+\pi)} - e^{-im\phi_{\hat{\xi}_0}}\right) = \frac{-i}{m2\pi}\left(1-e^{-im\pi}\right)e^{-im\phi_{\hat{\xi}_0}}. \end{aligned}$$

Certain remarks can be made about the Fourier coefficients, c_m. First of all, like expected, since the Heaviside function has real values, its complex conjugate, $\bar{c}_m$, is c_{-m}. Secondly, for m even, $c_m = 0$, since then $1 - e^{im\pi} = 0$.

Now note that

$$\beta u_0 \frac{\partial \xi_0}{\partial t} = \beta \mathrm{Re}\left\{\hat{u}_0 e^{-it}\right\}\mathrm{Re}\left\{(-i)\hat{\xi}_0 e^{-it}\right\} = \frac{\beta}{2}\mathrm{Re}\left\{(-i)\hat{u}_0\hat{\xi}_0 e^{-i2t}\right\} + \frac{\beta}{2}\mathrm{Re}\left\{i\hat{u}_0\hat{\xi}_0^*\right\}.$$

Denote

$$g_1 = \frac{-i\beta}{2}\hat{u}_0\hat{\xi}_0 \quad \text{and} \quad g_2 = \frac{i\beta}{2}\hat{u}_0\hat{\xi}_0^*.$$

Then, by shifting the indices of the sums,

$$\begin{aligned}
\beta u_0 \frac{\partial \xi_0}{\partial t} \mathcal{H}\left(-\frac{\partial \xi_0}{\partial t}\right) &= \mathrm{Re}\left\{g_1 e^{-i2t} + g_2\right\} \sum_{m\in\mathbb{Z}} c_m e^{imt} \\
&= \frac{1}{2}\left(g_1 e^{-i2t} + g_1^* e^{i2t} + g_2 + g_2^*\right) \sum_{m\in\mathbb{Z}} c_m e^{imt} \\
&= \frac{1}{2}\left(\sum_{m\in\mathbb{Z}} c_m g_1 e^{-i(2-m)t} + \sum_{m\in\mathbb{Z}} c_m g_1^* e^{i(2+m)t} + \sum_{m\in\mathbb{Z}} c_m (g_2 + g_2^*) e^{imt}\right) \\
&= \frac{1}{2}\left(\sum_{m\in\mathbb{Z}} c_{2-m} g_1 e^{-imt} + \sum_{m\in\mathbb{Z}} c_{-m-2} g_1^* e^{-imt} + \sum_{m\in\mathbb{Z}} c_{-m} (g_2 + g_2^*) e^{-imt}\right) \\
&= \frac{1}{2}\sum_{m\in\mathbb{Z}} \left(\underbrace{c_{2-m} g_1 + c_{2+m}^* g_1^* + c_m^* (g_2 + g_2^*)}_{p_m}\right) e^{-imt}.
\end{aligned}$$

Let's denote

$$\begin{aligned}
p_m &= c_{2-m} g_1 + c_{2+m}^* g_1^* + c_m^* (g_2 + g_2^*) \\
&= \frac{i\beta}{2}\left(c_{2+m}^* \hat{u}_0^* \hat{\xi}_0^* - c_{2-m} \hat{u}_0 \hat{\xi}_0\right) + c_m^* 2\mathrm{Re}\left\{g_2\right\} \\
&= \frac{i\beta}{2}\left(c_{2+m}^* \hat{u}_0^* \hat{\xi}_0^* - c_{2-m} \hat{u}_0 \hat{\xi}_0\right) - c_m^* \beta |\hat{u}_0||\hat{\xi}_0| \sin(\phi_{\hat{u}_0} - \phi_{\hat{\xi}_0})
\end{aligned}$$

Note that also $p_m^* = p_{-m}$,

$$p_m^* = c_{2-m}^* g_1^* + c_{2+m} g_1 + c_m (g_2^* + g_2) = c_{2+m} g_1 + c_{2-m}^* g_1^* + c_{-m}^* (g_2 + g_2^*) = p_{-m}.$$

Remembering that $c_0 = \frac{1}{2}$ and that $c_m = 0$ if m is even, yields

$$\begin{aligned}
\beta u_0 \frac{\partial \xi_0}{\partial t} \mathcal{H}\left(-\frac{\partial \xi_0}{\partial t}\right) &= \frac{1}{2} p_0 + \frac{1}{2}\sum_{m=1}^{\infty} (p_m)\, e^{-imt} + \frac{1}{2}\sum_{m=-\infty}^{-1} (p_m)\, e^{-imt} \\
&= \frac{1}{2}\left(\frac{1}{2} 2\mathrm{Re}\left\{g_2\right\}\right) + \sum_{m=1}^{\infty} \frac{1}{2}\left(p_m e^{-imt} + p_m^* e^{imt}\right) \\
&= \frac{1}{2}\mathrm{Re}\left\{g_2\right\} + \sum_{m=1}^{\infty} \mathrm{Re}\left\{p_m e^{-imt}\right\} \\
&= \frac{\beta}{4}\mathrm{Re}\left\{i\hat{u}_0 \hat{\xi}_0^*\right\} + \sum_{m=1}^{\infty} \mathrm{Re}\left\{p_m e^{-imt}\right\}
\end{aligned}$$

Calculation 3. The third calculation is the algebraic manipulations to arrive at equation (3.28),

$$\frac{\partial \bar{\xi}_1}{\partial x} = -\frac{1}{4}\frac{\partial |\hat{u}_0|^2}{\partial x} + |\hat{u}_0||\hat{\xi}_0|\left(r\cos(\phi_{\hat{u}_0} - \phi_{\hat{\xi}_0}) - \frac{\beta}{4}\sin(\phi_{\hat{u}_0} - \phi_{\hat{\xi}_0})\right).$$

from equation (3.27),

$$\int_{t_0}^{t_0+2\pi}\left[\frac{\partial u_1}{\partial t}+\frac{\partial \xi_1}{\partial x}+ru_1+u_0\frac{\partial u_0}{\partial x}-ru_0\xi_0-\beta u_0\frac{\partial \xi_0}{\partial t}\mathcal{H}\left(-\frac{\partial \xi_0}{\partial t}\right)\right]\,dt=0.$$

Since u_1 has period 2π and

$$u_0\frac{\partial u_0}{\partial x}=\frac{1}{2}\frac{\partial u_0^2}{\partial x},$$

equation (3.27) reduces to

$$\frac{\partial \bar{\xi}_1}{\partial x}=-r\bar{u}_1-\frac{1}{2}\frac{\partial \overline{u_0^2}}{\partial x}+r\overline{u_0\xi_0}+\frac{\beta}{4}\overline{\mathrm{Re}\left\{i\hat{u}_0\hat{\xi}_0^*\right\}}.$$

Then, substituting the solutions of $\bar{u}_1$, u_0 and ξ_0 and remembering Calculation 1,

$$\begin{aligned}
-r\bar{u}_1+r\overline{u_0\xi_0}=2\overline{u_0\xi_0}&=r\mathrm{Re}\left\{\hat{u}_0\hat{\xi}_0^*\right\}=|\hat{u}_0||\hat{\xi}_0|\cos(\phi_{\hat{u}_0}-\phi_{\hat{\xi}_0}),\\
-\frac{1}{2}\frac{\partial \overline{u_0^2}}{\partial x}=-\frac{1}{2}\frac{\partial}{\partial x}\int_{t_0}^{t_0+2\pi}&\left[\frac{1}{2}\mathrm{Re}\left\{\hat{u}_0^2e^{-i2t}\right\}+\frac{1}{2}\mathrm{Re}\left\{|\hat{u}_0|^2\right\}\right]\,dt=-\frac{1}{4}\frac{\partial|\hat{u}_0|^2}{\partial x},\\
\frac{\beta}{4}\overline{\mathrm{Re}\left\{i\hat{u}_0\hat{\xi}_0^*\right\}}=\frac{\beta}{4}\mathrm{Re}\left\{i\hat{u}_0\hat{\xi}_0^*\right\}&=-\frac{\beta}{4}\mathrm{Im}\left\{\hat{u}_0\hat{\xi}_0^*\right\}=-\frac{\beta}{4}|\hat{u}_0||\hat{\xi}_0|\sin(\phi_{\hat{u}_0}-\phi_{\hat{\xi}_0}).
\end{aligned}$$

Adding these yields equation (3.28).

Calculation 4. The fourth calculation is the algebraic manipulations needed to arrive at equation (3.30),

$$\begin{aligned}
&\sum_{m=0}^{\infty}\mathrm{Re}\left\{-\left(\frac{\partial^2\hat{\xi}_{1,m}}{\partial x^2}+(1+\beta)m(m+ri)\hat{\xi}_{1,m}\right)e^{-imt}\right\}\\
&\quad=\mathrm{Re}\left\{\underbrace{-2\beta\alpha\hat{\xi}_0}_{\mathrm{V}}e^{-it}\right\}+\mathrm{Re}\left\{\Big(\underbrace{i\frac{\partial}{\partial x}(\hat{u}_0\hat{\xi}_0)}_{\mathrm{IV}}\underbrace{+\frac{1}{4}\frac{\partial^2}{\partial x^2}(\hat{u}_0^2)}_{\mathrm{I}}\underbrace{-r\frac{\partial}{\partial x}(\hat{u}_0\hat{\xi}_0)}_{\mathrm{II}}\underbrace{+2\beta\alpha\hat{\xi}_0^2}_{\mathrm{V}}\Big)e^{-i2t}\right\}\\
&\qquad\underbrace{+\frac{1}{4}\frac{\partial^2}{\partial x^2}(|\hat{u}_0|^2)}_{\mathrm{I}}\underbrace{-r\mathrm{Re}\left\{\frac{\partial}{\partial x}(\hat{u}_0\hat{\xi}_0^*)\right\}}_{\mathrm{II}}\underbrace{-\frac{\beta}{4}\mathrm{Re}\left\{\frac{\partial}{\partial x}(i\hat{u}_0\hat{\xi}_0^*)\right\}-\sum_{m=1}^{\infty}\mathrm{Re}\left\{\frac{\partial p_m}{\partial x}e^{-imt}\right\}}_{\mathrm{III}}.
\end{aligned}$$

Substituting (3.23) in the left hand side of equation (3.22),

$$\begin{aligned}
(1+\beta)\frac{\partial^2\xi_1}{\partial t^2}-\frac{\partial^2\xi_1}{\partial x^2}+(1+\beta)r\frac{\partial\xi_1}{\partial t}=&\underbrace{-\frac{\partial^2}{\partial x\partial t}(u_0\xi_0)}_{\mathrm{IV}}\underbrace{+2\beta\alpha\frac{\partial^2\xi_0}{\partial t^2}-\beta\alpha\frac{\partial^2}{\partial t^2}\left(\xi_0^2\right)}_{\mathrm{V}}\underbrace{+\frac{1}{2}\frac{\partial^2}{\partial x^2}\left(u_0^2\right)}_{\mathrm{I}}\\
&\underbrace{-2r\frac{\partial}{\partial x}(u_0\xi_0)}_{\mathrm{II}}\underbrace{-\frac{\partial}{\partial x}\left(\beta u_0\frac{\partial\xi_0}{\partial t}\mathcal{H}\left(-\frac{\partial\xi_0}{\partial t}\right)\right)}_{\mathrm{III}}.
\end{aligned}$$

gives

$$\sum_{m=0}^{\infty} \mathrm{Re}\left\{\left(-(1+\beta)m^2\hat{\xi}_{1,m} - \frac{\partial^2\hat{\xi}_{1,m}}{\partial x^2} - (1+\beta)rim\hat{\xi}_{1,m}\right)e^{-imt}\right\}$$
$$= \sum_{m=0}^{\infty} \mathrm{Re}\left\{-\left(\frac{\partial^2\hat{\xi}_{1,m}}{\partial x^2} + (1+\beta)m(m+ri)\hat{\xi}_{1,m}\right)e^{-imt}\right\}.$$

For the right hand side we proceed term by term. Lemma B.1 is used multiple times.

$$\text{I}: \quad \frac{1}{2}\frac{\partial^2}{\partial x^2}\left(u_0^2\right) = \frac{1}{2}\frac{\partial^2}{\partial x^2}\left(\frac{1}{2}\mathrm{Re}\left\{\hat{u}_0^2 e^{-i2t}\right\} + \frac{1}{2}|\hat{u}_0|^2\right)$$
$$= \mathrm{Re}\left\{\frac{1}{4}\frac{\partial^2}{\partial x^2}(\hat{u}_0^2)e^{-i2t}\right\} + \frac{1}{4}\frac{\partial^2}{\partial x^2}(|\hat{u}_0|^2),$$

$$\text{II}: \quad -r\frac{\partial}{\partial x}(\hat{u}_0\hat{\xi}_0) = -2r\frac{\partial}{\partial x}\left(\frac{1}{2}\mathrm{Re}\left\{\hat{u}_0\hat{\xi}_0 e^{-i2t}\right\} + \frac{1}{2}\mathrm{Re}\left\{\hat{u}_0\hat{\xi}_0^*\right\}\right)$$
$$= -\mathrm{Re}\left\{r\frac{\partial}{\partial x}(\hat{u}_0\hat{\xi}_0)e^{-i2t}\right\} - \mathrm{Re}\left\{r\frac{\partial}{\partial x}(\hat{u}_0\hat{\xi}_0^*)\right\},$$

$$\text{III}: -\frac{\partial}{\partial x}\left(\beta u_0\frac{\partial\xi_0}{\partial t}\mathcal{H}\left(-\frac{\partial\xi_0}{\partial t}\right)\right) = -\frac{\beta}{4}\mathrm{Re}\left\{\frac{\partial}{\partial x}(i\hat{u}_0\hat{\xi}_0^*)\right\} - \sum_{m=1}^{\infty}\mathrm{Re}\left\{\frac{\partial p_m}{\partial x}e^{-imt}\right\},$$

$$\text{IV}: \quad -\frac{\partial^2}{\partial x\partial t}\left(u_0\xi_0\right) = -\frac{\partial^2}{\partial x\partial t}\left(\frac{1}{2}\mathrm{Re}\left\{\hat{u}_0\hat{\xi}_0 e^{-i2t}\right\} + \frac{1}{2}\mathrm{Re}\left\{\hat{u}_0\hat{\xi}_0^*\right\}\right)$$
$$= \mathrm{Re}\left\{i\frac{\partial}{\partial x}(\hat{u}_0\hat{\xi}_0)e^{-i2t}\right\},$$

$$\text{V}: \quad 2\beta\alpha\frac{\partial^2\xi_0}{\partial t^2} - \beta\alpha\frac{\partial^2}{\partial t^2}\left(\xi_0^2\right) = -2\beta\alpha\mathrm{Re}\left\{\hat{\xi}_0 e^{-it}\right\} - \beta\alpha\frac{\partial^2}{\partial t^2}\left(\frac{1}{2}\mathrm{Re}\left\{\hat{\xi}_0^2 e^{-i2t}\right\} + \frac{1}{2}|\hat{\xi}_0|^2\right)$$
$$= -2\beta\alpha\mathrm{Re}\left\{\hat{\xi}_0 e^{-it}\right\} + 2\beta\alpha\mathrm{Re}\left\{\hat{\xi}_0^2 e^{-i2t}\right\}.$$

Combing these terms and setting it equal to the left hand side yields equation (3.30).

Calculation 5. The fifth calculation is deriving the solution, (3.32),

$$\hat{\xi}_{1,m}(x) = \left(C_m + \frac{1}{2ik_m}\int_{a_1}^{x} e^{-ik_m s}f_m(s)\,ds\right)e^{ik_m x} + \left(D_m - \frac{1}{2ik_m}\int_{a_2}^{x} e^{ik_m s}f_m(s)\,ds\right)e^{-ik_m x},$$

of the ode (3.31),

$$\frac{\partial^2\hat{\xi}_{1,m}}{\partial x^2} + (k_m)^2\hat{\xi}_{1,m} = f_m(x).$$

The solution of the homogenous version of the equation is

$$\hat{\xi}_{1,m,\mathrm{hom}} = C_m e^{ik_m x} + D_m e^{-ik_m x},$$

with $C_m, D_m \in \mathbb{C}$. For every m, call the inhomogeneous part $f_m(x)$. Using the method of variation of parameters (see for example Bender and Orszag (1999)) we first calculate the Wronskian, W_m, of $e^{ik_m x}$ and $e^{-ik_m x}$,

$$W_m = e^{ik_m x}\frac{\partial}{\partial x}\left(e^{-ik_m x}\right) - e^{-ik_m x}\frac{\partial}{\partial x}\left(e^{ik_m x}\right) = -ik_m e^{ik_m x - ik_m x} - ik_m e^{ik_m x - ik_m x} = 2ik_m.$$

The particular solution is then

$$\hat{\xi}_{1,m,\mathrm{par}} = \frac{1}{2ik_m}\left(e^{ik_m x}\int_{a_1}^{x} e^{-ik_m s} f_m(s)\,ds - e^{-ik_m x}\int_{a_2}^{x} e^{ik_m s} f_m(s)\,ds\right),$$

with $a_1, a_2 \in \mathbb{R}$. Combing the $\hat{\xi}_{1,m,\mathrm{hom}}$ and $\hat{\xi}_{1,m,\mathrm{par}}$ yields, equation (3.32).

Calculation 6. The sixth calculation is the calculation of the right hand side of (3.34).

$$\begin{aligned}
&-\frac{1}{2}\frac{\partial}{\partial x}(u_0^2) - \frac{\partial \xi_1}{\partial x} + r u_0 \xi_0 + \beta u_0 \frac{\partial \xi_0}{\partial t}\mathcal{H}\left(-\frac{\partial \xi_0}{\partial t}\right)\\
&\quad = -\frac{1}{4}\mathrm{Re}\left\{\frac{\partial \hat{u}_0^2}{\partial x}e^{-i2t}\right\} - \frac{1}{4}\frac{\partial |\hat{u}_0|^2}{\partial x} - \sum_{m=1}^{\infty}\mathrm{Re}\left\{\frac{\partial \hat{\xi}_{1,m}}{\partial x}e^{-imt}\right\} - \frac{\partial \bar{\xi}_1}{\partial x} + \frac{r}{2}\mathrm{Re}\left\{\hat{u}_0\hat{\xi}_0 e^{-i2t}\right\}\\
&\qquad + \frac{r}{2}\mathrm{Re}\left\{\hat{u}_0\hat{\xi}_0^*\right\} - \frac{\beta}{4}\mathrm{Im}\left\{\hat{u}_0\hat{\xi}_0^*\right\} + \sum_{m=1}^{\infty}\mathrm{Re}\left\{p_m e^{-imt}\right\}\\
&= \mathrm{Re}\left\{-\left(\frac{1}{4}\frac{\partial \hat{u}_0^2}{\partial x} + \frac{\partial \hat{\xi}_{1,2}}{\partial x} - \frac{r}{2}\hat{u}_0\hat{\xi}_0 - p_2\right)e^{-i2t}\right\} + \sum_{\substack{m=1\\ m\neq 2}}^{\infty}\mathrm{Re}\left\{-\left(\frac{\partial \hat{\xi}_{1,m}}{\partial x} - p_m\right)e^{-imt}\right\}\\
&\qquad - \frac{1}{4}\frac{\partial |\hat{u}_0|^2}{\partial x} + \frac{r}{2}\mathrm{Re}\left\{\hat{u}_0\hat{\xi}_0^*\right\} - \frac{\beta}{4}\mathrm{Im}\left\{\hat{u}_0\hat{\xi}_0^*\right\} - \frac{\partial \bar{\xi}_1}{\partial x}\\
&= \mathrm{Re}\left\{-\left(\frac{1}{4}\frac{\partial \hat{u}_0^2}{\partial x} + \frac{\partial \hat{\xi}_{1,2}}{\partial x} - \frac{r}{2}\hat{u}_0\hat{\xi}_0 - p_2\right)e^{-i2t}\right\} + \sum_{\substack{m=1\\ m\neq 2}}^{\infty}\mathrm{Re}\left\{-\left(\frac{\partial \hat{\xi}_{1,m}}{\partial x} - p_m\right)e^{-imt}\right\}\\
&\qquad - \frac{1}{4}\frac{\partial |\hat{u}_0|^2}{\partial x} + \frac{r}{2}\mathrm{Re}\left\{\hat{u}_0\hat{\xi}_0^*\right\} - \frac{\beta}{4}\mathrm{Im}\left\{\hat{u}_0\hat{\xi}_0^*\right\} - \left(-\frac{1}{4}\frac{\partial}{\partial x}(|\hat{u}_0|^2) + r\mathrm{Re}\left\{\hat{u}_0\hat{\xi}_0^*\right\} - \frac{\beta}{4}\mathrm{Im}\left\{\hat{u}_0\hat{\xi}_0^*\right\}\right)\\
&= \mathrm{Re}\left\{-\left(\frac{1}{4}\frac{\partial \hat{u}_0^2}{\partial x} + \frac{\partial \hat{\xi}_{1,2}}{\partial x} - \frac{r}{2}\hat{u}_0\hat{\xi}_0 - p_2\right)e^{-i2t}\right\} + \sum_{\substack{m=1\\ m\neq 2}}^{\infty}\mathrm{Re}\left\{-\left(\frac{\partial \hat{\xi}_{1,m}}{\partial x} - p_m\right)e^{-imt}\right\} - \frac{r}{2}\mathrm{Re}\left\{\hat{u}_0\hat{\xi}_0^*\right\}.
\end{aligned}$$

CALCULATION 7. To implement $\hat{u}_1$ we we need te calculate

$$\frac{\partial \hat{\xi}_{1,m}}{\partial x}.$$

$$\begin{aligned}
\frac{\partial \hat{\xi}_{1,m}}{\partial x} &= \frac{\partial}{\partial x}\left[\left(C_m + \frac{1}{2ik_m}\int_{a_1}^{x} e^{-ik_m s} f_m(s)\,ds\right)e^{ik_m x} + \left(D_m - \frac{1}{2ik_m}\int_{a_2}^{x} e^{ik_m s} f_m(s)\,ds\right)e^{-ik_m x}\right] \\
&= \frac{1}{2ik_m}\frac{\partial}{\partial x}\left[e^{ik_m x}\int_{a_1}^{x} e^{-ik_m s} f_m(s)\,ds - e^{-ik_m x}\int_{a_2}^{x} e^{ik_m s} f_m(s)\,ds\right] \\
&= \frac{1}{2ik_m}\Bigg(e^{ik_m x}e^{-ik_m x} f_m(x) + (ik_m)e^{ik_m x}\int_{a_1}^{x} e^{-ik_m s} f_m(s)\,ds \\
&\quad - e^{-ik_m x}e^{ik_m x} f_m(x) - (-ik_m)e^{-ik_m x}\int_{a_2}^{x} e^{ik_m s} f_m(s)\,ds\Bigg) \\
&= \frac{(ik_m)e^{ik_m x}}{2ik_m}\int_{a_1}^{x} e^{-ik_m s} f_m(s)\,ds + \frac{(ik_m)e^{-ik_m x}}{2ik_m}e^{-ik_m x}\int_{a_2}^{x} e^{ik_m s} f_m(s)\,ds \\
&= \frac{e^{ik_m x}}{2}\int_{a_1}^{x} e^{-ik_m s} f_m(s)\,ds + \frac{e^{-ik_m x}}{2}\int_{a_2}^{x} e^{ik_m s} f_m(s)\,ds.
\end{aligned}$$

CALCULATION 8. Another thing to notice before implementing is that there is no need to calculate

$$\frac{\partial p_m}{\partial x}.$$

The terms where this term appears is in f_m. Denote

$$f_m = \tilde{f}_m + \frac{\partial p_m}{\partial x}$$

where $\tilde{f}_m = f_m - \frac{\partial p_m}{\partial x}$. The term, f_m, occurs in $\hat{\xi}_{1,m}$

$$\hat{\xi}_{1,m}(x) = \left(C_m + \frac{1}{2ik_m}\int_{a_1}^{x} e^{-ik_m s} f_m(s)\,ds\right)e^{ik_m x} + \left(D_m - \frac{1}{2ik_m}\int_{a_2}^{x} e^{ik_m s} f_m(s)\,ds\right)e^{-ik_m x}.$$

Now, notice that

$$\begin{aligned}
\int_{a_1}^{x} e^{-ik_m s} f_m(s)\,ds &= \int_{a_1}^{x} e^{-ik_m s}\tilde{f}_m(s)\,ds + \int_{a_1}^{x} e^{-ik_m s}\frac{\partial p_m}{\partial x}(s)\,ds \\
&= \int_{a_1}^{x} e^{-ik_m s}\tilde{f}_m(s)\,ds + e^{-ik_m x}p_m(x) - e^{-ik_m a_1}p_m(a_1) - \int_{a_1}^{x} -ik_m e^{-ik_m s}p_m(s)\,ds.
\end{aligned}$$

Similarly,

$$\int_{a_2}^{x} e^{ik_m s} f_m(s)\,ds = \int_{a_2}^{x} e^{ik_m s}\tilde{f}_m(s)\,ds + e^{ik_m x}p_m(x) - e^{ik_m a_2}p_m(a_2) - \int_{a_2}^{x} ik_m e^{ik_m s}p_m(s)\,ds.$$

APPENDIX C

The depth averaged shallow water equations

In this chapter we will derive depth averaged shallow water equations from the equations of motion. This consists of making the assumptions listed in Chapter 2 and integrate over the depth. Inspiration for this section is taken from Wesseling (2001), Parker (1984), Winant (2007) and Alebregtse et al. (2015). Figure 2.1 in Chapter 2 shows the domain and the placement of the x_1, x_2, x_3 axis. The free surface elevation, ξ, and the current velocity, u, are also explained in Chapter 2. In the main text h only depends on x_2, but it is not much more work to keep h more general. This way we derive a more general version of the depth averaged shallow water equations. When taking the average over the cross section we do assume h to be only dependent of x_2.

The equations of motion (see for example Cushman-Roisin and Beckers (2011)) consists of one equation that represents the balance of mass, also called the continuity equation,

$$\frac{\partial u_1}{\partial x_1} + \frac{\partial u_2}{\partial x_2} + \frac{\partial u_3}{\partial x_3} = 0,$$

and three equations that represent the balance of momentum,

$$\begin{aligned}
\frac{\partial u_1}{\partial t} + u_1\frac{\partial u_1}{\partial x_1} + u_2\frac{\partial u_1}{\partial x_2} + u_3\frac{\partial u_1}{\partial x_3} + f_* u_3 - f u_2 &= -\frac{1}{\rho}\frac{\partial p}{\partial x_1} + \frac{1}{\rho}\frac{\partial \tau_{11}}{\partial x_1} + \frac{1}{\rho}\frac{\partial \tau_{12}}{\partial x_2} + \frac{1}{\rho}\frac{\partial \tau_{13}}{\partial x_3},\\
\frac{\partial u_2}{\partial t} + u_1\frac{\partial u_2}{\partial x_1} + u_2\frac{\partial u_2}{\partial x_2} + u_3\frac{\partial u_2}{\partial x_3} + f u_1 &= -\frac{1}{\rho}\frac{\partial p}{\partial x_2} + \frac{1}{\rho}\frac{\partial \tau_{21}}{\partial x_1} + \frac{1}{\rho}\frac{\partial \tau_{22}}{\partial x_2} + \frac{1}{\rho}\frac{\partial \tau_{23}}{\partial x_3},\\
\frac{\partial u_3}{\partial t} + u_1\frac{\partial u_3}{\partial x_1} + u_2\frac{\partial u_3}{\partial x_2} + u_3\frac{\partial u_3}{\partial x_3} - f_* u_1 &= -g - \frac{1}{\rho}\frac{\partial p}{\partial x_3} + \frac{1}{\rho}\frac{\partial \tau_{31}}{\partial x_1} + \frac{1}{\rho}\frac{\partial \tau_{32}}{\partial x_2} + \frac{1}{\rho}\frac{\partial \tau_{33}}{\partial x_3}.
\end{aligned}$$

In these equations, $x = (x_1, x_2, x_3)$ is the spacial coordinate, t the time coordinate, u_1 (m s^{-1}) the horizontal velocity in the along channel direction, u_2 (m s^{-1}) the horizontal velocity in the cross section, u_3 (m s^{-1}) the vertical velocity, ρ (kg m^{-3}) the density, p (N m^{-2}) the pressure, g (m s^{-2}) the gravitational acceleration, f (rad s^{-1}) the Coriolis parameter, f_* (rad s^{-1}) the reciprocal Coriolis parameter and τ_{ij} (N m^{-2}) is the internal stress working in the x_i direction at a surface with normal pointing in the x_j direction.

We start with the assumption that the depth is much smaller than the both the length and the width of the channel. The momentum balances reduce to (see for example Parker (1984)),

(C.1)

$$\frac{\partial u_1}{\partial t} + u_1\frac{\partial u_1}{\partial x_1} + u_2\frac{\partial u_1}{\partial x_2} + u_3\frac{\partial u_1}{\partial x_3} + \cancel{f_* u_3} - f u_2 = -\frac{1}{\rho}\frac{\partial p}{\partial x_1} + \cancel{\frac{1}{\rho}\frac{\partial \tau_{11}}{\partial x_1}} + \cancel{\frac{1}{\rho}\frac{\partial \tau_{12}}{\partial x_2}} + \frac{1}{\rho}\frac{\partial \tau_{13}}{\partial x_3},$$

(C.2)
$$\frac{\partial u_2}{\partial t} + u_1\frac{\partial u_2}{\partial x_1} + u_2\frac{\partial u_2}{\partial x_2} + u_3\frac{\partial u_2}{\partial x_3} + f u_1 = -\frac{1}{\rho}\frac{\partial p}{\partial x_2} + \cancel{\frac{1}{\rho}\frac{\partial \tau_{21}}{\partial x_1}} + \cancel{\frac{1}{\rho}\frac{\partial \tau_{22}}{\partial x_2}} + \frac{1}{\rho}\frac{\partial \tau_{23}}{\partial x_3},$$

(C.3)
$$\cancel{\frac{\partial u_3}{\partial t}} + \cancel{u_1\frac{\partial u_3}{\partial x_1}} + \cancel{u_2\frac{\partial u_3}{\partial x_2}} + \cancel{u_3\frac{\partial u_3}{\partial x_3}} - \cancel{f_* u_1} = -g - \frac{1}{\rho}\frac{\partial p}{\partial x_3} + \cancel{\frac{1}{\rho}\frac{\partial \tau_{31}}{\partial x_1}} + \cancel{\frac{1}{\rho}\frac{\partial \tau_{32}}{\partial x_2}} + \cancel{\frac{1}{\rho}\frac{\partial \tau_{33}}{\partial x_3}}.$$

With the Equation (C.3) and the boundary condition, $p = p_a$ at the free surface, we can find a relation between the pressure, p, and the free surface elevation, ξ. The third momentum equation reduces to the so called hydrostatic balance,

(C.4)
$$0 = -g - \frac{1}{\rho}\frac{\partial p}{\partial x_3}.$$

Its interpretation of Equation (C.4) is that the pressure in the water at a certain level is only caused by the weight of the fluid above this level. Integrating Equation (C.4) yields

$$p(x_1, x_2, x_3) = C(x_1, x_2) - \rho g x_3,$$

with $C(x_1, x_2) \in \mathbb{R}$, determined by the fact that at the free surface $x_3 = \xi$ the pressure is the same as the atmospheric pressure p_a. We will assume that there are no strong storms surges traveling over the channel and take $p_a \in \mathbb{R}$ constant. This boundary condition gives us an expression for $C(x_1, x_2)$,

$$p_a = p(x_1, x_2, \xi) = C(x_1, x_2) + \rho g \xi.$$

Hence, from equation (C.3) we learn,

(C.5)
$$p = p_a + \rho g(\xi - x_3).$$

Consequently for $\alpha \in \{1, 2\}$,

(C.6)
$$\frac{1}{\rho}\frac{\partial p}{\partial x_\alpha} = g\frac{\partial \xi}{\partial x_\alpha}.$$

The next assumption is that the channel is not only shallow but also very narrow. In this case, the pressure gradient dominates the other terms in the second momentum equation and in the Coriolis term can be neglected in the first momentum equation. With this assumption and substituting (C.6), the equations (C.1) - (C.3) become (see Winant (2007), where the parameter α is very small)

(C.7)
$$\frac{\partial u_1}{\partial t} + u_1\frac{\partial u_1}{\partial x_1} + u_2\frac{\partial u_1}{\partial x_2} + u_3\frac{\partial u_1}{\partial x_3} - \cancel{f u_2} = -g\frac{\partial \xi}{\partial x_1} + \frac{1}{\rho}\frac{\partial \tau_{13}}{\partial x_3},$$

(C.8)
$$\cancel{\frac{\partial u_2}{\partial t}} + \cancel{u_1\frac{\partial u_2}{\partial x_1}} + \cancel{u_2\frac{\partial u_2}{\partial x_2}} + \cancel{u_3\frac{\partial u_2}{\partial x_3}} + \cancel{f u_1} = -g\frac{\partial \xi}{\partial x_2} + \cancel{\frac{1}{\rho}\frac{\partial \tau_{23}}{\partial x_3}}.$$

We conclude that in a shallow and very narrow channel, the momentum balance becomes

$$\frac{\partial u_1}{\partial t} + u_1\frac{\partial u_1}{\partial x_1} + u_2\frac{\partial u_1}{\partial x_2} + u_3\frac{\partial u_1}{\partial x_3} = -g\frac{\partial \xi}{\partial x_1} + \frac{1}{\rho}\frac{\partial \tau_{13}}{\partial x_3}, \tag{C.9}$$

$$0 = -g\frac{\partial \xi}{\partial x_2}, \tag{C.10}$$

and the continuity equation remains unchanged,

$$\frac{\partial u_1}{\partial x_1} + \frac{\partial u_2}{\partial x_2} + \frac{\partial u_3}{\partial x_3} = 0. \tag{C.11}$$

Note that Equation (C.10) implies that ξ is independent of x_2. Before taking integrals over the depth, we derive two equalities coming from the kinematic boundary conditions that water will not mix with the atmosphere or with the sand at the bottom. A water particle at position x at time t is at the free surface if $F(t,x) = x_3 - \xi(t,x_1,x_2) = 0$. Similarly a particle is at the bottom of the sea, if $H(t,x) = x_3 - (-h)(t,x_1,x_2) = 0$. A particle at the free surface will stay at the free surface and a particle that is at the bottom follows the shape of the bottom during a time interval. Hence,

$$\begin{aligned} 0 = \frac{DF}{Dt} &= \frac{Dx_3}{Dt} - \frac{D\xi}{Dt} && \text{at} \quad x_3 = \xi, \\ 0 = \frac{DH}{Dt} &= \frac{Dx_3}{Dt} - \frac{D(-h)}{Dt} && \text{at} \quad x_3 = -h. \end{aligned}$$

Since $Dx_3/Dt = u_3$, this gives us

$$u_1\frac{\partial \xi}{\partial x_1} + u_2\frac{\partial \xi}{\partial x_2} = u_3 - \frac{\partial \xi}{\partial t} \qquad \text{at} \quad x_3 = \xi, \tag{C.12}$$

$$u_1\frac{\partial (-h)}{\partial x_1} + u_2\frac{\partial (-h)}{\partial x_2} = u_3 - \frac{\partial (-h)}{\partial t} \quad \text{at} \quad x_3 = -h. \tag{C.13}$$

These equalities will be used later on.

3.1. Depth averaged continuity equation

In this section we will integrate the continuity equations over the depth of the channel to derive the depth averaged continuity equation. The average of u_1, over the depth is given by

$$\bar{u}_1 = \frac{1}{\xi + h}\int_{-h}^{\xi} u_1\, dx_3. \tag{C.14}$$

We integrate the continuity equation (C.11) over x_3 from $-h$ to ξ. This yields

$$0 = \int_{-h}^{\xi}\left[\frac{\partial u_1}{\partial x_1} + \frac{\partial u_2}{\partial x_2} + \frac{\partial u_3}{\partial x_3}\right] dx_3 = \int_{-h}^{\xi}\left[\frac{\partial u_1}{\partial x_1} + \frac{\partial u_2}{\partial x_2}\right] dx_3 + u_3|_{x_3=\xi} - u_3|_{x_3=-h}\,. \tag{C.15}$$

Using the Leibniz's rule,

$$\frac{\partial}{\partial t}\int_{a(t)}^{b(t)} f(t,x)\, dx = \int_{a(t)}^{b(t)} \frac{\partial f(t,x)}{\partial t}\, dx - f(t,a(t))\frac{\partial a(t)}{\partial t} + f(t,b(t))\frac{\partial b(t)}{\partial t}, \tag{C.16}$$

notice that

$$\int_{-h}^{\xi}\left[\frac{\partial u_1}{\partial x_1} + \frac{\partial u_2}{\partial x_2}\right] dx_3 = \sum_{j=1}^{2}\left[\frac{\partial}{\partial x_j}\int_{-h}^{\xi} u_j\, dx_3 + u_j|_{x_3=-h}\frac{\partial (-h)}{\partial x_j} - u_j|_{x_3=\xi}\frac{\partial \xi}{\partial x_j}\right].$$

Substituting this in (C.15) and using (C.12) and (C.13) yields

$$\begin{aligned} 0 &= \sum_{j=1}^{2} \left[\frac{\partial(\xi+h)\bar{u}_j}{\partial x_j} + u_j|_{x_3=-h} \frac{\partial(-h)}{\partial x_j} - u_j|_{x_3=\xi} \frac{\partial \xi}{\partial x_j} \right] + u_3|_{x_3=\xi} - u_3|_{x_3=-h} \\ &= \sum_{j=1}^{2} \frac{\partial(\xi+h)\bar{u}_j}{\partial x_j} + \frac{\partial \xi}{\partial t} - \frac{\partial(-h)}{\partial t}. \end{aligned}$$

We conclude that the depth averaged continuity equation is

$$\frac{\partial(\xi+h)}{\partial t} + \frac{\partial(\xi+h)\bar{u}_1}{\partial x_1} + \frac{\partial(\xi+h)\bar{u}_2}{\partial x_2} = 0.$$

If h is constant in t and x_1 this reduces to

$$\frac{\partial \xi}{\partial t} + \frac{\partial(\xi+h)\bar{u}_1}{\partial x_1} + \frac{\partial(\xi+h)\bar{u}_2}{\partial x_2} = 0.$$

3.2. Depth averaged momentum balance

In this section we take the integral of the momentum balance equations over the depth of the channel to derive a depth averaged momentum balance. The third equation in the momentum balance gave us a relation between p and ξ and the second equation only tells us we consider ξ to be independent of x_2. For the remaining equation (C.9) we take the average over the depth,

$$\frac{1}{\xi+h} \int_{-h}^{\xi} \left[\frac{\partial u_1}{\partial t} + u_1 \frac{\partial u_1}{\partial x_1} + u_2 \frac{\partial u_1}{\partial x_2} + u_3 \frac{\partial u_1}{\partial x_3} \right] dx_3 = \frac{1}{\xi+h} \int_{-h}^{\xi} \left[-\frac{1}{\rho} \frac{\partial p}{\partial x_1} + \frac{1}{\rho} \frac{\partial \tau_{13}}{\partial x_3} \right] dx_3. \tag{C.17}$$

We start with the left hand side of equation (C.17). With corollary C.16, the continuity equation and equations (C.12) and (C.13), we find,

$$\frac{1}{\xi+h} \int_{-h}^{\xi} \left[\frac{\partial u_1}{\partial t} + u_1 \frac{\partial u_1}{\partial x_1} + u_2 \frac{\partial u_1}{\partial x_2} + u_3 \frac{\partial u_1}{\partial x_3} \right] dx_3 = \frac{\partial(\xi+h)\bar{u}_1}{\partial t} + \sum_{j=1}^{2} \left[\frac{\partial}{\partial x_j} \int_{-h}^{\xi} u_1 u_j \, dx_3 \right]. \tag{C.18}$$

Details of the calculation are given in the box below.

First notice that, by the continuity equation,

$$\sum_{j=1}^{3} \frac{\partial u_1 u_j}{\partial x_j} = \sum_{j=1}^{3} \left[u_1 \frac{\partial u_j}{\partial x_j} + u_j \frac{\partial u_1}{\partial x_j} \right] = \sum_{j=1}^{3} u_j \frac{\partial u_1}{\partial x_j}.$$

The left hand side of equation (C.17) therefore equals

$$\frac{1}{\xi+h} \int_{-h}^{\xi} \left[\underbrace{\frac{\partial u_1}{\partial t}}_{\text{I}} + \underbrace{\sum_{j=1}^{2} \frac{\partial u_1 u_j}{\partial x_j}}_{\text{II}} + \underbrace{\frac{\partial u_1 u_3}{\partial x_3}}_{\text{III}} \right] dx_3.$$

The terms I, II, III are worked out separately.

$$\text{I}: \qquad \int_{-h}^{\xi} \frac{\partial u_1}{\partial t}\, dx_3 = \frac{\partial(\xi+h)\bar{u}_1}{\partial t} + u_1|_{x_3=-h}\, \frac{\partial(-h)}{\partial t} - u_1|_{x_3=\xi}\, \frac{\partial \xi}{\partial t}.$$

$$\begin{aligned}
\text{II}: \int_{-h}^{\xi} \sum_{j=1}^{2} \frac{\partial u_1 u_j}{\partial x_j}\, dx_3 &= \sum_{j=1}^{2} \left[\frac{\partial}{\partial x_j} \int_{-h}^{\xi} u_1 u_j\, dx_3 \right] + u_1|_{x_3=-h} \left(\sum_{j=1}^{2} u_j|_{x_3=-h}\, \frac{\partial(-h)}{\partial x_j} \right) \\
&\quad - u_1|_{x_3=\xi} \left(\sum_{j=1}^{2} u_j|_{x_3=\xi}\, \frac{\partial \xi}{\partial x_j} \right) \\
&= \sum_{j=1}^{2} \left[\frac{\partial}{\partial x_j} \int_{-h}^{\xi} u_1 u_j\, dx_3 \right] + u_1|_{x_3=\xi} \left(u_3|_{x_3=-h} - \frac{\partial(-h)}{\partial t} \right) \\
&\quad - u_1|_{x_3=\xi} \left(u_3|_{x_3=\xi} - \frac{\partial \xi}{\partial t} \right) \\
&= \sum_{j=1}^{2} \left[\frac{\partial}{\partial x_j} \int_{-h}^{\xi} u_1 u_j\, dx_3 \right] + u_1|_{x_3=-h}\, u_3|_{x_3=-h} - u_1|_{x_3=-h}\, \frac{\partial(-h)}{\partial t} \\
&\quad - u_1|_{x_3=\xi}\, u_3|_{x_3=\xi} + u_1|_{x_3=\xi}\, \frac{\partial \xi}{\partial t},
\end{aligned}$$

$$\text{III}: \qquad \int_{-h}^{\xi} \frac{\partial u_1 u_3}{\partial x_3}\, dx_3 = u_1|_{x_3=\xi}\, u_3|_{x_3=\xi} - u_1|_{x_3=-h}\, u_3|_{x_3=-h}\,.$$

Many terms cancel, combining all them yields equation (C.18).

In order to arrive at a momentum balance dependent of $\bar{u}_1$ and independent of u_1, we need the second term on the right hand side of (C.18) also to be expressed in terms of the depth averaged velocity. Let $u_1 = \bar{u}_1 + \tilde{u}_1$ and the same for u_2. So $\tilde{u}_1$ is the difference between the actual value and the depth averaged value. We assume

$$\frac{\partial}{\partial x_1} \int_{-h}^{\xi} \tilde{u}_1 \tilde{u}_1\, dx_3 + \frac{\partial}{\partial x_2} \int_{-h}^{\xi} \tilde{u}_1 \tilde{u}_2\, dx_3 = 0, \tag{C.19}$$

so for the horizontal velocities the derivative with respect to x_1 and x_2 of the difference between the average value over one tidal period and its actual value is neglected. Another option would be to parameterize these terms. The second term in equation (C.18) becomes

$$\sum_{j=1}^{2} \frac{\partial}{\partial x_j} \int_{-h}^{\xi} u_1 u_j\, dx_3 = \sum_{j=1}^{2} \frac{\partial}{\partial x_j} \int_{-h}^{\xi} \bar{u}_1 \bar{u}_j\, dx_3 = \sum_{j=1}^{2} \frac{\partial(\xi+h)\bar{u}_1 \bar{u}_j}{\partial x_j}.$$

Details of the calculation is giving in the box below.

Clearly, integrating $\tilde{u}_1 = u_1 - \bar{u}_1$, gives

$$\int_{-h}^{\xi} \tilde{u}_1\, dx_3 = \int_{-h}^{\xi} u_1\, dx_3 - (\xi+h)\bar{u}_3 = 0.$$

Then,

$$\begin{aligned}
&\sum_{j=1}^{2} \frac{\partial}{\partial x_j} \int_{-h}^{\xi} u_1 u_j \, dx_3 \\
&\quad = \sum_{j=1}^{2} \frac{\partial}{\partial x_j} \int_{-h}^{\xi} (\bar{u}_1 + \tilde{u}_1)(\bar{u}_j + \tilde{u}_j) \, dx_3 \\
&\quad = \sum_{j=1}^{2} \Big[\frac{\partial}{\partial x_j} \int_{-h}^{\xi} \bar{u}_j \bar{u}_1 \, dx_3 + \frac{\partial}{\partial x_j} \left(\bar{u}_j \int_{-h}^{\xi} \tilde{u}_1 \, dx_3 \right) + \frac{\partial}{\partial x_j} \left(\bar{u}_1 \int_{-h}^{\xi} \tilde{u}_j \, dx_3 \right) \\
&\qquad + \frac{\partial}{\partial x_j} \int_{-h}^{\xi} \tilde{u}_1 \tilde{u}_j \, dx_3 \Big] \\
&\quad = \sum_{j=1}^{2} \left[\frac{\partial}{\partial x_j} \int_{-h}^{\xi} \bar{u}_1 \bar{u}_j \, dx_3 + \frac{\partial}{\partial x_j} \int_{-h}^{\xi} \tilde{u}_1 \tilde{u}_j \, dx_3 \right] \\
&\quad = \sum_{j=1}^{2} \frac{\partial}{\partial x_j} \int_{-h}^{\xi} \bar{u}_1 \bar{u}_j \, dx_3.
\end{aligned}$$

We found the left hand side of equation (C.17) to be

$$\frac{1}{\xi + h} \left(\frac{\partial (\xi + h) \bar{u}_1}{\partial t} + \frac{\partial (\xi + h) \bar{u}_1 \bar{u}_1}{\partial x_1} + \frac{\partial (\xi + h) \bar{u}_1 \bar{u}_2}{\partial x_2} \right). \tag{C.20}$$

For the pressure gradient term we get

$$\frac{1}{\xi + h} \int_{-h}^{\xi} -g \frac{\partial \xi}{\partial x_1} \, dx_3 = -g \frac{\partial \xi}{\partial x_1}.$$

We neglect (wind) stress at the free surface and write $\tau = \tau_{13}|_{x_3 = -h}$, for the stress at the bottom in the direction of x_1. For the internal friction terms we obtain,

$$\frac{1}{\xi + h} \int_{-h}^{\xi} \frac{1}{\rho} \frac{\partial \tau_{13}}{\partial x_3} \, dx_3 = \frac{1}{\rho(\xi + h)} \left(\tau_{13}|_{x_3 = \xi} - \tau_{13}|_{x_3 = -h} \right) = -\frac{\tau}{\rho(\xi + h)}.$$

Moving $\xi + h$ to the other side, we now found the depth averaged shallow water equations,

$$\begin{aligned}
\frac{\partial (\xi + h)}{\partial t} + \frac{\partial (\xi + h) \bar{u}_1}{\partial x_1} + \frac{\partial (\xi + h) \bar{u}_2}{\partial x_2} &= 0, \\
\frac{\partial (\xi + h) \bar{u}_1}{\partial t} + \frac{\partial (\xi + h) \bar{u}_1 \bar{u}_1}{\partial x_1} + \frac{\partial (\xi + h) \bar{u}_1 \bar{u}_2}{\partial x_2} &= -g(\xi + h) \frac{\partial \xi}{\partial x_1} - \frac{\tau}{\rho}, \\
0 &= -g \frac{\partial \xi}{\partial x_2}.
\end{aligned}$$

Adding the assumption that h only dependents on x_2, reduces the equations to,

$$\frac{\partial \xi}{\partial t} + \frac{\partial (\xi + h)\bar{u}_1}{\partial x_1} + \frac{\partial (\xi + h)\bar{u}_2}{\partial x_2} = 0,$$
$$\frac{\partial (\xi + h)\bar{u}_1}{\partial t} + \frac{\partial (\xi + h)\bar{u}_1\bar{u}_1}{\partial x_1} + \frac{\partial (\xi + h)\bar{u}_1\bar{u}_2}{\partial x_2} = -g(\xi + h)\frac{\partial \xi}{\partial x_1} - \frac{\tau}{\rho},$$
$$0 = -g\frac{\partial \xi}{\partial x_2}.$$

These are Equations (2.3) - (2.5) that are used in the main text when we take the average over the width of the channel. However, with the continuity equation (see box below) we can write the first momentum equation in a cleaner form as

$$\frac{\partial \bar{u}_1}{\partial t} + \bar{u}_1\frac{\partial \bar{u}_1}{\partial x_1} + \bar{u}_2\frac{\partial \bar{u}_1}{\partial x_2} = -g\frac{\partial \xi}{\partial x_1} - \frac{\tau}{\rho(\xi + h)}. \tag{C.21}$$

Note that with the product rule and the depth averaged continuity equation (2.3),

$$\begin{aligned}
&\frac{\partial (\xi + h)\bar{u}_1}{\partial t} + \sum_{j=1}^{2}\frac{\partial (\xi + h)\bar{u}_1\bar{u}_j}{\partial x_j} \\
&\quad = (\xi + h)\frac{\partial \bar{u}_1}{\partial t} + \bar{u}_1\frac{\partial (\xi + h)}{\partial t} + \sum_{j=1}^{2}\left[\bar{u}_1\frac{\partial (\xi + h)\bar{u}_j}{\partial x_j} + (\xi + h)\bar{u}_j\frac{\partial \bar{u}_1}{\partial x_j}\right] \\
&\quad = (\xi + h)\frac{\partial \bar{u}_1}{\partial t} - \bar{u}_1\sum_{j=1}^{2}\frac{\partial (\xi + h)\bar{u}_j}{\partial x_j} + \sum_{j=1}^{2}\left[\bar{u}_1\frac{\partial (\xi + h)\bar{u}_j}{\partial x_j} + (\xi + h)\bar{u}_j\frac{\partial \bar{u}_1}{\partial x_j}\right] \\
&\quad = (\xi + h)\left(\frac{\partial \bar{u}_1}{\partial t} + \sum_{j=1}^{2}\bar{u}_j\frac{\partial \bar{u}_1}{\partial x_j}\right).
\end{aligned}$$

Therefore,

$$\frac{1}{\xi + h}\left(\frac{\partial (\xi + h)\bar{u}_1}{\partial t} + \sum_{j=1}^{2}\frac{\partial (\xi + h)\bar{u}_1\bar{u}_j}{\partial x_j}\right) = \frac{\partial \bar{u}_1}{\partial t} + \bar{u}_1\frac{\partial \bar{u}_1}{\partial x_1} + \bar{u}_2\frac{\partial \bar{u}_1}{\partial x_2},$$

which allows us to write the depth averaged momentum balance as equation (C.21).

Bibliography

Alebregtse, N. C., H. E. de Swart, J.-W. Meijerink, and J. T. F. Zimmerman
2015. *The effect of intertidal areas on velocity in tidal channels; momentum sink and overtopping.* PhD thesis, Utrecht University.

Bender, C. M. and S. A. Orszag
1999. *Advanced Mathematical Methods for Scientists and Engineers I, Asymptotic Methods and perturbation Theory.* Springer.

Boon, J. D. and R. J. Byrne
1981. On basin hypsometry and the morphodynamic response of coastal inlet systems. *Marine Geology*, 40:27–48.

Cushman-Roisin, B. and J.-M. Beckers
2011. *Introdroduction To Geophysical Fluid Dynamics.* Academic Press, Elsevier.

Dronkers, J. J.
1964. *Tidal computations in rivers and coastal waters.* Amsterdam: North-Holland Publishing Co.

Friedrichs, C. T. and D. G. Aubrey
1988. Non-linear tidal distortion in shallow well-mixed estuaries, a synthesis. *Estuarine, Coastal and Shelf Science*, 27:521–545.

Friedrichs, C. T. and D. G. Aubrey
1994. Tidal propagation in strongly convergent channels. *Journal of Geophysical Research.*, 99:3321–3336.

Holmes, M. H.
2013. *Introduction to Pertubation Methods*, second edition edition. Springer.

McCully, J. G.
2006. *Beyond the Moon.* World Scientific Publishing Co Pte Ltd.

Open University Course Team
2001. *Waves, tides and shallow water processes.* Pergamon Press, Oxford.

Parker, B. B.
1984. *Frictional effects on the tidal dynamics of a shallow estuary.* PhD thesis, University Baltimore.

Parker, B. B.
1991. *Tidal Hydrodynamics.* John Wiley and Sons, Inc.

Prandle and Rahman
1980. Tidal response in estuaries. *Journal of physical oceanography.*

Renardy, M. and R. C. Rogers
2004. *An Introduction to Partial Differential Equations*, second edition edition. Springer.

Ridderinkhof, W., H. E. de Swart, M. van der Vegt, N. C. Alebregtse, and P. Hoekstra
2014. Geometry of tidal basin systems: A key factor for the net sediment transport in tidal inlets. *Journal of Geophysical Research: Oceans*, (119):6988–7006.

Speer, P. E. and D. G. Aubrey
1985. A study of non-linear tidal propagation in shallow inlet/estuarine systems part ii: Theory. *Estuarine, Coastal and Shelf Science*, (21):207–224.
Vandersmissen, H.
1993. *Wadverhalen*. Hollandia.
Wesseling, P.
2001. *Principles of Computational Fluid Dynamics*. Springer.
Winant, C. D.
2007. Three-dimensional tidal flow in a elongated, rotating basin. *Journal of physical oceanography*, 37:1278–1295.
Zimmerman, J. T. F.
1982. On the lorenz linearization of a quadratically damped forced oscillator. *Physics letters*, 89A(3):123–124.

The photo on the title page of the common ringed plover on top of the logo of Utrecht University is made by Henk Laverman.